

**THE USE OF ELECTRICAL RESISTIVITY TO
MONITOR THE MODIFICATION OF Al-Si-Mg
CASTING ALLOYS**

by

Karen Lindsay Pirie

A thesis submitted to the Faculty of
Graduate Studies and Research in partial
fulfillment of the requirements for the
Degree of Master of Engineering

Department of Mining and Metallurgical Engineering
McGill University
Montreal, Canada
April 1984 ©

1

ABSTRACT

The modification of A356, Al-Si-Mg alloy has been studied using electrical resistivity. It is shown that an unmodified alloy exhibits a higher resistivity than a modified alloy. Resistivity is directly related to the morphology of eutectic silicon and can therefore also be used to follow the heat treatment of Al-Si-Mg alloys in which the eutectic silicon undergoes ripening and spheroidization. Resistivity generally increases on solution treatment and decreases on subsequent aging. Modified alloys exhibit a greater increase in resistivity on solution treatment than do unmodified alloys.

Resistivity can also be used to study modification in A356 alloys with unusually high iron contents. Magnesium, however, has an inherent modifying effect and alloys with high magnesium contents such as A357 show no variation in resistivity upon modification.

Both a D.C. and a differential A.C. resistivity technique can be used. The former measures the potential drop across a bar through which a current of 40 Amps is passed. The differential technique compares the voltage across a standard non-modified sample with the voltage across an unknown sample. The A.C. technique would be favoured in foundry practice since it is temperature independent and is associated with very small instrumental errors. Differential measurement

requires the standard and sample bar to be of similar porosity content and also to be of similar diameter since eutectic segregation occurs towards the centre of bar samples.

RESUME

La technique de la résistivité électrique a été utilisée dans l'étude de la modification des alliages Al-Si-Mg (A356). Il a été montré que l'alliage non modifié présente une résistivité plus élevée que l'alliage modifié. La résistivité électrique peut être directement reliée à la morphologie du silicium de l'eutectique. Cette technique trouve aussi une application dans l'étude du traitement thermique des alliages Al-Si-Mg dans lesquels le silicium de l'eutectique subit une globularisation et une coalescence. Le traitement de mise en solution augmente la résistivité tandis que le traitement de précipitation diminue la résistivité. Après le traitement thermique de mise en solution les alliages modifiés présentent une augmentation de la résistivité électrique nettement supérieure à celle des alliages non modifiés.

La résistivité a aussi été utilisée dans l'étude des alliages A356 contenant de fortes teneurs en fer. Cependant, les alliages A357, à haute teneur en magnésium, ne subissent qu'une très faible variation de la résistivité avec le degré de modification. Il a été montré que ces faibles changements sont imputables au pouvoir modificateur du magnésium.

Deux techniques de mesure de résistivité peuvent être employées, l'une utilise le courant continu, l'autre, différentielle, utilise le courant alternatif. La première mesure la

différence de potentiel à travers une barre dans laquelle on a fait passer un courant de 40 ampères. La méthode différentielle compare la différence de potentiel dans un échantillon de référence, non modifié, avec la différence de potentiel dans un échantillon de mesure. La technique différentielle semble être d'une utilisation plus pratique en fonderie parcequ'elle est indépendante de la température ambiante et qu'elle n'introduit que de faibles erreurs expérimentales. Cependant, la méthode du courant alternatif requiert des échantillons de référence et de mesure ayant une porosité identique afin d'éviter les incertitudes de mesure susceptibles d'être introduites par une ségrégation existant entre la surface et le centre de la barre.

ACKNOWLEDGEMENTS

The author wishes to extend her deepest thanks to Professor J.E. Gruzleski and Dr. B. Closset for their great help and guidance throughout the course of the work.

Thanks are also due to the entire staff of the Department of Mining and Metallurgical Engineering, especially Dr. R.A.L. Drew for guidance in differential resistivity analysis.

The technical assistance of Mr. M. Knoepfel and Mr. B. Grondin, the help of Mr. R. Paquette in performing casting experiments, and the assistance of Mrs. H. Campbell in spectrochemical analyses are all gratefully acknowledged.

The author is also indebted to Robert Mitchell Inc. for the radiography of the bars, and to Mr. M. Ross, School of Occupational Health and Safety, McGill University, for the assistance in analysis of silicon eutectic content of the bars.

Sincere appreciation and gratitude is extended to Mr. Stephen R. Cameron, to fellow graduate students and to all others whose assistance and encouragement have been invaluable.

TABLE OF CONTENTS

	Page
ABSTRACT	i
RESUMÉ	iii
ACKNOWLEDGEMENTS	v
TABLE OF CONTENTS	vi
LIST OF FIGURES	ix
LIST OF TABLES	xiii
1. INTRODUCTION	1
1.1 Aluminum-Silicon-Magnesium Alloys	1
1.2 Modification	4
1.2.1 General Discussion	4
1.2.2 Modifying Agents	9
1.2.3 Theory of Modification	12
1.3 Heat Treatment of Al-Si-Mg Alloys	15
1.3.1 Introduction	15
1.3.2 Solution Treatment	15
1.3.3 Aging	17
1.4 The Effects of Increasing Magnesium and Iron Contents on the Structure and Mechanical Properties of Al-Si-Mg Alloys	17
1.5 Porosity	24
1.6 Monitoring the Modification Process in the Foundry	24
1.6.1 Metallography	26
1.6.2 Thermal Analysis	26
1.6.3 Electrical Resistivity	31
1.7 Aims of the Present Investigation	39

	Page
2. EXPERIMENTAL PROCEDURES	43
2.1 Parameters and Variables	43
2.2 Statistical Analysis of Results	44
2.3 Foundry Procedure and Sample Preparation	46
2.3.1 The Pattern and Sand Mould	46
2.3.2 Melting and Strontium Addition	48
2.3.3 Alloy Additions	52
2.3.4 Bar Preparation	52
2.3.5 Spectrochemical Analysis	52
2.3.6 Metallography	54
2.4 Electrical Resistivity Measurement	55
2.4.1 D.C. Resistivity Measurement	55
2.4.2 A.C. Resistivity Measurement	55
2.5 The Factors Affecting Resistivity	61
2.5.1 Temperature	61
2.5.2 Porosity	61
2.5.3 Eutectic Segregation	63
2.5.4 Solute Concentrations	66
2.6 Heat Treatment	68
3. RESULTS	73
3.1 Electrical Resistivity	73
3.1.1 D.C. Resistivity	73
3.1.2 A.C. Resistivity	78
3.2 The Factors Affecting Resistivity	87
3.2.1 Temperature	87
3.2.2 Porosity	92
3.2.3 Eutectic Segregation	92
3.2.4 Solute Concentrations	97
3.3 Heat Treatment	97
3.3.1 Heat Treatment of A356 Alloys	97

	Page
3.3.2 Heat Treatment of A357 and A356 (0.48 wt.% Fe) Alloys	110
4. DISCUSSION	118
4.1 Experimental Inaccuracies	118
4.1.1 Instrumental Inaccuracies	118
4.1.2 Inaccuracies due to Inherent Differences Between Similar Bars	119
4.1.3 Dimensional Inaccuracies	119
4.1.4 Total Inaccuracies of the D.C. and A.C. Techniques	120
4.2 D.C. and A.C. Resistivity	121
4.2.1 A356 Alloy	121
4.2.2 A357 Alloy	123
4.2.3 A356 Alloy containing 0.48wt.% Fe	124
4.3 Factors Affecting Resistivity	124
4.3.1 Temperature	125
4.3.2 Porosity	126
4.3.3 Eutectic Segregation	128
4.4 Heat Treatment	128
4.4.1 Introduction	128
4.4.2 Heat Treatment and Resistivity	129
4.5 Comparison Between D.C. and A.C. Resistivity Techniques	132
5. SUMMARY	134
6. CONCLUSIONS AND SUGGESTIONS FOR FURTHER WORK	136
REFERENCES	140
APPENDIX	143

LIST OF FIGURES

Figure		Page
1	The Al-Si binary phase diagram	2
2	Microstructures of A356 alloy	8
3	Variation in the quality index with relation to strontium content	11
4	Suggested sequence by Thall and Chalmers showing how aluminum might occlude silicon at an advancing duplex solid-liquid front	14
5	Microstructures of an unmodified A356 alloy, as-cast and heat treated	18
6	Microstructures of a modified A356 alloy as-cast and heat treated	19
7	Tensile properties of degassed aluminum -7%Si alloys containing various amounts of magnesium	22
8	The effect of iron on tensile properties of permanent mold cast alloy 356-T6	23
9	Influence of hydrogen porosity on the tensile strength of sand cast bars of Al-5.0% Si alloy	25
10	Schematic of the system for thermal analysis	27
11	Simple thermal analysis curves near the eutectic plateau	29
12	The derived thermal analysis curve and the simple thermal analysis curve near the eutectic plateau	30
13	The total heat of solidification curve and the simple thermal analysis curve near the eutectic plateau	32
14	Circuit design for differential resistivity measurement	35

Figure		Page
15	Schematic of the apparatus used in D.C. resistivity measurement by Oger, Closset and Gruzleski	37
16	Variation of electrical resistivity with strontium content	38
17	Variation of electrical resistivity (voltage) with magnesium content	40
18	An Al-Si-Mg alloy casting showing the four test bars with the risers and gating systems	49
19	Graphite plunger used for strontium additions	50
20	Copper mould used for casting spectrometer samples	51
21	The magnesium rod and iron powder pellets used for alloying the Al-Si-Mg melts	53
22	Schematic of the apparatus used in D.C. electrical resistivity measurement	56
23	The jig used to hold the Al-Si-Mg test bars in D.C. electrical resistivity measurement	57
24	The jig used in A.C. resistivity measurement	58
25	Circuit design for differential resistivity measurement	59
26	Apparatus used to measure resistivity at various temperatures	62
27	The apparatus used in porosity measurement	64
28	Determination of the amount of eutectic across the bar diameter	67
29	Cross section of the wire mesh jig used to hold the bars during heat treatment	71

Figure

Page

30	Variation of D.C. resistivity with strontium content for A356 alloy	74
31	Microstructures of A356 alloy at various strontium contents	75
32	Microstructures of A357 alloy at various strontium contents	77
33	Variation of D.C. resistivity with strontium content for A357 alloy	80
34	Variation of D.C. resistivity with strontium content for alloy A356 (0.48 wt.% Fe)	81
35	Microstructures of A356 alloy containing 0.48 wt.% Fe at various strontium contents	82
36	Variation of ΔV with strontium content for A356 alloy	86
37	Variation of ΔV with strontium content for A357 alloy	88
38	Variation of ΔV with strontium content for A356 alloy containing 0.48 wt.% Fe	89
39	Variation of D.C. resistivity with temperature for A356 alloy	91
40	X-ray images of the test bars. The bars were found to be homogeneous	95
41	Porosity on the surface of a metallographic sample	96
42	Variation of the amount of eutectic with radial distance from the centre of bars	100
43	Variation of silicon content in the primary aluminum matrix with strontium content	102
44	The difference in D.C. resistivity between as-cast and solution treated A356 bars of various strontium contents	107

Figure		Page
45	The difference in ΔV between as-cast and solution treated A356 bars of various strontium contents	108
46	The difference in D.C. resistivity between as-cast and completely heat treated A356 bars of various strontium contents	109
47	The difference in ΔV between as-cast and completely heat treated bars of various strontium contents	111
48	Metallographic samples of unmodified and modified bars subject to complete heat treatment A,B, and C	112
49	An Al-Si-Mg alloy casting showing the location of bars A,B,C and D	145

LIST OF TABLES

Table		Page
I	Composition ranges for the Al-7%Si-Mg alloys	3
II	Heat treatments for separately cast test bars of alloys 356 and A356	5
III	Mechanical properties of A356 T6	6
IV	Mass, thermal and electrical properties of alloy 356, T6, sand cast	7
V	Comparison of strontium modified alloys with unmodified alloys. Both alloys are sand cast and heat treated	20
VI	Statistical results of the strontium content vs. D.C. resistivity data	45
VII	F tables for 95% significance level	47
VIII	Calibration of density apparatus	65
IX	Temperature variations within the Blue M Power Omatic 80 Furnace (Model No RG-3080 C)	69
X	Temperature variations within the Griffin-Grundy Furnace (Model No 661530)	70
XI	Results of statistical analysis on the ΔV versus $S\bar{r}$ wt.% data for the three diameter ranges using A356 alloy	85
XII	D.C. resistivity values of A356 bars at various temperatures	90
XIII	ΔV values from A.C. resistivity measurements at various temperatures, for alloy A356	93
XIV	The influence of porosity on electrical resistivity	94
XV	Variation of D.C. resistivity with machined sample diameter	98

Table		Page
XVI	Variation of percent eutectic present with radial distance from the centre of a bar	99
XVII	Correlation between percent silicon in the aluminum matrix with strontium content	101
XVIII	The average change in D.C. resistivity as a result of solution treatment and as a result of aging for A356 alloy heat treatments A, B and C	103
XIX	A comparison of the changes in resistivity brought about by various solution treatments and aging treatments, between unmodified and modified A356 alloys	105
XX	The average change in D.C. resistivity as a result of solution treatment and as a result of aging for A357 alloy	115
XXI	The average change in D.C. resistivity as a result of solution treatment and as a result of aging for A356 alloy containing 0.48 wt.%Fe	116

1. INTRODUCTION

1.1 Aluminum-Silicon-Magnesium Alloys

The Al-7%Si-Mg alloys have excellent castability, good weldability, pressure tightness and good corrosion resistance, and have therefore found applications in aircraft structures, aircraft engine controls, aircraft fittings and pump parts, water-cooled cylinder blocks and nuclear installations. These products are usually sand castings, permanent mold castings or investment castings of intricate design due to the excellent castability of the alloy. Castability is a property dependant upon composition and freezing temperatures. The composition of the alloy is near the eutectic composition (12.6% Si-Al) and therefore has a small freezing range and solidifies quickly in the mold. Additionally the freezing temperatures are low enabling casting to be performed at 675 C to 790 C (figure 1).

The specific application of a 7%Si-Al alloy is related to its precise composition. The composition ranges of these alloys incorporates the 356, A356, 357, and A357 alloys (Table I). It is important that the compositional limits are not exceeded in order to maintain superior properties; for example high copper or nickel contents decrease ductility and resistance to corrosion, and high iron contents decrease strength and ductility.

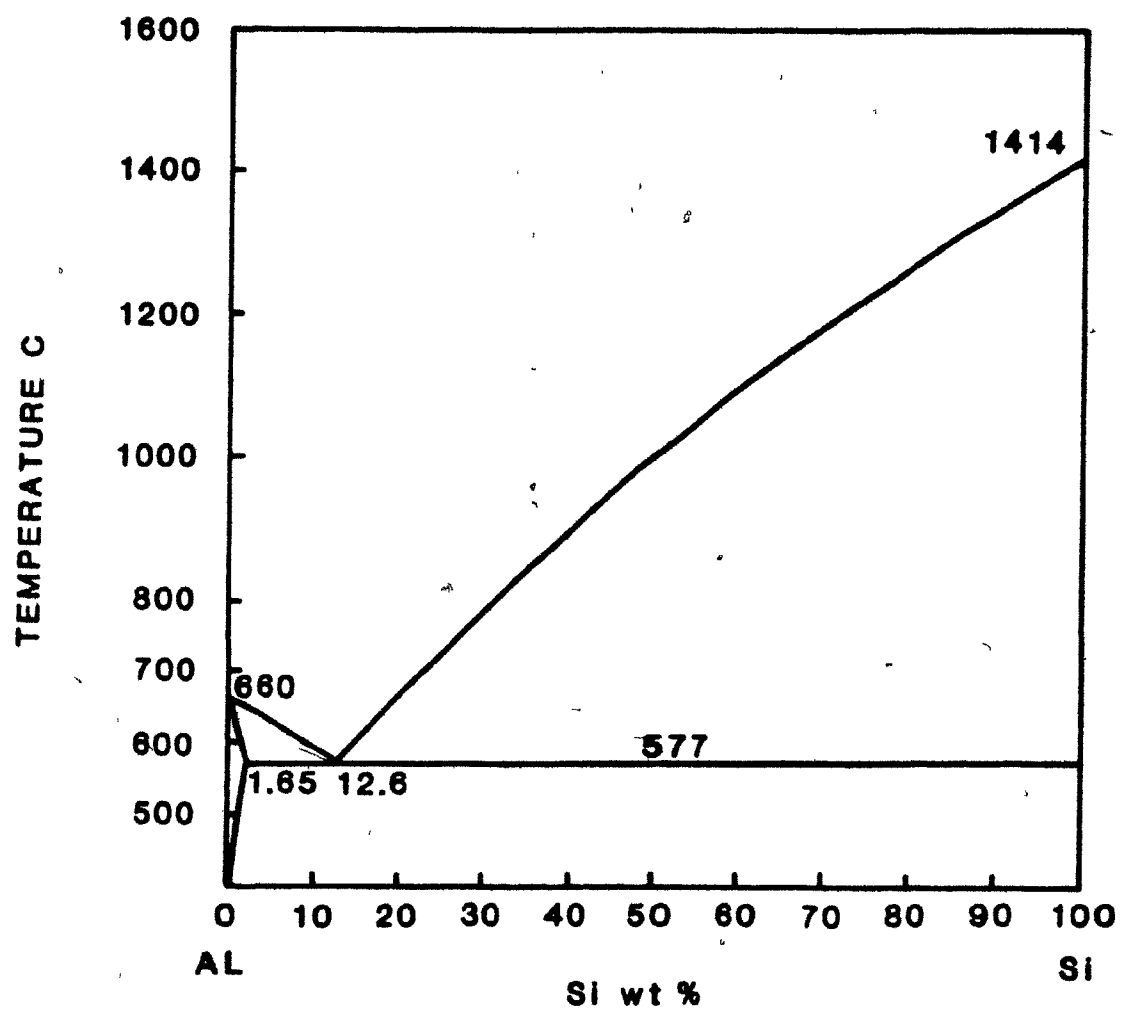


Figure 1⁽¹⁾: The Al-Si binary phase diagram

Element	Composition (wt.%)			
	Alloy			
	356	A356	357	A357
Si	6.5 → 7.5	6.5 → 7.5	6.5 → 7.5	6.5 → 7.5
Mg	0.20 → 0.45	0.25 → 0.45	0.45 → 0.60	0.40 → 0.70
Cu	0.25 max	0.20 max	0.05 max	0.20 max
Mn	0.35 max	0.10 max	0.03 max	0.10 max
Fe	0.60 max	0.20 max	0.15 max	0.20 max
Zn	0.35 max	0.10 max	0.05 max	0.10 max
Ti	0.25 max	0.20 max	0.20 max	0.10 - 0.20

Table I⁽²⁾: Composition ranges for the Al- 7%Si-Mg alloys

Another important consideration in the production of 7%Si-Al alloy castings is heat treatment. These alloys are seldom used in the as-cast condition, and the type of heat treatment performed will greatly influence the properties of the final product. Generally, heat treatment confers increased strength and hardness, obtained by a high temperature solution treatment, followed by a quench and natural aging. This sequence of processes produces T6 and T7 type tempers. Alloys in T6-type tempers generally have the highest strength possible without sacrifice of other properties and characteristics, and alloys in T7-type tempers are stabilized by "overaging" which means that some degree of strength has been sacrificed to improve one or more other characteristics such as dimensional stability. The temperature and time limits in the various stages of tempers T6 and T7 are shown in table II, and table III shows the mechanical properties of heat treated alloy 356 T6.

The mass, thermal and electrical properties of alloy 356 are given in table IV.

1.2 Modification

1.2.1 General Discussion

Modification is a widely used process which enhances the mechanical properties of Al-Si-Mg alloys by altering the morphology of the eutectic silicon. An unmodified alloy (figure 2a) has an acicular eutectic structure where the silicon is in the form of large brittle plates. With a successful modification

Purpose (and resulting temper)	Temperature C	Time hrs.
Sand Castings; Solution treatment	535 to 540	12
Aging T6 T7	150 to 155 225 to 230	2 to 5 7 to 9
Permanent Mold Castings; Solution treatment	535 to 540	8
Aging T6	150 to 155	3 to 5

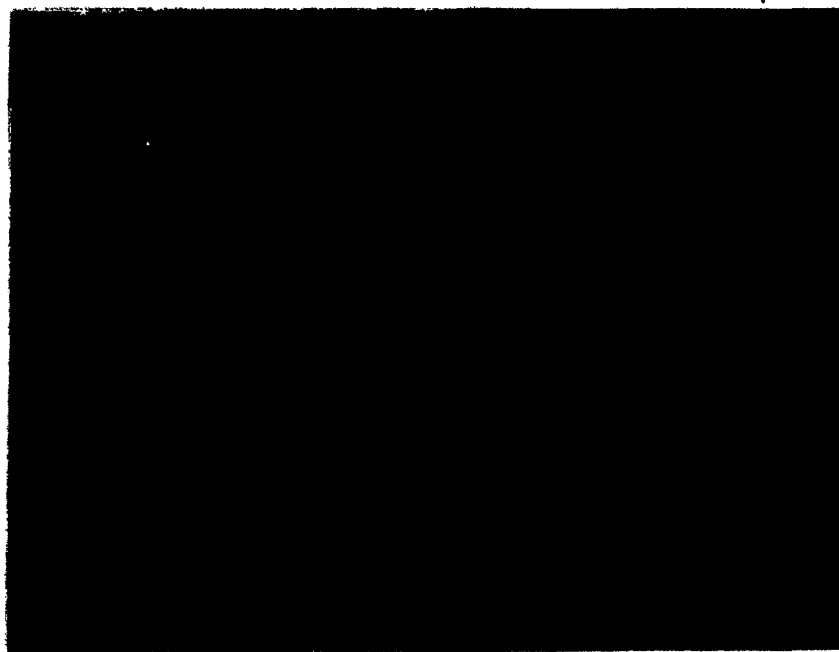
Table II⁽²⁾: Heat treatments for separately cast test bars of alloys 356 and A356

Property	Value
Tensile strength	228 MPa
Yield strength	165 MPa
Elongation	3.5%
Hardness HB	70
Shear strength	180 MPa
Fatigue strength	60 MPa
Compressive yield strength	170 MPa
Poisson's ratio	0.33
Elastic modulus: Tension	72.4 GPa
Shear	27.2 GPa

Table III⁽²⁾: Mechanical properties of A356 T6

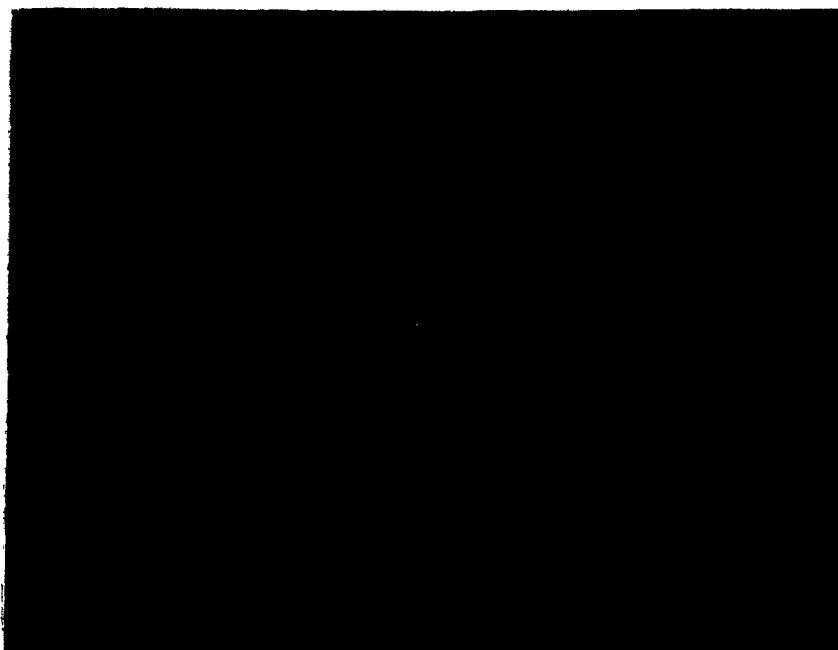
Property	Value
Density at 20 C	2.685 g cm ⁻³
Liquidus temperature	615 C
Solidus temperature	555 C
Coefficient of thermal expansion 20 — 100 C	21.5 m m ⁻¹ K ⁻¹
Specific heat	963 J Kg ⁻¹ K ⁻¹
Latent heat of fusion	389 KJ Kg ⁻¹
Thermal conductivity at 25 C	151 W m ⁻¹ K ⁻¹
Electrical Conductivity	39 IACS
Electrical Resistivity at 20 C	44.2 nΩ.m

Table IV⁽²⁾: Mass, thermal and electrical properties of alloy 356, T6, sand cast



(mag x 200)

2a; Unmodified 0.000 wt.% Sr



(mag x 200)

2b; Undermodified 0.007 wt.% Sr

Figure 2: Microstructures of A356 Alloy

treatment the silicon assumes a fine fibrous morphology (figure 2c). This modified, fibrous structure transmits cracks for short distances because individual strands of silicon do not extend over large areas in any one plane, as in the unmodified case. The modified alloy therefore exhibits a higher ductility and higher strength than the unmodified alloy.

The process of modification is performed by the addition of a modifying agent to the melt. The amount of agent used is of prime importance for successful modification since too little modifying agent will produce an undermodified alloy (figure 2b) with lamellar eutectic silicon, while too much modifying agent will produce an overmodified structure containing intermetallics. Work by Closset and Gruzleski⁽³⁾ using strontium as a modifying agent, showed that optimum mechanical properties are obtained in the strontium range from 0.005 wt.% Sr to 0.015 wt.% Sr where the alloy is modified (figure 3). An overmodified alloy has poorer mechanical properties caused by the formation of Al-Si-Sr intermetallics.

1.2.2 Modifying Agents

Strontium, sodium and antimony are the three most well known modifying agents. Only strontium and sodium have found extensive commercial application because antimony produces a lamellar eutectic⁽⁴⁾, the result of a refinement process rather than a modification process. Both strontium and sodium



(mag x 200)

2c; Modified 0.015 wt.% Sr



(mag x 200)

2d; Overmodified 0.069 wt.% Sr

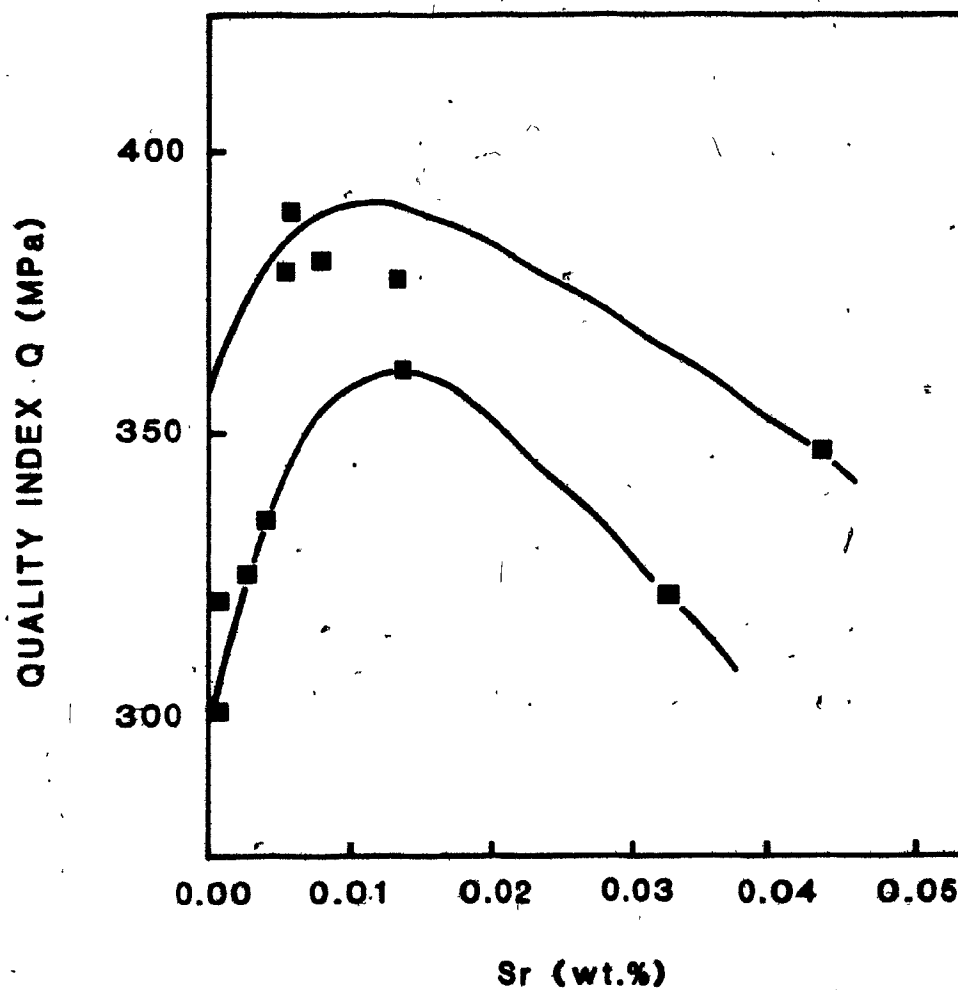


Figure 3⁽³⁾: Variation in the quality index with relation to strontium content.

$$Q = \text{Tensile Strength} + 150 \log (\% \text{ elongation})$$

produce equivalent modified structures, but behave in a different way. Sodium has good dissolution characteristics, however it has only a limited effect in time as it will disappear rapidly by evaporation or oxidation during holding of the molten metal. Strontium, on the other hand, has poorer dissolution characteristics; however, it does not evaporate from the melt during holding and can be easily added via master alloys giving reduced oxidation problems.

1.2.3 Theory of Modification

The early theories⁽⁵⁾ of modification all supposed that some poisoning action by the modifying agent prevented the silicon crystals from growing at the same rate as aluminum (or vice versa) so that the interface advanced by some repetitive nucleation process. However, since modified forms of silicon are now known to be continuous, more recent theories have concentrated on the shape of the eutectic solid-liquid interface.

Two main theories have been forwarded as to how the sodium modifies the actual growth process:

a) by surface adsorption which may poison the growth mechanisms of silicon.

b) by altering the solid-solid or solid-liquid interfacial energies and consequently changing the solid-liquid profile.

Thall and Chalmers⁽⁶⁾ suggested the theory of surface adsorption. They assumed that aluminum projects ahead of the silicon

(figure 4a), and as the solid-liquid front progresses, the aluminum occludes the silicon (figure 4). During modification it is supposed that sodium adsorption occurs at the Al-Si-liquid interfaces, reducing the surface energy and increasing the solid-liquid contact angle at these triple junctions, again leading to overgrowth until further nucleation occurs.

The most accepted theory of modification based on work by Davies and West⁽⁷⁾ suggests that the preferential adsorption of sodium on the solid-liquid interface changes the profile because the growth kinetics of the silicon are affected. Although the authors are unable to comment on the shape of the solid-liquid profile, they note that "the failure of silicon to develop faceted faces (evident in the modification of primary crystals) must mean that rapidly growing faces or active growth sites are affected"⁽⁷⁾ The need only for surface activity explains why the sodium or other elements are effective at such low concentrations. It is not known why the alkali and alkaline earth metals should be effective modifying agents; one suggestion⁽⁷⁾ is that they have the most polarized atoms and lowest ionization potentials, which account for their retention on the electronegative elements such as silicon.

Phosphorus is often present in Al-Si alloys and produces a eutectic refining effect changing the morphology of silicon from flakes to a granular form. It has an effect upon modification since Crosley and Mondolfo⁽⁸⁾ proved that the growth process in the presence of phosphorus is not hindered in the

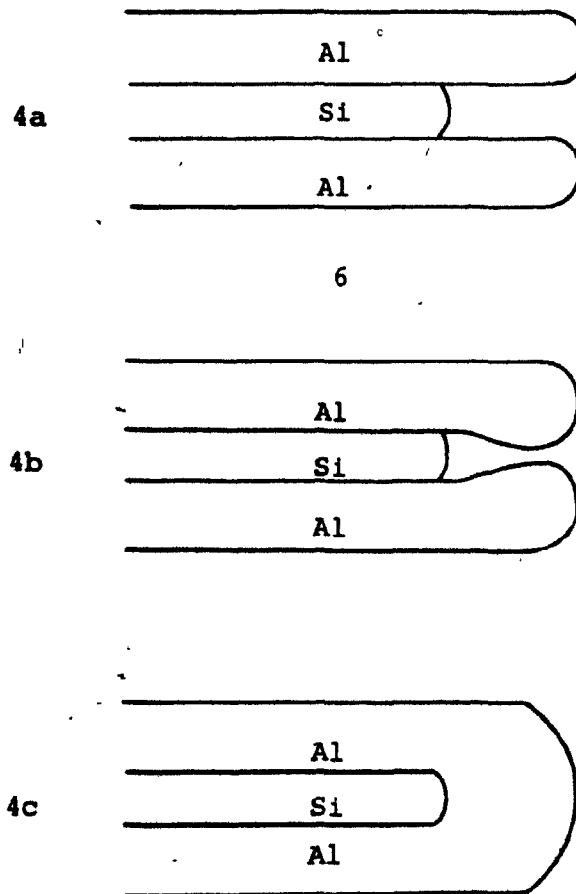


Figure 4: Suggested sequence by Thall and Chalmers⁽⁶⁾ showing how aluminum might occlude silicon at an advancing duplex solid-liquid front

same way as it is in modified alloys. They suggested that the active ingredient in the refining action is the compound AlP which acts as a heterogeneous nucleating agent for silicon, and in the presence of sodium, forms a quaternary P-Al-Na-Si compound which does not act as a heterogeneous nucleating agent.

In summary, the theories of modification suggest kinetic limitations of silicon, either by the imposed growth rate and inability of the faceted material to grow as quickly as the metal, or because the growth process is susceptible to poisoning.

1.3 Heat Treatment of Al-Si-Mg Alloys

1.3.1 Introduction

The typical heat treatment of A356 alloys⁽²⁾ (Table II) involves solution treatment at 535 to 540 C for 12 hours, followed by quenching and aging at 150 to 155 C for 2 to 5 hours. The main purpose of solution treatment is to dissolve alloying atoms in solution so that upon quenching, these atoms are held in solid solution. The final process of aging then allows these alloying elements to form finely dispersed precipitates which increase the alloy strength and hardness.

1.3.2 Solution Treatment

There are four main processes that occur on solution treatment of A356 alloys; dissolution, spheroidization, ripening, and homogenization. Dissolution is primarily that of

silicon and magnesium and they are held in solid solution when the alloy is quenched. Spheroidization is a diffusion controlled process with the minimization of surface area acting as the driving force. Diffusion of silicon from the surface of particles with a high degree of curvature to adjacent surfaces with low degrees of curvature occurs, and as a result, particles become more spheroidal. The plate-like eutectic silicon of unmodified alloys is obviously able to undergo more extensive spheroidization than the already spheroidal-like eutectic silicon of the modified alloys.

The third process, ripening is also diffusion controlled with the minimization of surface energy acting as the driving force. Ripening appears as a coarsening of the eutectic where silicon diffuses from smaller particles (relatively high surface energy) to larger particles (lower surface energy). As a result, smaller particles dissolve and the larger ones increase in size. The effects of ripening are more pronounced in modified alloys because the distance between eutectic particles is relatively small allowing diffusion from one particle to another to occur readily. The plates of unmodified alloys are widely spaced and diffusion between them takes considerably more time.

Homogenization is also diffusion controlled where solute concentrations throughout the alloy become uniform.

Since spheroidization, ripening and homogenization are diffusion controlled they therefore occur to a greater extent upon solution treatment at 540 C than upon aging at 155 C.

1.3.3 Aging

Silicon and magnesium are the two main elements held in solid solution when the alloy is quenched. With subsequent aging at temperatures of 155 C the precipitation process can be represented as:

Guinier Preston zones \longrightarrow intermediate precipitate \longrightarrow equilibrium phase Mg_2Si

Mg_2Si forms as fine precipitates between the dendritic silicon particles, and there is a depletion of the average silicon and magnesium concentration in the matrix.

Figures 5 and 6 show the microstructures of as-cast and heat treated modified and unmodified alloys. In the modified alloy, the fine fibrous eutectic undergoes coalescence upon heat treatment to give a coarser structure than in the as-cast condition. In the unmodified alloy, the eutectic silicon plates become less angular. The heat treated modified alloy exhibits superior mechanical properties than the as-cast modified alloys or the as-cast and heat treated unmodified alloys. Table V compares the mechanical properties of modified and non-modified, heat treated Al-Si-Mg bars.

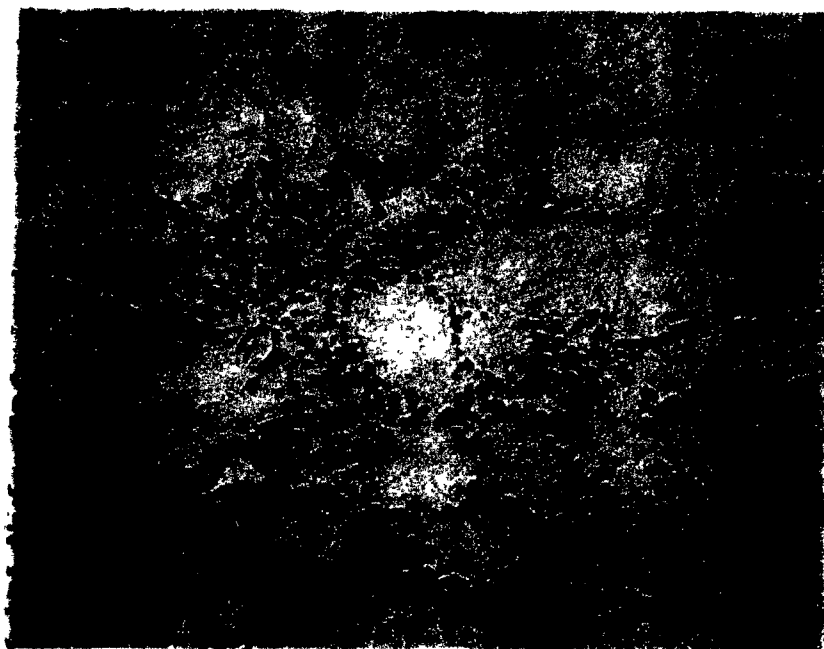
1.4 The Effects of Increasing Magnesium and Iron Contents on the Structure and Mechanical Properties of Al-Si-Mg Alloys

Aluminum-silicon-magnesium alloys are renowned for their extreme sensitivity to magnesium content, which could be attributed to the 0.3 wt.% Mg solubility limit at the solution treatment temperature. With increasing magnesium content, up



(mag x 200)

5a: As-cast microstructure



(mag x 200)

5b: Heat treated microstructure

Figure 5: Microstructure of an unmodified A356 alloy, as-cast and heat treated (8 hours solution treatment at 540 C, and 12 hours aging at 155 C)



(mag x 200)

6a: As-cast microstructure



(mag x 200)

6b: Heat treated microstructure

Figure 6: Microstructure of a modified A356 alloy
(0.015 wt.% Sr) as-cast and heat treated
(8 hours solution treatment at 540 C, 12
hours aging at 155 C)

Property	Unmodified Alloy ⁽²⁾	Modified Alloy ⁽³⁾
Ultimate tensile strength (MPa)	230	285
Yield strength (MPa)	165	208
Elongation (pct)	3.5	12
Quality Index (Q) (MPa)	312	447

Table V^(2,3): Comparison of strontium modified alloys with unmodified alloys. Both alloys are sand cast and heat treated. The unmodified alloy is heat treated to the T6 designation, and the modified alloy is solution treated for 72 hours at 540 C, naturally aged for 48 hours at room temperature and artificially aged for 8 hours at 155 C

to 0.3 wt.% Mg, the tensile strength of the alloy is greatly increased and its ductility is decreased due to the increase of magnesium in solid solution (figure 7) ⁽⁹⁾. At concentrations greater than 0.3 wt.% Mg the tensile strength and percent elongation remain constant because Mg_2Si forms and therefore any further increase in magnesium has relatively little effect on the structure and composition of the aluminum matrix. At very high magnesium concentrations (0.65 wt.% Mg) the $Al_8FeMg_3Si_6$ intermetallics have been found ⁽³⁾ dispersed throughout the microstructure thus leading to inferior mechanical properties.

Heat treatment of Al-Si-Mg alloys with high magnesium contents tends to increase the tensile properties due to the fine re-dispersion of Mg_2Si during aging ⁽¹⁰⁾. Unlike Al-Si-Mg alloys, with increasing magnesium contents, alloys with increasing iron contents show a slight decrease in tensile strength together with a decrease in ductility ⁽¹¹⁾ (figure 8). These effects can be attributed to the low solubility limit of iron in aluminum, above which needles of Al_5FeSi form, imparting brittle fracture characteristics and poor mechanical properties to the alloy. Heat treatment does not produce superior mechanical properties in the Al-Si-Mg alloy with a high iron content because the Al_5FeSi needles do not dissolve during the heat treatment process.

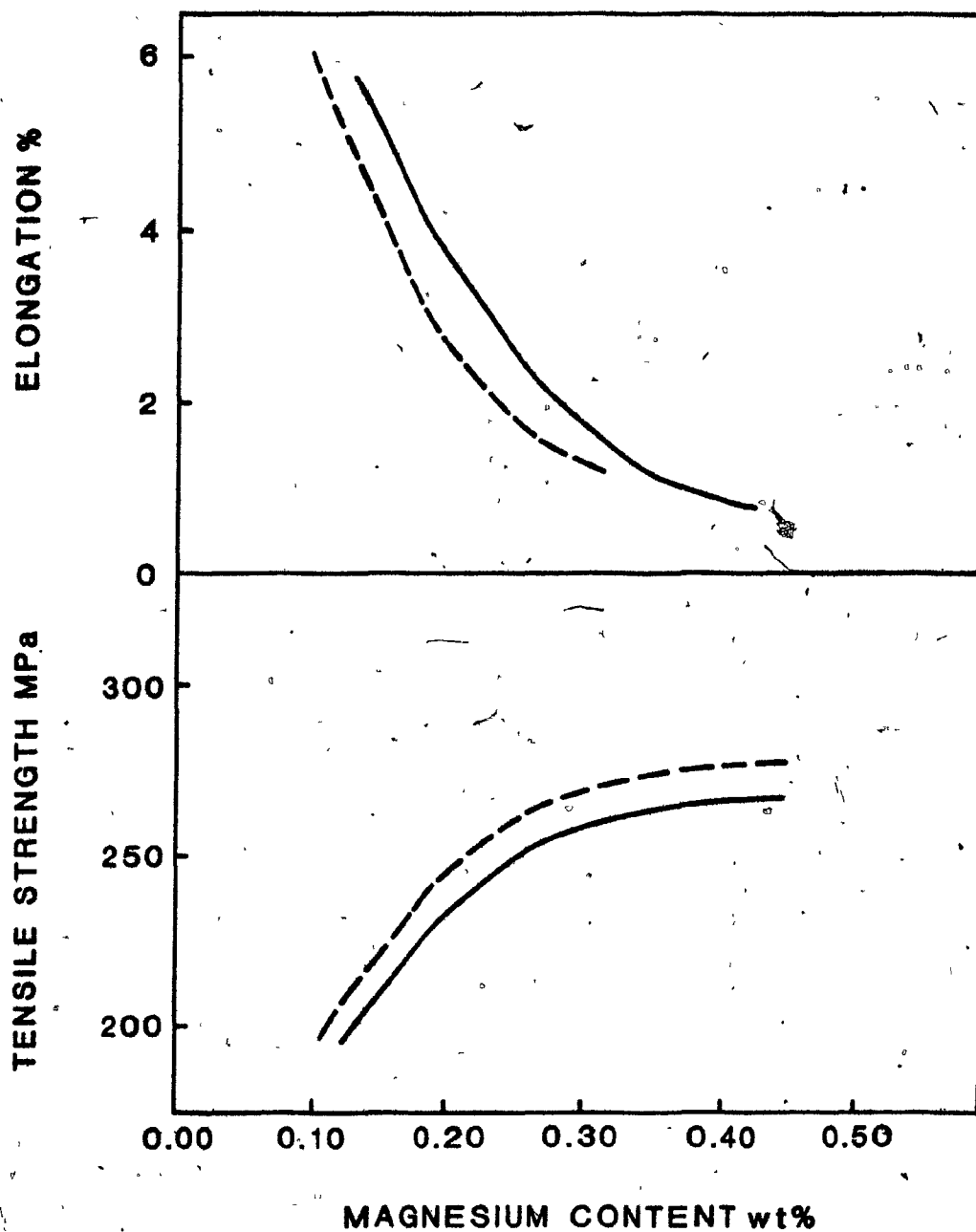


Figure 7⁽⁹⁾: Tensile properties of degassed aluminum -7% Si alloys containing various amounts of magnesium. All alloys are solution treated for 16 hours at 538 C aged for 6 hours at 204 C

-- non-modified alloys
— modified alloys

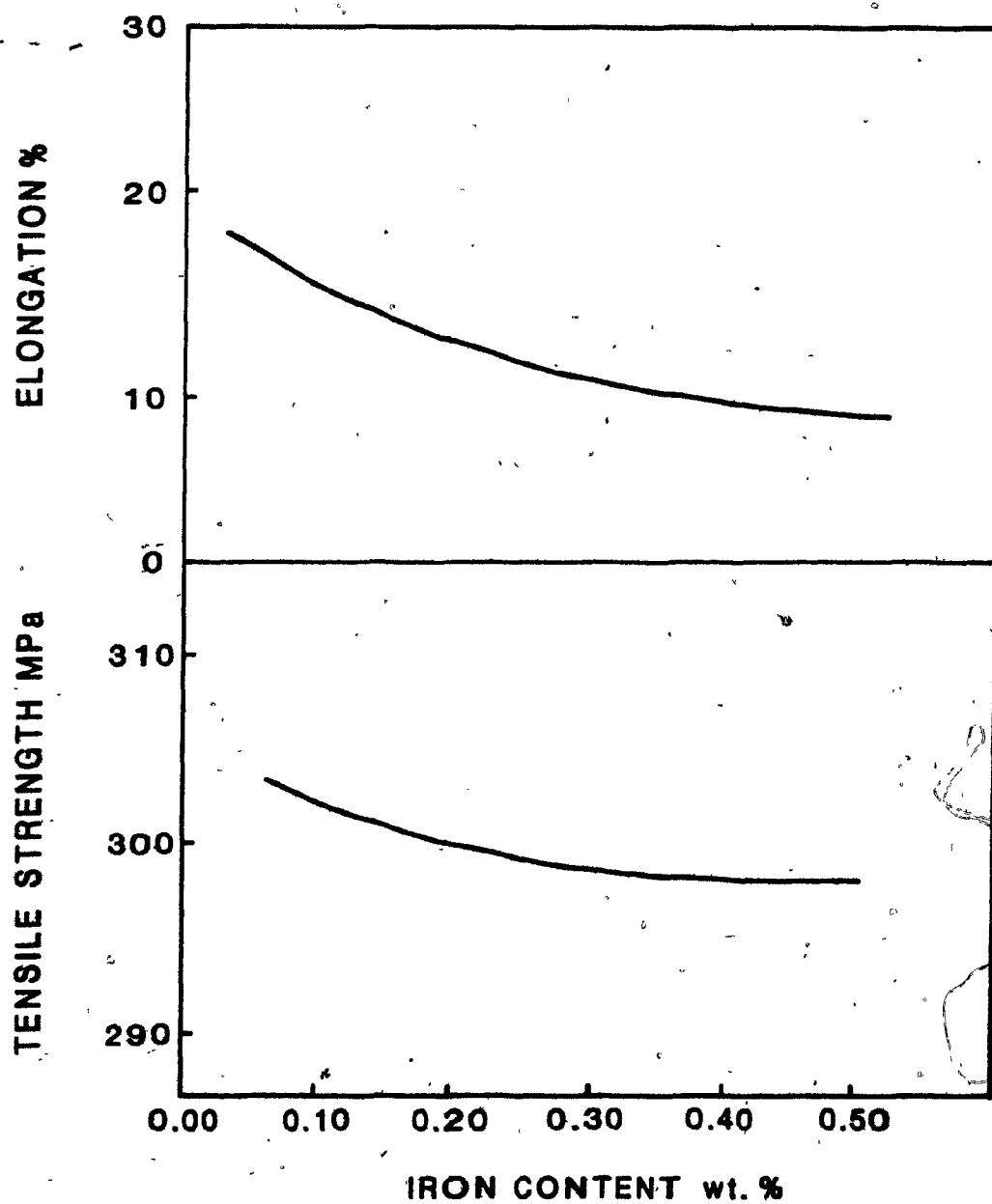


Figure 8⁽¹¹⁾: The effect of iron on tensile properties of permanent mold cast alloy 356 - T6

1.5 Porosity

Porosity is a well known casting defect especially in aluminum castings where hydrogen porosity is a major problem. Porosity, which has deleterious effects on mechanical properties, occurs as an internal gas phase or void. It has been shown⁽¹²⁾ that there is a tendency for the tensile strength to decrease with increasing amounts of porosity (figure 9).

Porosity can be reduced by degassing the melt with an inert gas before casting. Work by Closset and Gruzleski⁽¹³⁾ has shown that the total amount of dissolved hydrogen in an Al-Si-Mg casting decreases with increase in volume of nitrogen gas bubbled through the melt and the density of the casting accordingly increases. Although degassing has the advantageous effect of reducing porosity it also has the disadvantageous effect of causing loss of the modifying agent from the melt, particularly when degassing is carried out with a chlorine containing gas.

1.6 Monitoring the Modification Process in the Foundry

It is desirable in foundry practice to be able to maintain close control over all aspects of melt chemistry in order to guarantee casting quality. For modification of aluminum-silicon alloys, the morphology of the eutectic silicon is so sensitive to very small variations in modifying agent, that some control method must be used to ensure that modification is successful. The extent of modification cannot always be

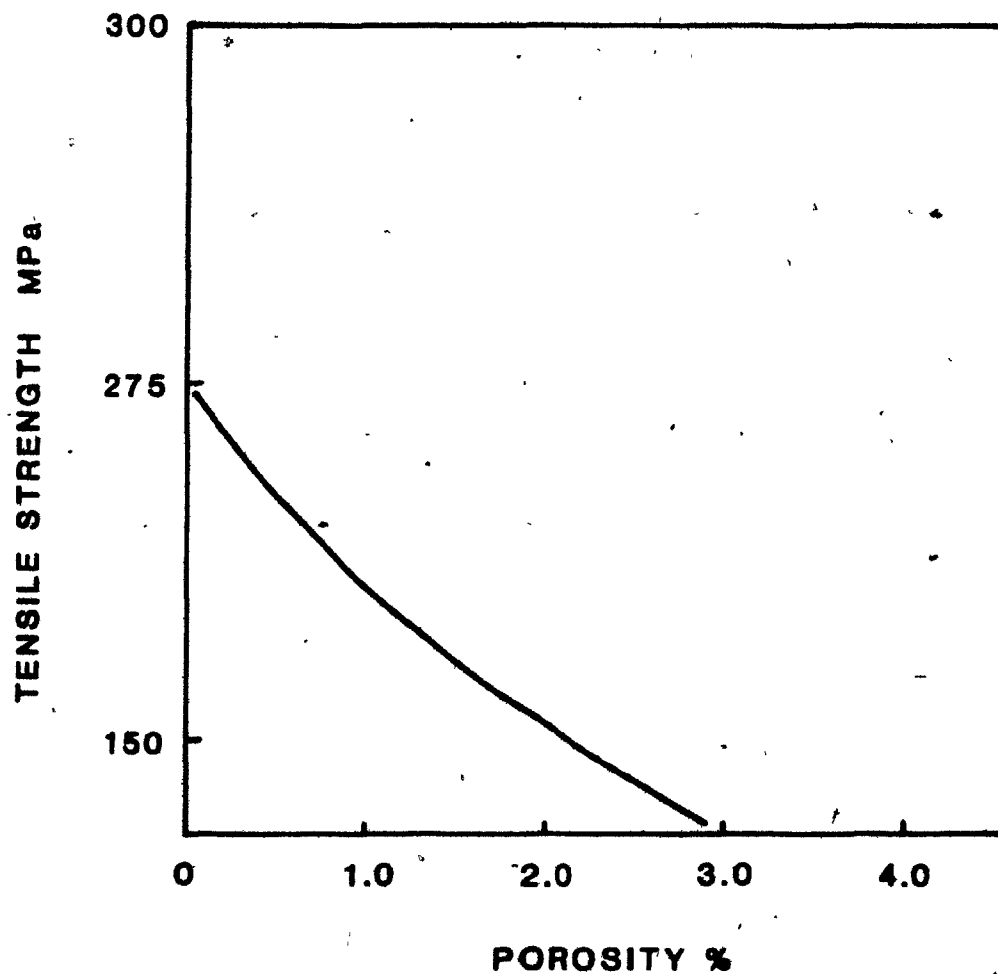


Figure 9⁽¹⁷⁾: Influence of hydrogen porosity on the tensile strength of sand cast bars of Al-5.0% Si alloy

determined simply by using the amount of modifying agent introduced, since dissolution characteristics and loss of the agent vary from one melt to another. In addition, a chemical analysis for the level of modifier present is often inadequate since modification depends on actual solidification rates in the casting as well as the amount of phosphorus present.

1.6.1 Metallography

Metallography is the usual foundry control technique used with modification. It is a direct method with which to examine the structure of a metal involving sampling, grinding, polishing, etching, and microscopic examination. Metallography has the disadvantages that it is expensive, and if performed during the casting process, the sample solidification and examination are time consuming resulting in melt holding costs. Additionally, metallography on the final product may entail destruction of expensive castings.

There has been a significant desire to develop a quick, simple, non-destructive method with which to control the modification process. Possible approaches that have been studied are thermal analysis and electrical resistivity.

1.6.2 Thermal Analysis

Work by Closset et al^(14,15) uses a thermal analysis system (figure 10) consisting of a k-type thermocouple which records the temperature of a cooling Al-Si alloy. The analog signal thus obtained is converted to a digital signal by an electronic board and stored on a floppy disc. The system

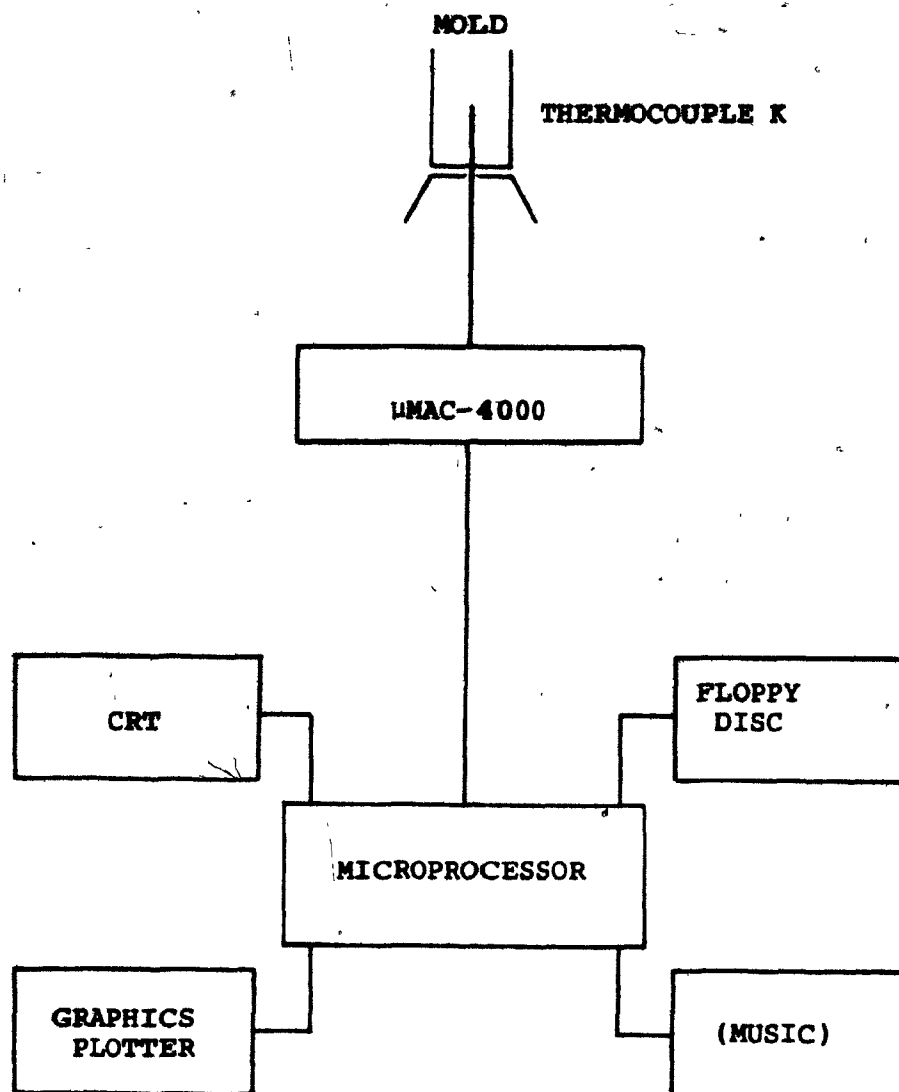


Figure 10⁽¹⁵⁾: Schematic of the system for thermal analysis

5(performs three types of analyses: simple thermal analysis, derived thermal analysis, and total heat of solidification analysis.

Simple thermal analysis can easily be interpreted graphically using a plot of temperature versus time during the phase changes associated with solidification (figure 11). Strontium addition affects only the portion of the curves concerned with the eutectic and solidus transformation, causing a variation in $\Delta\theta$ (the change in the difference between the eutectic growth temperature and the eutectic nucleation temperature). A small strontium addition (0.0022 wt.%) producing an undermodified alloy results in an increase of $\Delta\theta$ from 2.3 C to 4.3 C. At the higher strontium concentrations of the modified alloy, (0.0044 wt.% to 0.0079 wt.%) $\Delta\theta$ decreases to 3.2 C and stabilizes. With further increase in strontium level to 0.018 wt.%, $\Delta\theta$ drops sharply, a characteristic observed with overmodified alloys.

Derived thermal analysis can also be interpreted graphically using a plot of cooling rate versus time during solidification. Figure 12 shows the derived thermal analysis curves and corresponding simple thermal analysis curves for various levels of strontium. The derived curve has a liquidus undercooling peak, S_0 , a binary Al-Si-Mg eutectic undercooling peak S_1 and a ternary eutectic Al-Mg₂Si-Si inflection. With increasing strontium the peak S_1 gradually disappears and there is no further change in the peak S_0 , or ternary eutectic inflection.

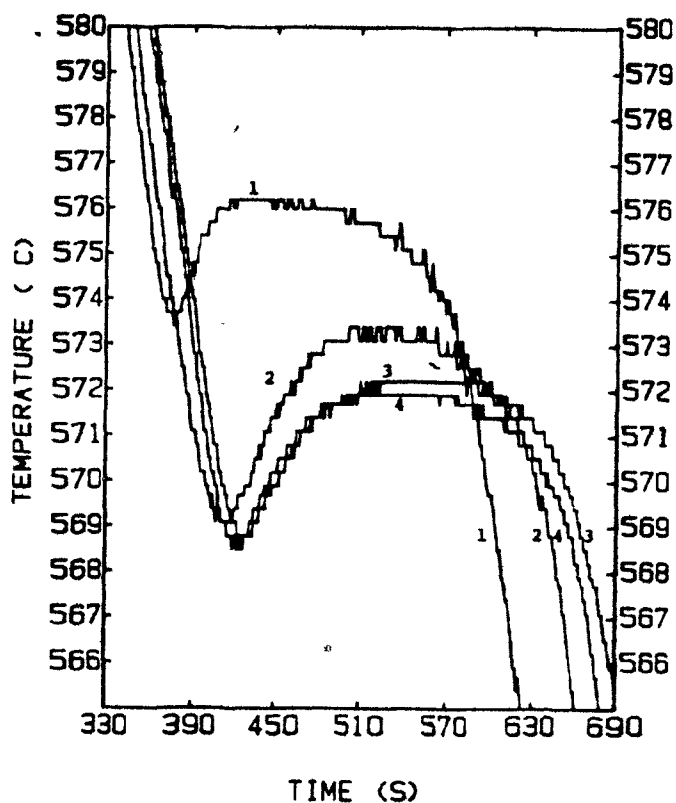
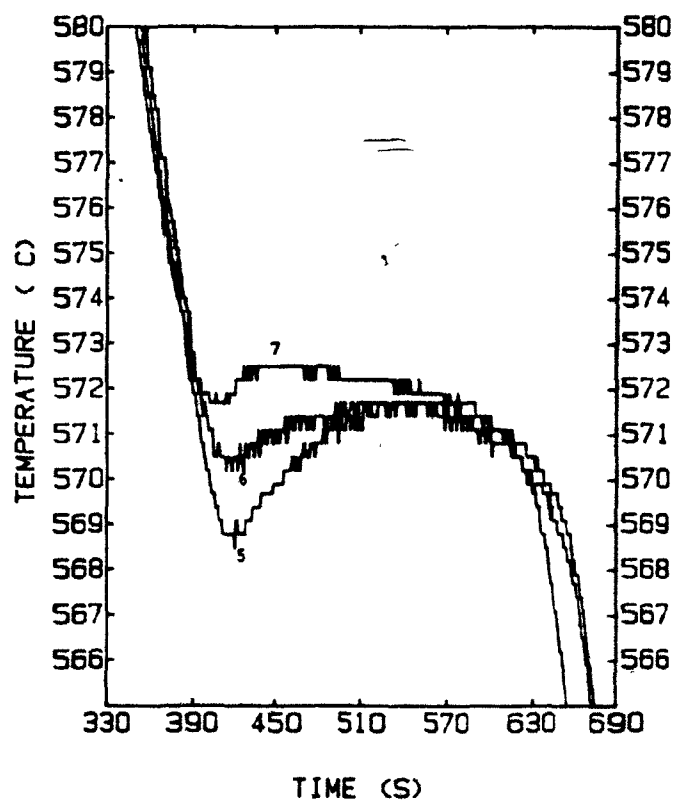


Figure 11

Simple thermal
analysis curves
near eutectic
plateau

- 1) 0.000 wt.% Sr
- 2) 0.002 wt.% Sr
- 3) 0.004 wt.% Sr
- 4) 0.005 wt.% Sr



- 5) 0.008 wt.% Sr
- 6) 0.011 wt.% Sr
- 7) 0.018 wt.% Sr

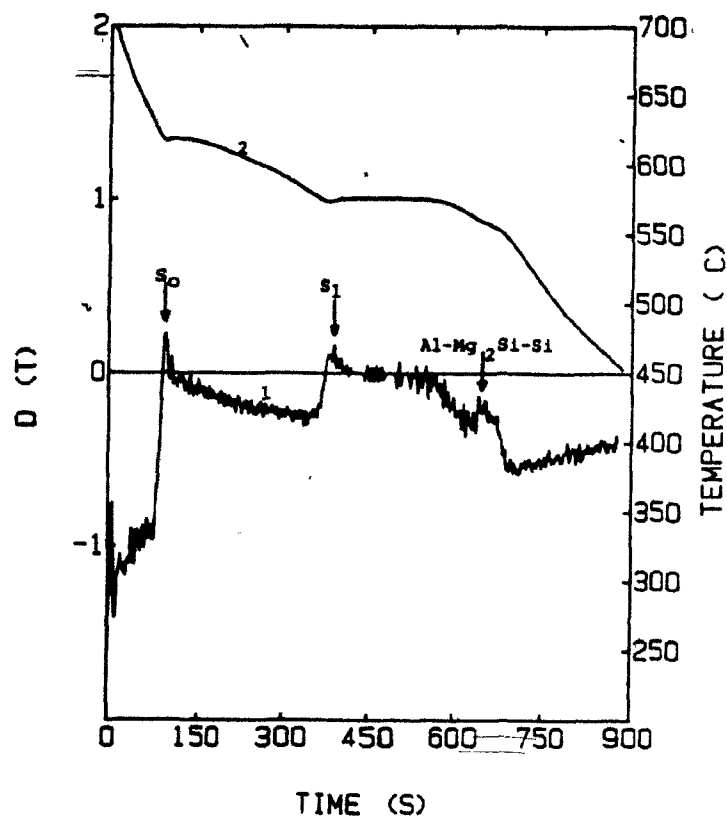
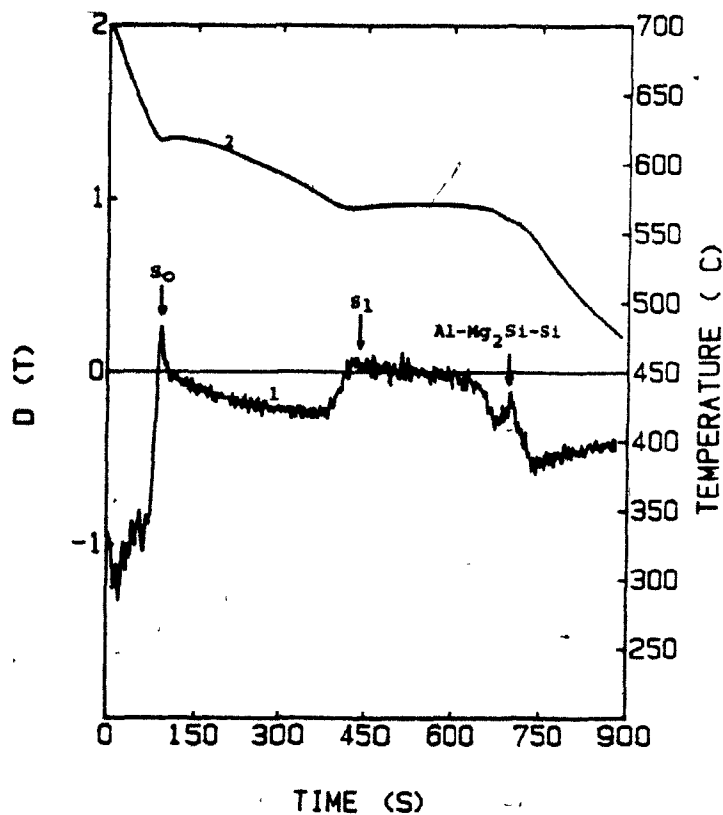


Figure 12

Unmodified alloy
strontium content

0.000 wt.% Sr

- 1) Derived thermal analysis curve
- 2) Simple thermal analysis curve



Modified alloy
strontium content

0.008 wt.% Sr

- 1) Derived thermal analysis curve
- 2) Simple thermal analysis curve

The third technique of thermal analysis involves the calculation of the heat of solidification evolved between the liquidus and the solidus temperatures, using experimental measurements and applying Newtonian heat transfer. The results again can be plotted graphically (figure 13) for various levels of strontium. It can be seen that modification results in the disappearance of the eutectic undercooling peak S_1 and perhaps some sharpening of the ternary eutectic $\text{Al-Mg}_2\text{Si-Si}$ peak. The total heat of solidification, Q_T , can be calculated and is found to increase with increase in strontium concentration (or degree of modification) reaching a maximum for modified melts.

Thermal analysis techniques enable evaluations to be made upon the degree of modification both qualitatively and quantitatively. Qualitatively, the four main states of modification can be determined graphically, and quantitatively, values such as $\Delta\theta$, T_E (the eutectic transformation temperature), T_C (the nucleation temperature), the cooling rate, and Q_T are characteristics which define modification.

1.6.3 Electrical Resistivity

Electrical resistivity is defined⁽¹⁶⁾ as "a characteristic proportionality factor equal to the resistance of a centimeter cube of a substance to the passage of an electric current perpendicular to two parallel faces" and is a measure of the ability of an electric current, or the movement of electrons to flow through a material. The resistivity of a metal is the sum of the resistivities caused by various defects;

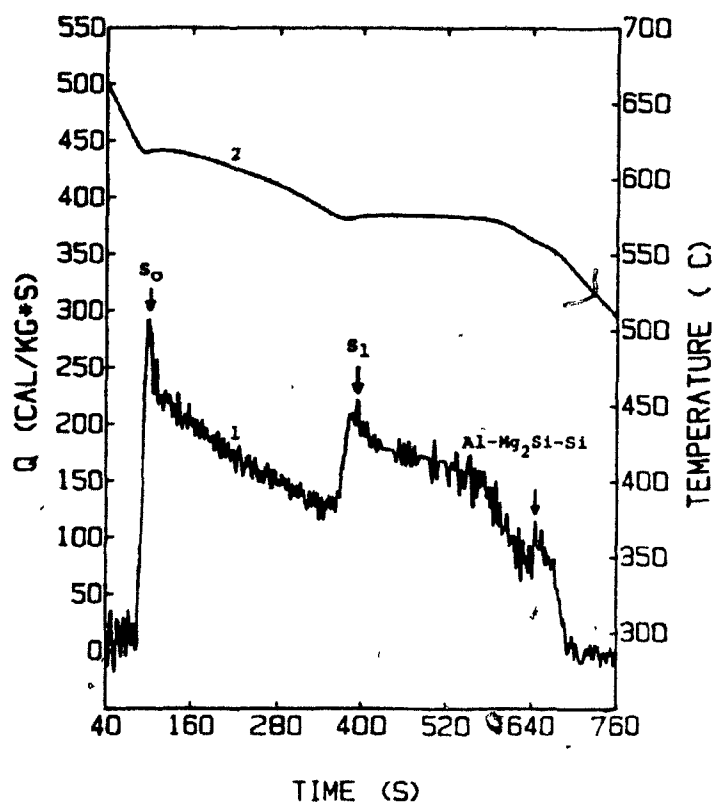


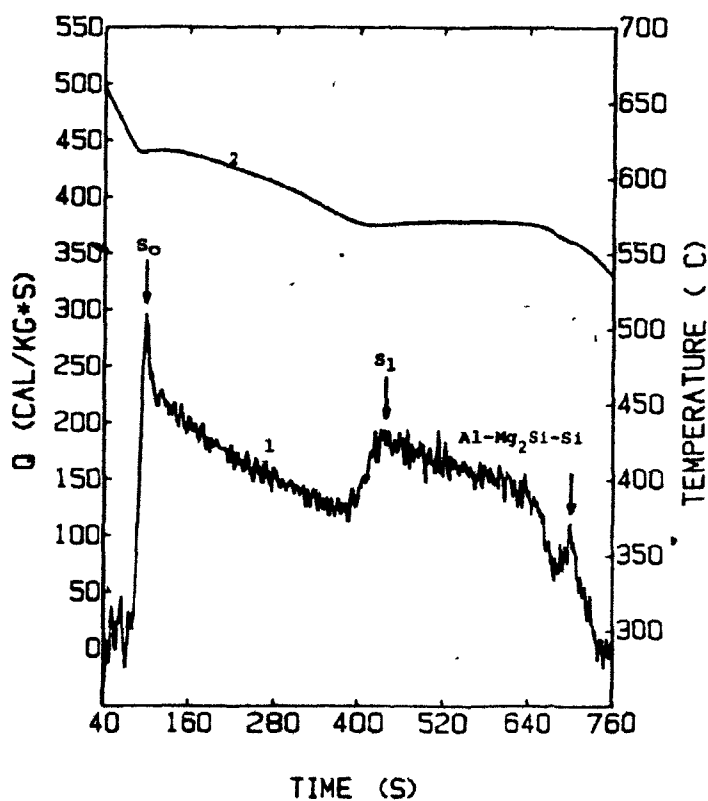
Figure 13

Unmodified alloy
strontium content

0.000 wt.% Sr

1) Total heat of
solidification
curve

2) Simple thermal
analysis curve



Modified alloy
strontium content

0.008 wt.% Sr

1) Total heat of
solidification
curve

2) Simple thermal
analysis curve

$$\rho(T) = \rho_T + \rho_I + \rho_E + \rho_D + \rho_{GB} \quad (\text{n}\Omega.\text{m}) \quad (1)$$

where $\rho(T)$ = the resistivity at a particular temperature

ρ_T = the temperature-dependent resistivity

ρ_I = resistivity due to impurity atoms

ρ_E = resistivity due to eutectic phase (if present)

ρ_D = resistivity due to dislocations and vacancies

and ρ_{GB} = the resistivity due to scattering by grain boundaries.

Alternatively, the resistivity of a metal can be expressed as;

$$\rho = R (A/l) \quad (\text{n}\Omega.\text{m}) \quad (2)$$

where R is the resistance of a uniform conductor, l is its length, A its cross section and ρ its resistivity.

One simple method of measuring resistivity employs equation (2). A D.C. current (I) can be passed through a sample and the potential drop (V) between two fixed points recorded. The resistance R of the metal is then given by:

$$R = \frac{V}{I}$$

The principle disadvantage of this technique is that the final resistivity measurement is the sum of the various resistivities given in equation (1) and yields no information about the effect of a single factor upon the total resistivity.

A differential method, however, developed by Drew et al⁽¹⁷⁾ is a comparison technique and can measure changes in individual

resistivity effects. The method uses a standard reference specimen (figure 14) and compares this with the sample under examination. In this way, the effects of resistivity due to factors that are present in both the standard and the sample are eliminated. The technique uses an A.C. current which passes in series through the standard and the sample, and a lock-in amplifier which measures the voltage difference (ΔV *) between the two samples. The relative change in resistivity is then equal to the relative change in voltage:

$$\frac{\Delta \rho}{\rho_s} = \frac{\Delta V}{V_s} \quad (3)$$

where ρ_s is the resistivity of the standard and V_s is the voltage across the standard.

Electrical resistivity has been used in many metallurgical situations because of its sensitivity to microstructure. Early work by Schröder⁽¹⁸⁾ studied the yield phenomena in copper-arsenic alloys, and Cuddy⁽¹⁹⁾ used electrical resistivity to study deformation and recovery of iron at low temperatures. Uses of electrical resistivity in metallurgy have included the temperature dependence of the resistivity of a metal with dislocations⁽²⁰⁾; the study of the stability of intermediate precipitates⁽²¹⁾ in an Al-4.07 wt.% Cu alloy, and the study of lattice defects⁽²²⁾ in deformed iron.

Resistance ratios, the ratio of electrical resistance at room temperature to that at 4.2K have been used⁽²³⁾ widely for

* where $\Delta V = \Delta V_{\text{standard}} - \Delta V_{\text{experimental}}$

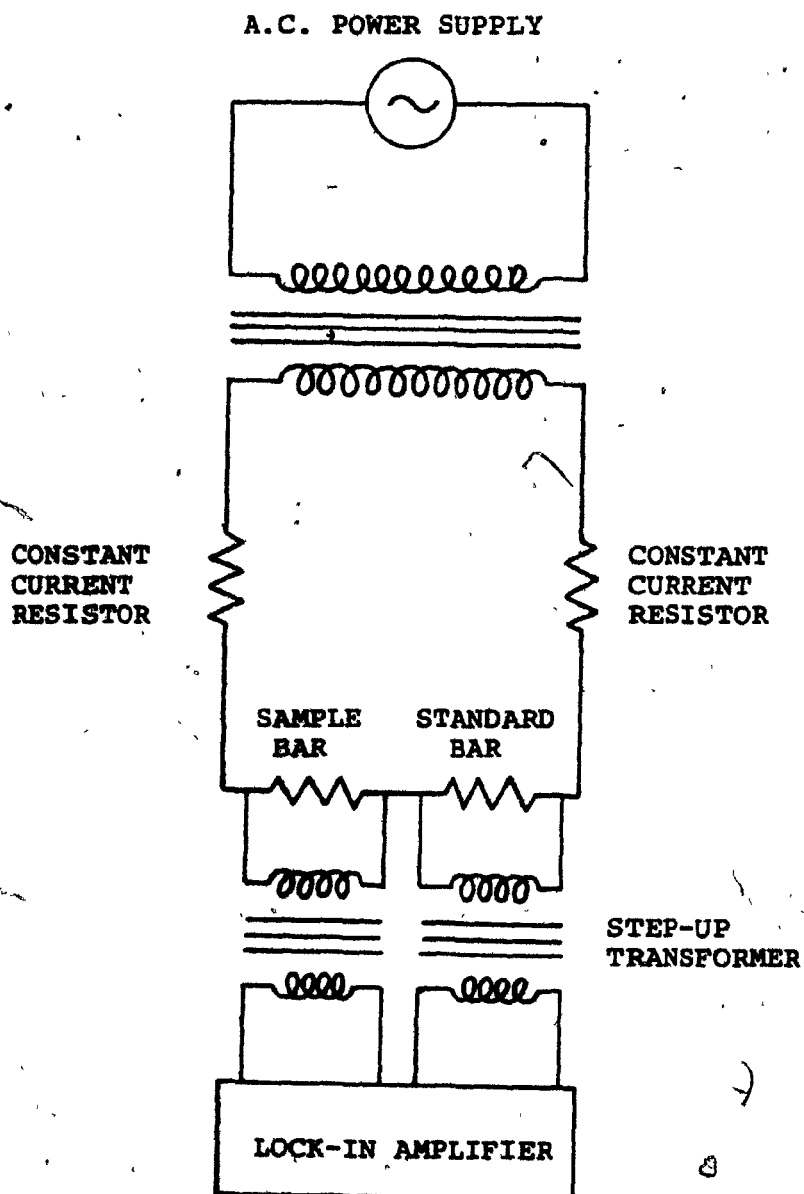


Figure 14 (17): Circuit design for differential resistivity measurement

assessing the ultra purity of a metal. The suitability of a metal for studies of its electronic structure is found with resistance ratios since an impurity that lowers the resistance ratio also obscures the measurement of electronic structure.

With the knowledge of the sensitivity of resistivity to structure, Oger, Closset and Gruzleski⁽¹⁵⁾ worked on electrical resistivity as a method with which to monitor the modification of Al-Si-Mg alloys. Al-Si-Mg alloy bars of constant diameter (D) and various degrees of modification (various % Sr contents) were cast and the resistivity measured by passing a D.C. current (I) through them. The voltage (V) in millivolts was recorded between two points separated by a constant distance, l .

The electrical resistivity ρ was calculated using

$$\rho = \frac{\pi V D^2}{4 I l} \quad (4)$$

Figure 15 shows the electrical circuit used for these D.C. resistivity measurements.

Non-modified bars were found to have a higher resistivity than modified bars, with a resistivity difference of 10% between the two (figure 16)⁽²⁴⁾. The acicular silicon of the unmodified alloy was said to have interfered with current passage through the bar to a greater extent than in the case of the modified alloy with a fibrous eutectic and therefore continuous matrix.

It was also found⁽²⁴⁾ that samples cast from degassed melts had a lower resistivity than those from non-degassed melts (figure 16); for example the electrical resistivity

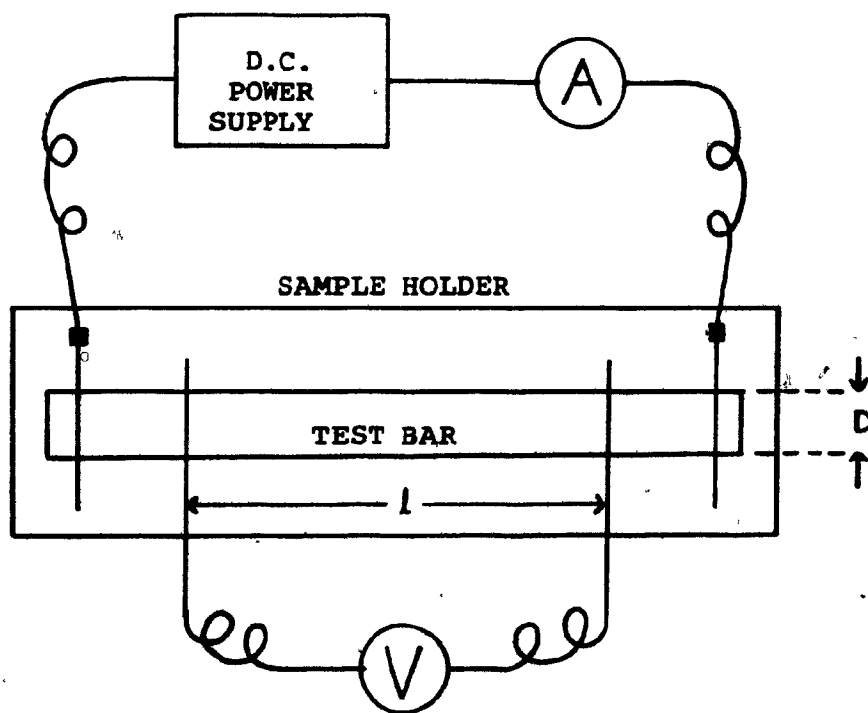


Figure 15⁽¹⁵⁾: Schematic of the apparatus used in D.C. electrical resistivity measurement by Oger, Closset and Gruzleski

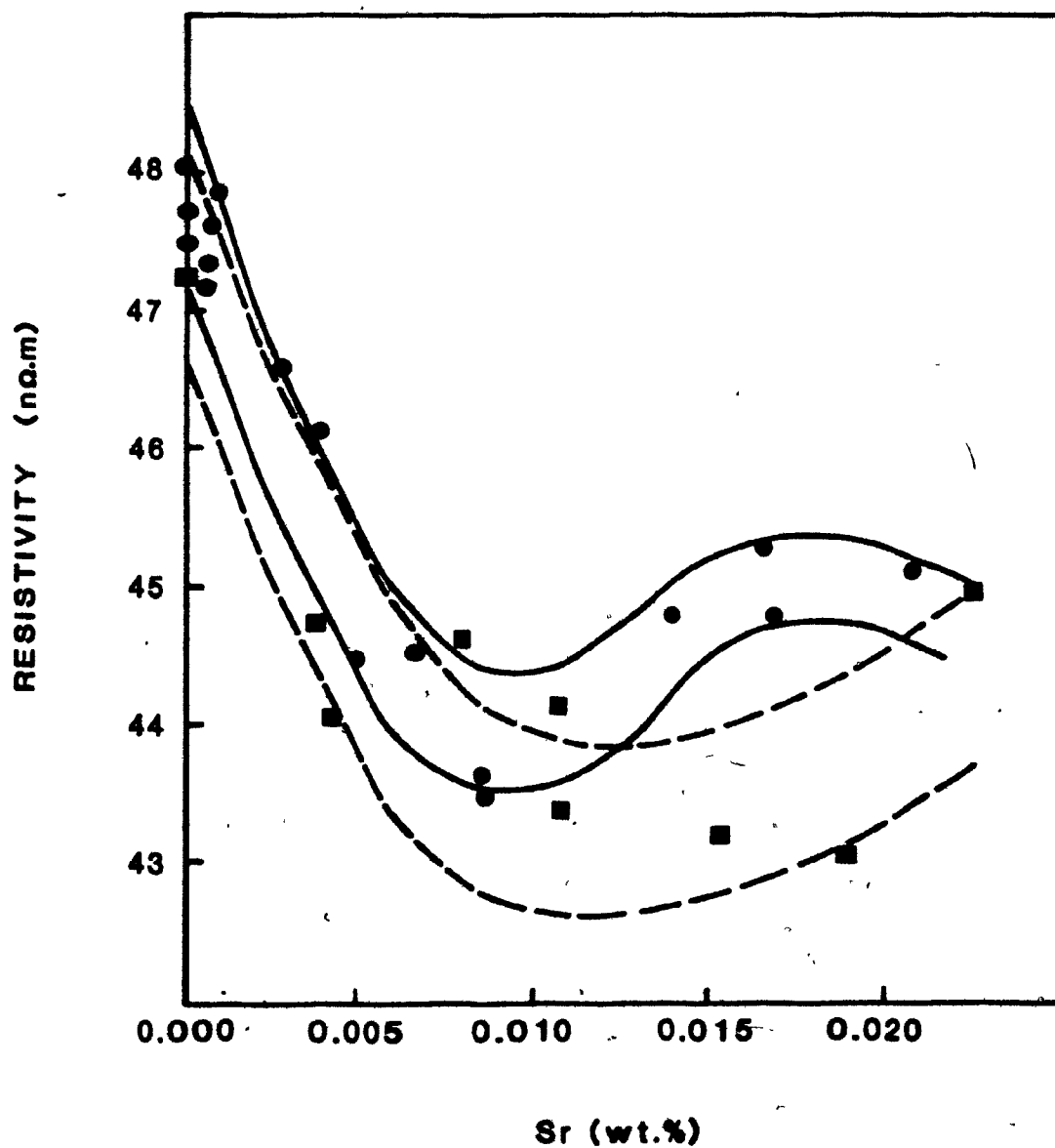


Figure 16 (24): Variation of electrical resistivity with strontium content. Separate test bars

—●— non-degassed melts
---■--- degassed melts

varied from 49 nΩ.m to 44 nΩ.m for non degassed melts, and from 47 nΩ.m to 43 nΩ.m for degassed melts. The difference in electrical resistivity was assumed to be due to hydrogen porosity. Upon solidification, the dissolved atomic hydrogen in a melt will recombine to form bubbles and eventually voids in the solidified metal. A non degassed melt will contain more dissolved hydrogen than a degassed melt and therefore a casting from a non degassed melt will contain more voids than a casting from a degassed melt. It is the voids in the solidified casting that cause the electrical resistivity to increase because they increase impedance to electron flow.

Heat treatment performed⁽¹⁵⁾ on cast bars indicated that coalescence of eutectic silicon during solution treatment produces a 3% increase in electrical resistivity, and that the aging treatment produces a subsequent 5% decrease. The electrical resistivity therefore decreases by 2% after the complete heat treatment cycle. The solution treatment times for these experiments were varied and no change in electrical resistivity was found.

The influence of composition on resistivity⁽¹⁵⁾ was also studied, (figure 17). The results show that magnesium does not significantly affect the electrical resistivity and the authors stated that the principle cause of electrical resistivity changes is the modification of the eutectic microstructure.

1.7 Aims of the Present Investigation

As discussed previously, electrical resistivity has been used⁽¹⁵⁾ in one instance, to study the modification of Al-Si-Mg

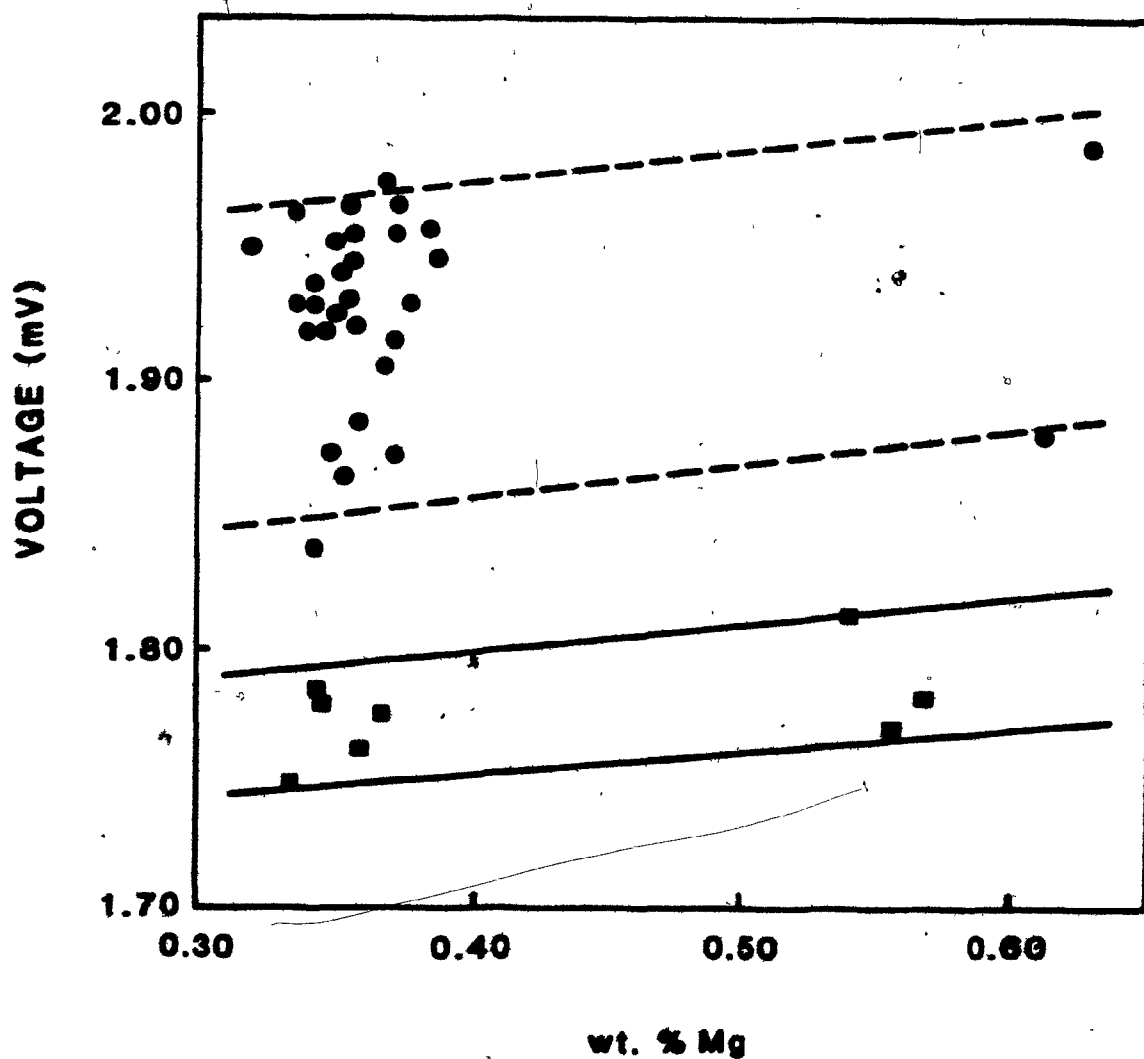


Figure 17⁽¹⁵⁾: Variation of electrical resistivity (voltage) with magnesium content

- melts modified
- melts unmodified

alloys; however, this work was not extensive. It is known that modified alloys have a lower resistivity than unmodified alloys and the reason has been speculatively attributed to a change in the form of the eutectic silicon from acicular to fibrous. This work has also shown porosity to be a contributing factor in the resistivity. However, no evidence was given as to whether porosity varied with strontium content and whether in fact the changes in resistivity with variations in strontium were due to changes in porosity. The resistivity results obtained were scattered and no attempt was made to determine whether this scatter was due to the apparatus or due to other inherent factors. Work^(10,15) has been carried out on the effects of magnesium and iron upon modification and mechanical properties, however no extensive electrical resistivity measurements have been made on these alloys, and resistivity has not been used to examine modification or heat treatment of these alloys.

This study was therefore undertaken with the general objective of developing the electrical resistivity technique and of studying its feasibility for use in foundry situations.

More specifically, the following questions were to be answered:

1. - Is the change in resistivity between modified and unmodified Al-Si-Mg alloys due to the change in the form of the eutectic silicon or due to some other change such as composition of the aluminum matrix?

2. To what degree does resistivity due to porosity affect the resistivity measurements, and is the resistivity of the Al-Si-Mg alloy due primarily to porosity or microstructure?
3. Are the inaccuracies observed in the results by Closset and Gruzleski⁽¹⁵⁾ due to poor apparatus or sample variation, and does differential electrical resistivity yield more accurate results?
4. Can electrical resistivity techniques be used to study compositional influences at various levels of modification?
5. Can the electrical resistivity technique be used to study heat treatment of Al-Si-Mg alloys at various levels of modification?

2. EXPERIMENTAL PROCEDURES

2.1 Parameters and Variables

In order to study modification using electrical resistivity techniques, a number of A356 alloy bars were cast with different strontium levels. Their D.C. resistivity was then measured. An alternative method using differential A.C. resistivity was also employed to try to reduce the scatter in results obtained with the D.C. technique. This differential method works on the principle that the standard bar and sample are of the same dimensions, however due to machining tolerances this was not the case. Statistical analyses were performed on the results and only bars within a specified diameter range were used.

Three heat treatments differing only in solution treatment time were performed and resistivity measurements were taken after solution treatment and after complete heat treatment. The effects of solution treatment time were studied on the resistivity behaviour of both unmodified and modified bars.

The above procedure was performed on three alloys:

- i, A356 (composition shown in table I)
- ii, A357 (A356 alloy containing 0.7 wt.% Mg)
- iii, A356 containing 0.48 wt.% Fe.

In order to find the effects of compositional changes on resistivity. Magnesium and iron were varied because they are common elements in aluminum alloys with a relatively wide range of permissible composition.

In order to gain an insight into the scatter observed in both D.C. and A.C. resistivity results, a number of factors that affect resistivity were examined. These include both porosity and temperature. Bar diameter was found to affect the resistivity and therefore experiments were performed to investigate the change in the amount of eutectic present across the diameter of the bar.

The silicon content in the aluminum phase was investigated in samples showing various degrees of modification in order to see if changes in the matrix composition could account for changes in resistivity.

2.2 Statistical Analysis of Results

The experimental data was analysed graphically and the curve with the best fit through the points was found. The analysis was performed using a computer based statistical package programme and the F-test. To simplify the statistical analysis explanation, the correlation between strontium content and D.C. resistivity is discussed. The F-test was performed on the data for six possible types of curve, that is, for six degrees of polynomial. Each polynomial was characterised by a particular F value (table VI). The second degree polynomial had the largest F value of 39.0 and was therefore considered to be the most accurate graphical representation of the data (the second degree polynomial was the curve with the best fit through the points).

Degree of Polynomial	F Value
1	9.67
2	39.00
3	34.53
4	25.57
5	20.64
6	18.50

Table VI: Statistical results of the strontium content vs. D.C. resistivity data

In order to determine the validity of the F value (39.0) for the second degree polynomial, the F value is compared with F values in a 95% significance table (table VII)⁽²⁵⁾. The horizontal and vertical axis of this table represent the number of degrees of freedom in the statistical analysis and these degrees of freedom can be found from the computer read out. In the case of the strontium content versus D.C. resistivity data, these degrees of freedom are 2 and 23 for the horizontal and vertical axes respectively. The degrees of freedom are used to find the table F values for 95% significance level. The experimental F value, 39.0, is greater than the F value from tables, 3.42, which means that over 95% of the results are significant. This 95% significance level allows no more than 5% of the results to be accounted for in terms of experimental error, and is therefore a satisfactory concept when dealing with experimental data.

The F-test can be used to compare the graphical representations of two sets of data. The set of data exhibiting the highest F value will have the curve with the least amount of scatter between the points.


2.3 Foundry Procedure and Sample Preparation

2.3.1 The Pattern and Sand Mould

The casting procedure employed was sand casting. The pattern was designed to obtain four cylindrical bars

F_1	1	<u>2</u>	3	4	5	6	7	8	9	10	12	15	20	24	30
F_2															
1	160-45	100-00	210-71	220-00	220-10	220-00	220-77	220-00	240-04	240-00	240-01	240-05	240-01	240-05	240-10
2	10-01	10-00	10-10	10-20	10-20	10-20	10-25	10-27	10-20	10-40	10-41	10-43	10-45	10-45	10-45
3	10-13	0-05	0-20	0-12	0-01	0-04	0-00	0-05	0-01	0-70	0-74	0-70	0-60	0-04	0-02
4	7-71	0-04	0-00	0-20	0-20	0-10	0-00	0-04	0-00	0-00	0-01	0-05	0-00	0-77	0-75
5	0-01	0-70	0-41	0-10	0-05	0-05	0-00	0-02	0-77	0-74	0-00	0-02	0-00	0-02	0-00
6	0-00	0-14	0-70	0-03	0-30	0-20	0-21	0-15	0-10	0-00	0-00	0-04	0-07	0-04	0-01
7	0-00	0-74	0-35	0-12	0-07	0-07	0-70	0-73	0-00	0-04	0-07	0-01	0-04	0-41	0-20
8	0-02	0-40	0-07	0-04	0-00	0-00	0-00	0-44	0-30	0-35	0-20	0-22	0-15	0-12	0-00
9	0-12	0-20	0-00	0-03	0-40	0-37	0-20	0-23	0-10	0-14	0-07	0-01	0-04	0-00	0-05
10	0-00	0-10	0-71	0-40	0-33	0-22	0-14	0-07	0-02	0-00	0-01	0-04	0-77	0-74	0-70
11	0-04	0-00	0-00	0-30	0-20	0-00	0-01	0-05	0-00	0-05	0-70	0-72	0-05	0-01	0-07
12	0-75	0-00	0-40	0-25	0-11	0-00	0-01	0-05	0-00	0-75	0-00	0-02	0-04	0-01	0-07
13	0-07	0-01	0-41	0-10	0-00	0-02	0-03	0-77	0-71	0-07	0-00	0-03	0-40	0-42	0-20
14	0-00	0-74	0-34	0-11	0-00	0-05	0-70	0-70	0-00	0-00	0-03	0-40	0-20	0-20	0-21
15	0-04	0-00	0-20	0-00	0-00	0-70	0-71	0-04	0-00	0-04	0-40	0-40	0-33	0-20	0-20
16	0-40	0-03	0-24	0-01	0-05	0-74	0-00	0-00	0-04	0-40	0-42	0-30	0-20	0-24	0-10
17	0-40	0-00	0-20	0-00	0-01	0-70	0-01	0-00	0-40	0-40	0-30	0-31	0-23	0-10	0-10
18	0-41	0-00	0-10	0-03	0-77	0-00	0-00	0-01	0-40	0-41	0-34	0-27	0-10	0-10	0-11
19	0-30	0-02	0-13	0-00	0-74	0-03	0-04	0-40	0-42	0-30	0-31	0-23	0-10	0-11	0-07
20	0-25	0-40	0-10	0-07	0-71	0-00	0-01	0-40	0-40	0-30	0-30	0-20	0-12	0-00	0-04
21	0-32	0-47	0-07	0-04	0-00	0-07	0-40	0-42	0-37	0-32	0-25	0-10	0-10	0-05	0-01
22	0-30	0-44	0-05	0-02	0-00	0-05	0-40	0-40	0-34	0-30	0-23	0-15	0-07	0-03	0-00
<u>23</u>	0-20	<u>0-42</u>	0-03	0-00	0-04	0-03	0-44	0-37	0-32	0-27	0-20	0-13	0-05	0-01	0-00
24	0-20	0-40	0-01	0-70	0-02	0-01	0-42	0-30	0-30	0-25	0-10	0-11	0-03	0-00	0-04
25	0-24	0-30	0-00	0-70	0-00	0-40	0-40	0-34	0-20	0-24	0-10	0-00	0-01	0-00	0-02
26	0-23	0-37	0-00	0-74	0-00	0-47	0-30	0-32	0-27	0-22	0-15	0-07	0-00	0-00	0-00
27	0-21	0-30	0-00	0-73	0-07	0-40	0-37	0-31	0-25	0-20	0-13	0-00	0-07	0-03	0-00
28	0-20	0-34	0-00	0-71	0-00	0-40	0-30	0-20	0-24	0-10	0-12	0-04	0-00	0-01	0-07
29	0-10	0-33	0-00	0-70	0-05	0-43	0-30	0-20	0-22	0-10	0-10	0-03	0-04	0-00	0-00
30	0-17	0-32	0-02	0-60	0-03	0-42	0-33	0-27	0-21	0-16	0-00	0-01	0-03	0-00	0-04
40	0-00	0-23	0-04	0-01	0-40	0-34	0-25	0-10	0-12	0-00	0-00	0-02	0-04	0-70	0-74
60	0-00	0-15	0-70	0-03	0-37	0-25	0-17	0-10	0-04	0-00	0-02	0-04	0-75	0-70	0-00
100	0-00	0-07	0-00	0-40	0-20	0-10	0-00	0-00	0-00	0-00	0-00	0-75	0-00	0-01	0-00
∞	0-04	0-00	0-00	0-27	0-27	0-10	0-01	0-00	0-00	0-00	0-75	0-07	0-07	0-02	0-40

Table VII: F tables for 95% significance level. The outlined numbers refer to the text on statistical analysis of D.C. resistivity vs. strontium content



each approximately 16 cm in length and 2 cm in diameter. Figure 18 shows one of the castings with the gating and riser systems attached. Four bars were incorporated into each casting in order to obtain repeat samples and in order to provide sufficient samples for various heat treatments.

An oil bonded (Petro Bond) silica sand was used, and mixing was done in a standard sand mixer. An iron flask was used to make the mould.

2.3.3 Melting and Strontium Addition

The A356 alloy was melted in a gas fired furnace in a silicon carbide crucible (depth 22 cm, diameter 14 cm). The melt temperature was monitored using a chromel-alumel K type thermocouple. A calculated weight of strontium was cut from an extruded 99% pure strontium bar, wrapped in aluminum foil and introduced into the melt at temperatures between 730 C and 750 C using a graphite plunger (figure 19). Dissolution took approximately 15 minutes. The final strontium contents of the various melts ranged from 0.0 wt.% Sr to 0.068 wt.% Sr. De-gassing was performed after every strontium and alloying addition by bubbling 1.75 litres per minute of Argon through the melt, using a graphite lance, for twenty minutes. Spectrometer samples were taken from the melt using a ladle and cast in a standard copper mold (figure 20). Each melt was finally poured at temperatures of 725 C to 730 C.

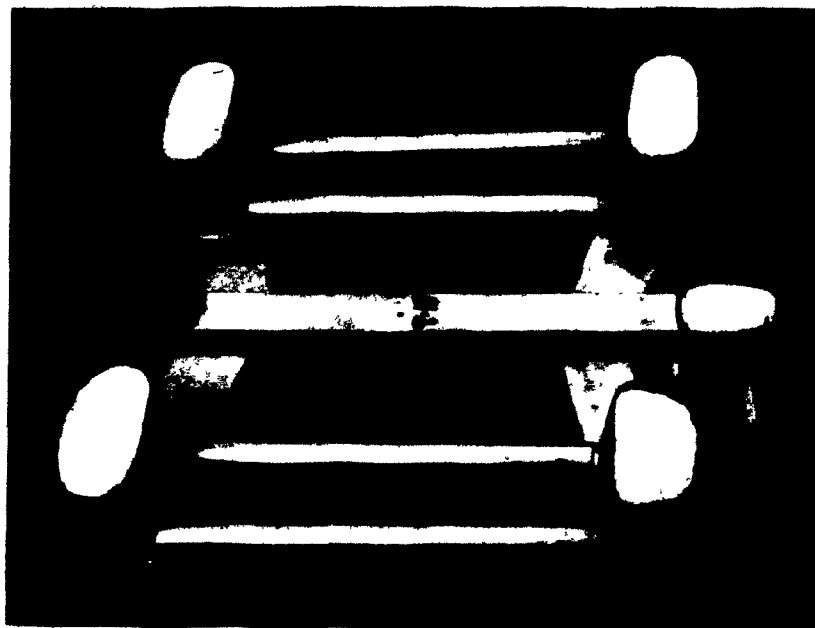


Figure 18: An Al-Si-Mg alloy casting showing the four test bars with the risers and gating system.



Figure 19: Graphite plunger used for strontium additions



Figure 20: Copper mould used for casting spectrometer samples

2.3.3 Alloy Additions

The two alloying agents used were magnesium and iron. Calculated weights of pure magnesium (99.9% pure) were added to increase the 0.35 wt.% Mg content of the A356 alloy, producing an A357 alloy containing 0.7 wt.% Mg. The magnesium was added in the form of rods (figure 21) (diameter 5 mm) to the surface of the melt at a temperature of 730 C.

Iron additions were also made at 730 C in the form of compressed powder pellets (figure 21) containing 25% aluminum powder (100 mesh) and 75% iron powder (100 mesh electrolytic 99+ % pure, or 20.3 mesh, granular). No difference in dissolution behaviour was found between the two different iron powders. Calculated weights of pellets were used in order to increase the 0.2 wt.% Fe content of the A356 alloy to 0.48 wt.% Fe.

2.3.4 Bar Preparation

The risers and gating systems were cut off the castings leaving the bars. Metallographic samples were taken from the ends of the bars. The bars were then machined and sanded to a smooth surface finish to produce a dimensionally uniform bar.

2.3.5 Spectrochemical Analysis

The spectrochemical samples cast in the copper mould were disc-like and measured approximately 1.5 cm in height and 4 cm in diameter. They were machined to obtain a flat smooth surface for analysis in a vacuum emission spectrometer (Baird-Atomic Spectrovac 1000 Model No. DV2) equipped with a micro-

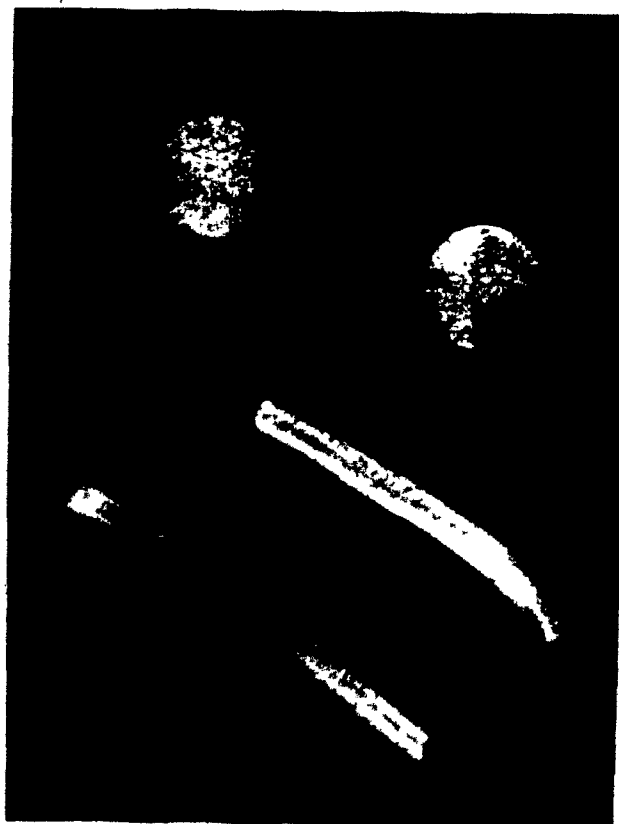


Figure 21: The magnesium rod and iron powder pellets used for alloying the Al-Si-Mg melts

computer (Baird-Atomic Spectrocamp System Model No. SCE-14). Aluminum-strontium standards were used to obtain calibration curves and the samples were analysed for the main elements strontium, iron, magnesium and the impurities (copper, nickel, etc.). Results of these analyses are given in appendix 1.

2.3.6 Metallography

For metallographic analysis transverse slices were cut from the 4 bars in each casting and mounted in a cold resin mount or a bakelite mount for polishing and grinding. Rough grinding was done using a standard silicon-carbide belt grinder and fine grinding was done on a series of grinding wheels of grit 240, 320, 400 and 600 in that order, using water as the flow medium. Subsequent polishing was performed on two polishing wheels using metron polishing cloth and alumina powder suspended in water as the polishing agent; 5 μ m and 0.3 μ m powder was used for rough and fine polishing respectively. After polishing, the samples were cleaned in alcohol and dried. The A 356 alloy samples were not etched, while the A357 and A356 (0.48 wt.% Fe) alloy samples were etched in 0.5% HF solution to darken the magnesium and iron intermetallics.

A Neophot microscope (Leco Model No. 21) was used to examine the polished samples at a magnification of X200. This magnification proved to be sufficiently high to examine the morphology of the eutectic yet sufficiently low to encompass a representative area of the eutectic and primary phases.

2.4 Electrical Resistivity Measurement

2.4.1 D.C. Resistivity Measurement

The electrical circuit used in D.C. resistivity measurement (figure 22) consisted of a Kepco generator capable of passing a 40 Amp current through a bar using crocodile clips as electrical contacts. The bar was placed in a jig (figure 23) consisting of two knife edge contacts which touched the bar 10.03 cm apart. These two knife edges were connected to a voltmeter. In order to obtain a representative resistivity result the voltage was read for three different bar positions between the knife edges, using forward as well as reversed current. The resistivity was calculated using the average of the six voltage readings and an average of three bar diameter readings, (measured with a micrometer screw gauge).

2.4.2 A.C. Resistivity Measurement

A.C. resistivity measurement, was done using an F-41 signal generator in combination with a Kikusui bipolar power supply (Model No. POW 35-S) which passed an A.C. current of 1 Amp and frequency 135 Hz through a standard bar (A) and sample bar (B) in series (figure 24). The ballast resistor served as a means to reduce the voltage in the circuit so that small voltage differences between A and B could be accurately detected. The voltmeter was used to check the current periodically. The step-up transformers increased the voltage across the bars so that the lock-in amplifier could be used to read the voltage differences. Figure 25 shows the A.C. electrical circuit.

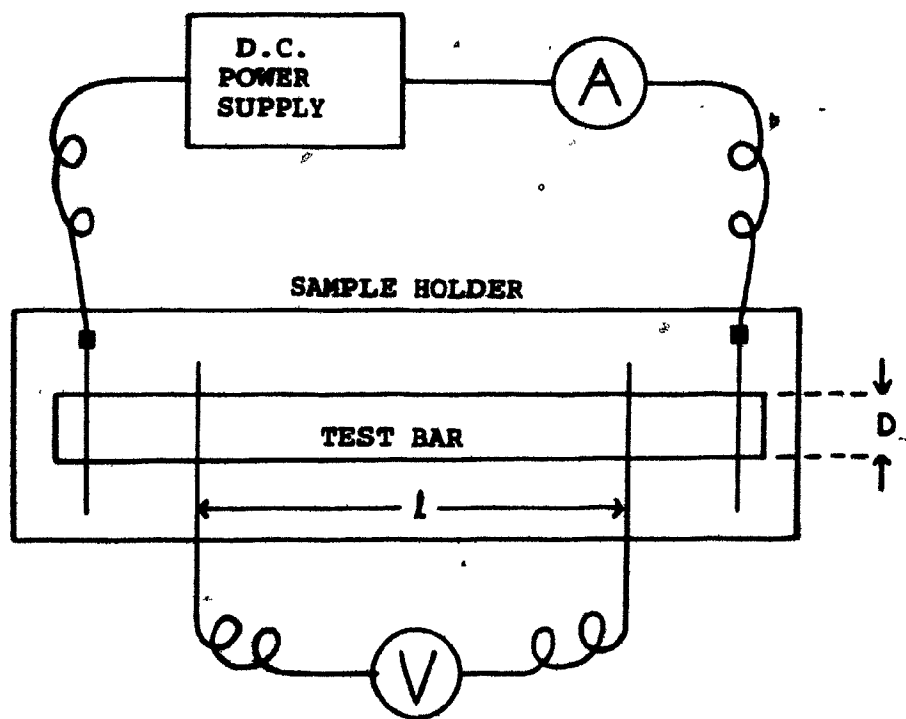


Figure 22: Apparatus for D.C. resistivity measurement

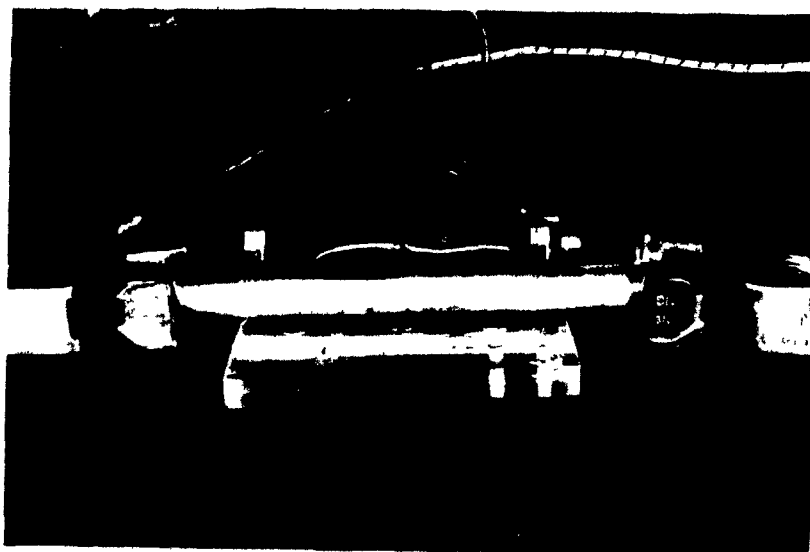


Figure 23: The jig used to hold the Al-Si-Mg test bars in D.C. electrical resistivity measurement

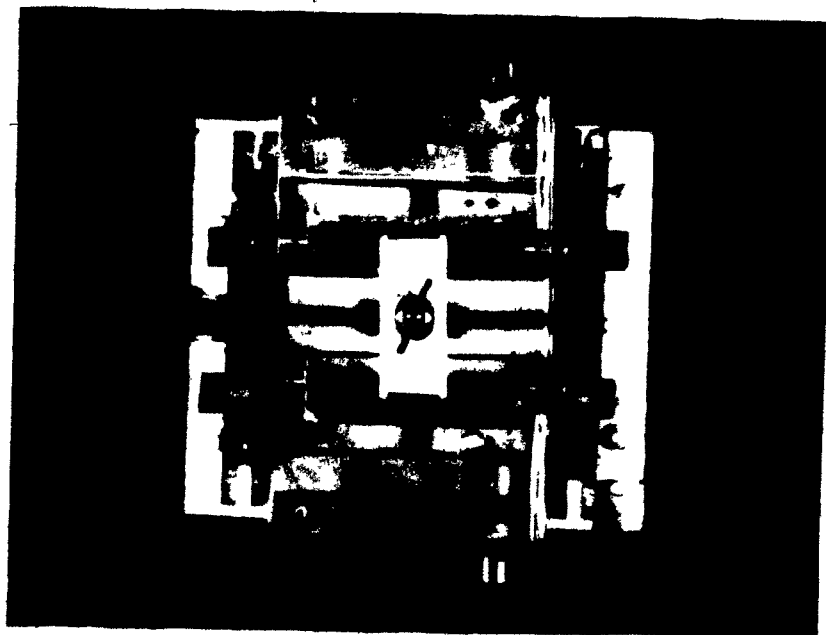


Figure 24: The jig used in A.C. resistivity measurement

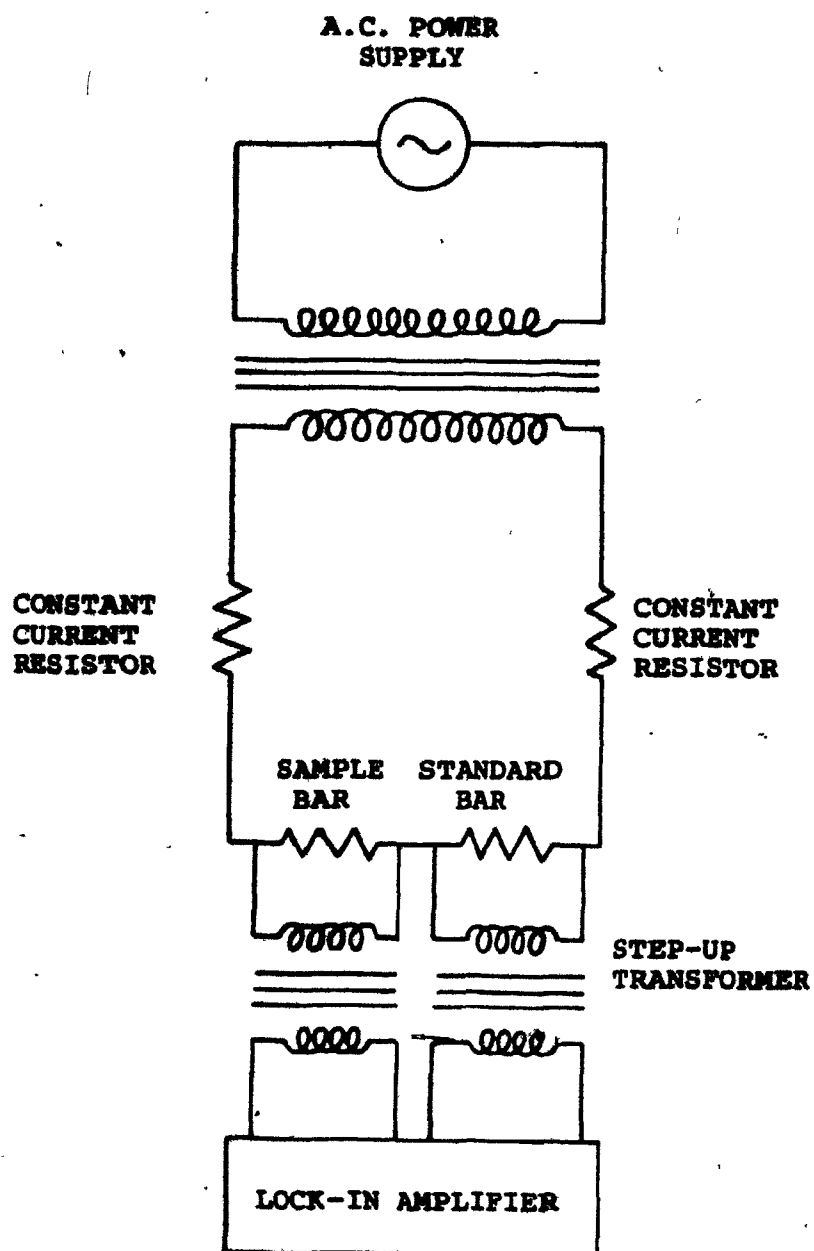


Figure 25: Circuit design for differential resistivity measurement

In all measurements the same unmodified, unheat-treated standard was used so that valid result comparisons could be made.

Since the A.C. technique is a comparison method it requires the bars to be of the same diameter. All bars were therefore machined, however the unavoidable machining tolerances gave bar diameters ranging from 15.17 mm to 15.35 mm. This 0.18 mm maximum bar diameter difference (δD) that could be exhibited between the standard and sample bars would introduce an error on ΔV of ± 0.212 mV (Appendix 2). In order to reduce this error, the bars were grouped into three diameter ranges.

Range A ; 15.17 mm to 15.35 mm ($\delta D = 0.18$ mm)

B ; 15.22 mm to 15.31 mm ($\delta D = 0.09$ mm)

C ; 15.25 mm to 15.29 mm ($\delta D = 0.04$ mm)

Three graphs were produced of ΔV versus strontium content for the A356 alloy. The first used bars within range A (130 bars), the second used bars within range B (80 bars) and the third used bars within range C (52 bars).

Although range C exhibits the greatest accuracy in terms of diameter, the resistivity values were only the average values of a small number of bars. Statistical analyses, i.e. F tests, were therefore performed on the three graphs to determine which gave the most accurate graphical representation of the data, that is, which diameter range yielded the graph with the least amount of scatter between the points.

2.5 The Factors Affecting Resistivity

In order to gain an insight into the scatter observed in both D.C. and A.C. resistivity results, a number of factors that affect resistivity were examined such as temperature and porosity. During the course of experiments it was found that resistivity was affected by bar diameter. Factors such as percent eutectic that could vary with bar diameter were therefore studied. The silicon content in the aluminum phase was also investigated in bars having various degrees of modification.

2.5.1 Temperature

D.C. and A.C. resistivity measurements were performed on A356 bars at various temperatures from -10 C to 24 C (room temperature). The resistivity jigs were placed in an insulated box (figure 26) on a mesh stand under which was placed dry ice. A T-type thermocouple (copper-constantin) was placed through the box wall and attached to one of the bars. Resistivity measurements were recorded when the temperature was at a steady -10 C. The lid of the box was then removed and the apparatus allowed to warm up. Further measurements were taken at 0 C and 24 C. The standard used for the A.C. technique was an unmodified A356 bar.

2.5.2 Porosity

A density technique was used to measure the amount of porosity in each sample bar. This technique allows the evaluation of porosity in volume percent by comparison of theoreti-

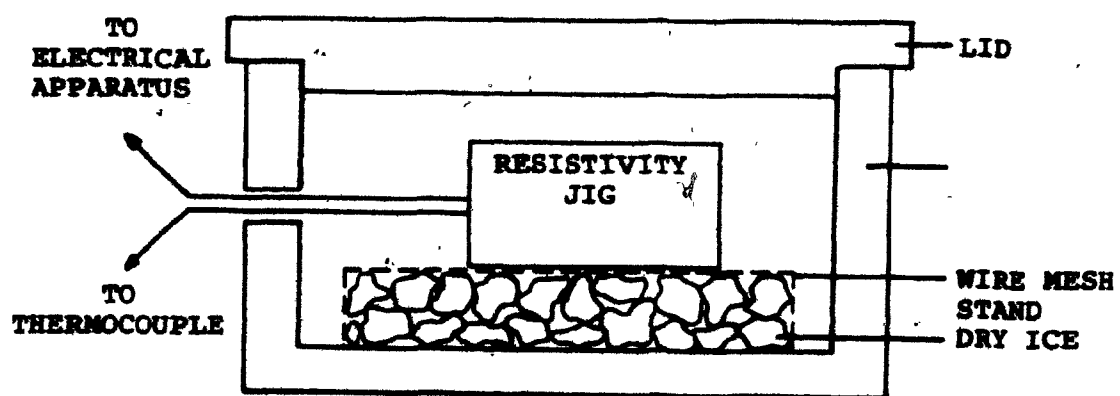


Figure 26: Apparatus used to measure resistivity at various temperatures

cal and experimental density. The experimental density was determined using Archimedes' Principle where the mass of a bar in air was compared with the mass of the same bar in another medium of known density (e.g. water, which was used in this study). Figure 27 shows the density apparatus used in porosity measurement. A wetting agent of 0.01% teepol was added to the distilled water in which the samples were weighed to minimize any error arising from entrapment of air bubbles on the surface of the sample. A thermometer monitored the temperature of the water so that accurate water density data could be used in the calculations.

To ensure accurate measurements, the density measuring device was calibrated by evaluating the densities of pure aluminum, copper and tin and comparing the results with published values. Table VIII shows that the measured densities agreed to within 0.38% of the published values.

The experimental density of the Al-Si-Mg bars was calculated from experimental results (Appendix 3) and the theoretical density was determined from compositional bar data (Appendix 4). Knowing the experimental and theoretical densities of the bars, the porosity in volume percent was calculated (Appendix 3).

2.5.3 Eutectic Segregation

Experiments were carried out using a Zeiss interactive image analysis system, IBAS 1, semi automatic evaluation unit to measure the variation in amount of eutectic from the centre to the outside of the sample bar. Four positions across the

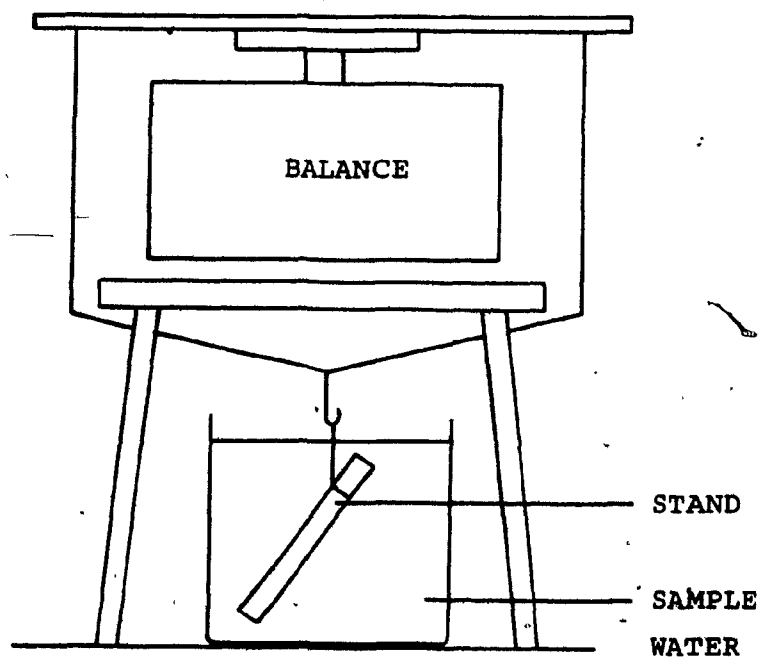


Figure 27: The apparatus used in porosity measurement .

Sample	Experimental Density* gm/cm ³	Reported Density ⁽²⁶⁾ gm/cm ³	Difference between experimental and reported density
Sn	7.29	7.28	0.38
Cu	8.90	8.92	0.23*
Al	2.69	2.70	0.14

* average of 6 measurements on one sample.

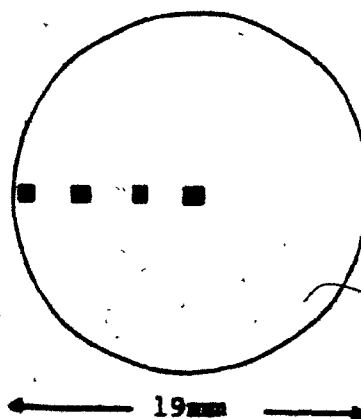
Table VIII: Calibration of density apparatus

diameter of a metallographic sample were chosen (figure 28): the centre, 3.75 mm from the centre, 7.5 mm from the centre, and the edge. At each position three photographs were taken, magnification X200, using a Neophot microscope (Leco Model No. 21). The amount of eutectic in each photograph was measured by drawing around the eutectic areas with a pen (figure 28) on the screen surface of the IBAS 1. The system then calculated the percent eutectic by area. At each position across the sample diameter the results of the three photographs were averaged. The above procedure was performed on three samples of different levels of modification, (unmodified, undermodified, and modified).

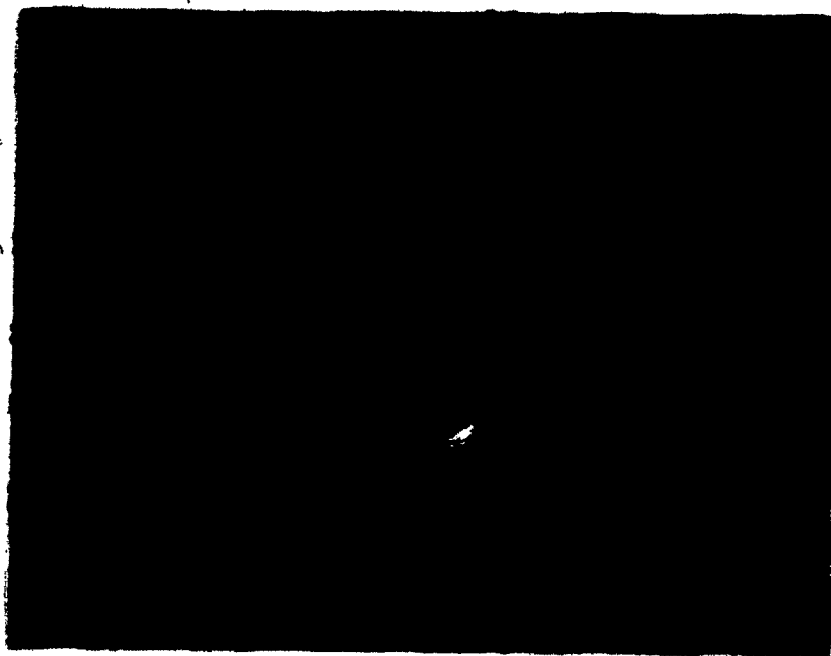
2.5.4 Solute Concentrations

Sections of the bars were cut 2 mm thick and mounted in resin for grinding and polishing (see 2.3.6 Metallography). They were then carbon coated and analysed using an electron microprobe (Cameca Comebax Microbeam system. Model no. MB1) with a 15 KV voltage and a 15 nA current.

Analysis of silicon was performed. Strontium analysis, however, was not possible due to the unavailability of low concentration strontium standards. The analyses could not be carried out in the modified eutectic phase because the eutectic silicon was too finely dispersed. They were therefore carried out in the centre of aluminum dendrites. Spot analyses were performed in the centre of samples with various strontium contents in order to study the variation of solute content with modification.



28a: The positions of analysis
across the diameter of the
bar



(mag x 200)
28b: The eutectic areas outlined in pen

Figure 28: Determination of the amount of
eutectic across the bar diameter

2.6 Heat Treatment

Each of the four bars in each casting was heat treated in a different way as follows;

Bar 1. As-cast, no heat treatment.

Bar 2. Solution treated for 8 hours at 540 C, quenched, aged at room temperature for 24 hours, and aged at 155 C for 12 hours.

Bar 3. Solution treated for 24 hours at 540 C, quenched, aged at room temperature for 24 hours, and aged at 155 C for 12 hours.

Bar 4. Solution treated for 48 hours at 540 C, quenched, aged at room temperature for 24 hours, and aged at 155 C for 12 hours.

For convenience the heat treatments on bars 2, 3 and 4 will be termed heat treatments A, B and C corresponding to 8, 24 and 48 hour solution treatments respectively.

Solution treatment was carried out in a Blue M Power Omatic 80 Furnace (Model No RG-3080 C) and aging in a Griffin-Grundy Furnace (Model No. 661530). In order to test the temperature uniformity of the furnaces, six thermocouples were placed in various positions in the furnaces, (Tables IX and X). The greatest variation in temperature in both furnaces occurred between the back and front, therefore bars were placed centrally in the furnaces, standing vertically in a wire mesh jig (figure 29). A chromel-alumel K-type thermocouple was placed vertically between the central bars in the jig throughout the heat treatments. The bars in the jig were not allowed to touch

Position in furnace	Temperature C
Top	544
Back	548
Left side	537
Bottom	538
Front	530
Right side	536

Table IX: Temperature variations within the Blue M
Power Omatic 80 Furnace (Model No RG-3080 C)

Position in furnace	Temperature C
Top	159
Back	160
Left side	153
Bottom	155
Front	149
Right side	154

Table X: Temperature variations within the Griffin-Grundy Furnace (Model no. 661530)



Figure 29: Cross section of the wire mesh jig used to hold the bars during heat treatment. The jig holds 16 bars.

in order to allow air circulation and therefore uniform heating. Similarly, on quenching the bars in the jig, cooling was rapid and uniform.

D.C. and A.C. resistivity measurements were made one hour after solution treatment at which time the bars had reached room temperature. After 24 hours room temperature aging the bars were aged at 155 C for another 24 hours, slowly cooled, and their resistivities measured again. The diameters of the bars were measured throughout the course of the heat treatments and no dimensional change was found. For the A.C. resistivity measurements, an unmodified, nonheat treated A356 bar was used as the standard. Metallographic samples of the heat treated bars were also prepared.

3. RESULTS

3.1 Electrical Resistivity

3.1.1 D.C. Resistivity

Resistivity was evaluated by passing a current through a bar and measuring the potential difference between two fixed points along the bar. The procedure was carried out on bars of various degrees of modification and the results obtained (Appendix 5) were presented as graphs of D.C. resistivity versus strontium content.

In the case of the A356 alloy (figure 30), the resistivity decreases by 4.07 n Ω .m from 44.67 n Ω .m to 40.60 n Ω .m with an increase in strontium concentration from 0.000 wt.% Sr to 0.044 wt.% Sr. The resistivity then appears to increase with strontium concentrations greater than 0.044 wt.% Sr, however it must be noted that there are few points with which to derive this portion of the curve. The corresponding microstructures (figure 31) show the alloy with 0.000 wt.% Sr (figure 31a) to have an unmodified acicular silicon structure, 0.007 wt.% Sr gives an undermodified structure (figure 31b) and 0.015 wt.% Sr exhibits a modified structure. The alloy with 0.069 wt.% Sr is overmodified.

An increase in magnesium concentration to that of an A357 alloy produces a partially modified alloy at concentrations of 0.000 wt.% Sr (figure 32a). At strontium contents of 0.007 wt.% Sr and higher, the microstructures are modified and overmodified

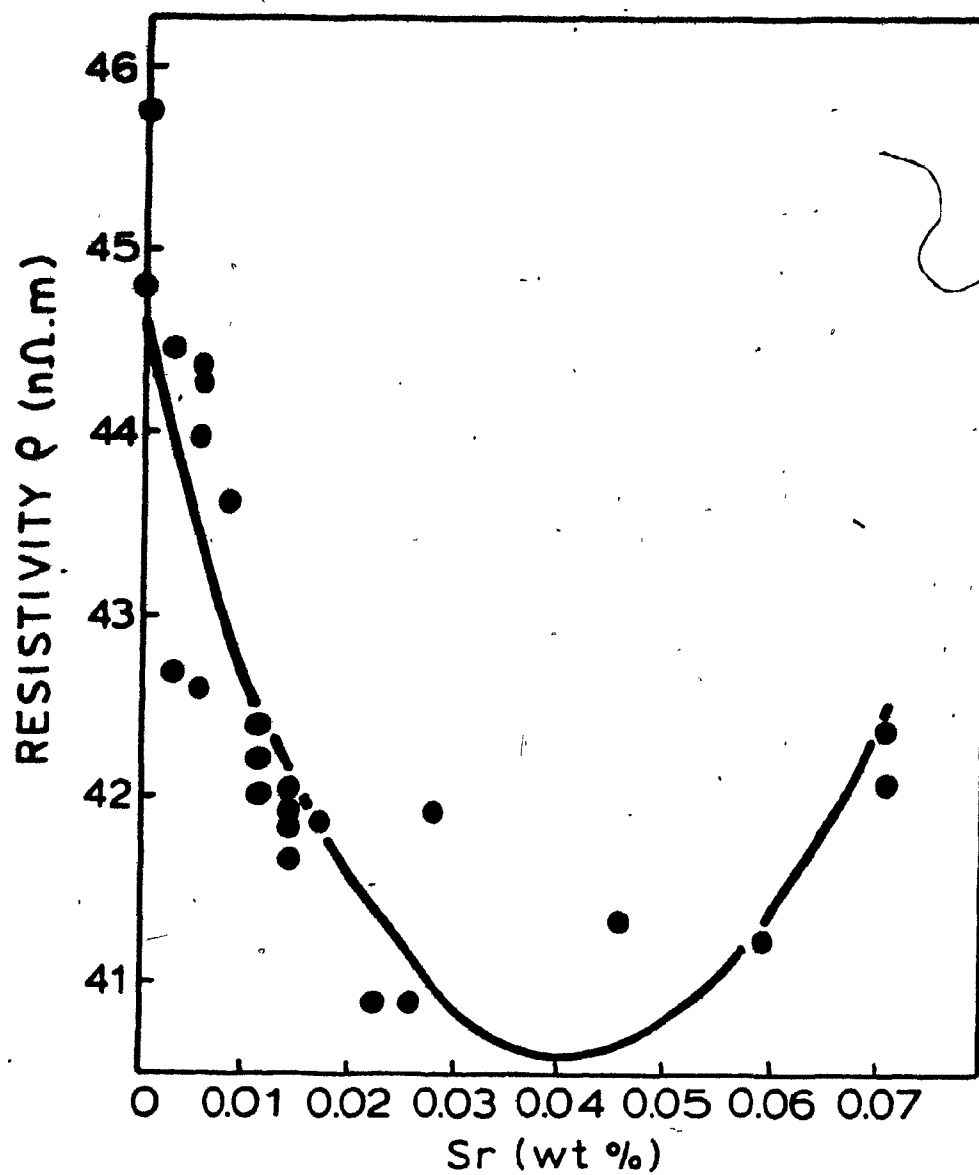
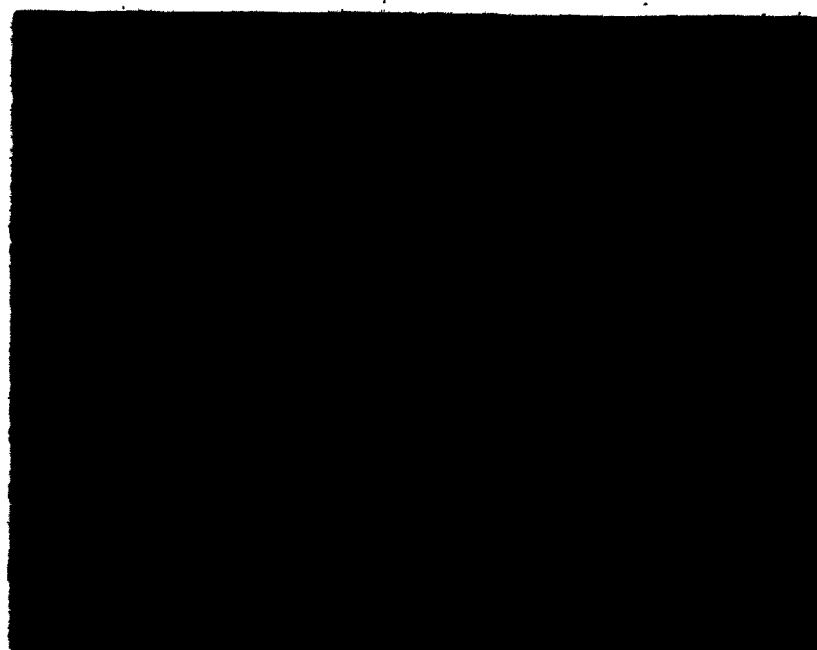


Figure 30: Variation of D.C. resistivity with strontium content for A356 alloy



(mag x 200)

31a: Unmodified 0.000 wt.% Sr

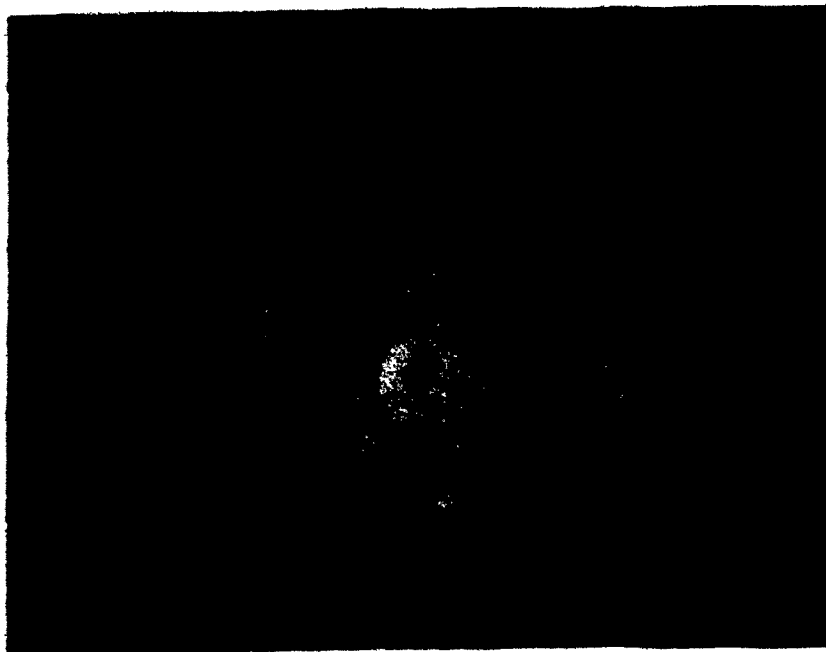


(mag x 200)

31b: Undermodified 0.007 wt.% Sr

Figure 31: Microstructure of A356 alloy at
various strontium contents

continued..



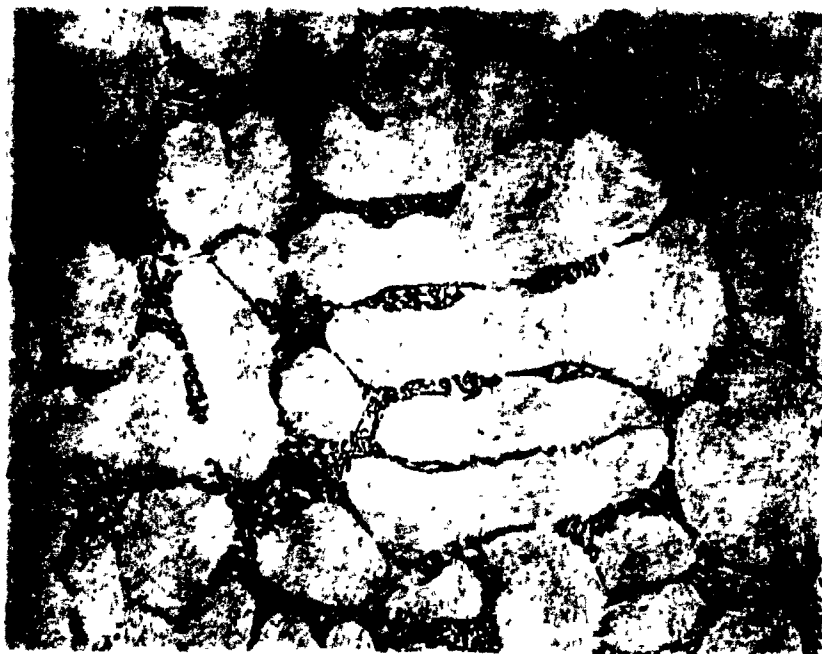
(mag x 200)

31c: Modified 0.015 wt.% Sr



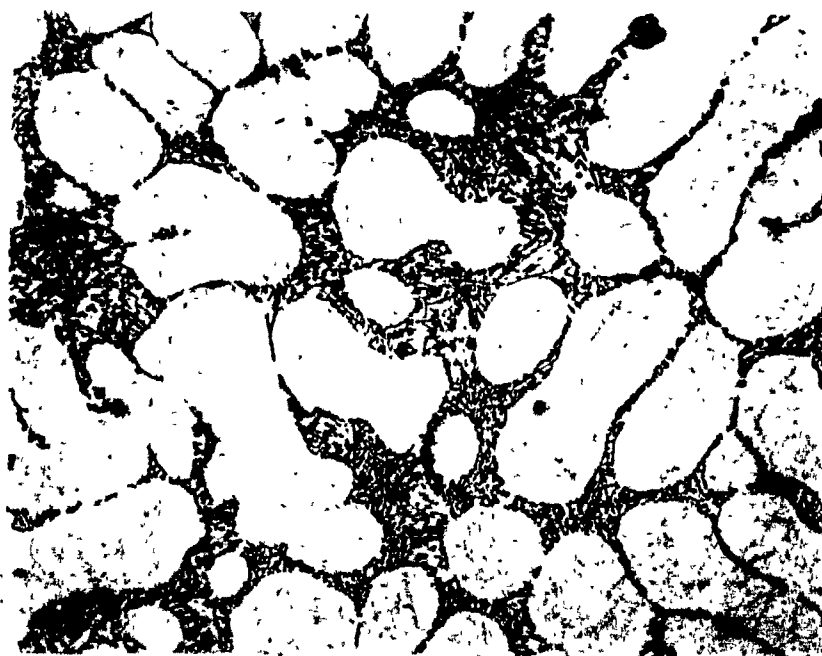
(mag x 200)

31d: Overmodified 0.069 wt.% Sr



(mag x 200)

32a: Partially modified 0.000 wt.% Sr



(mag x 200)

32b: Modified 0.007 wt.% Sr

Figure 32: Microstructure of A357 alloy at various strontium contents. Dark Chinese script intermetallic is Mg_2Si

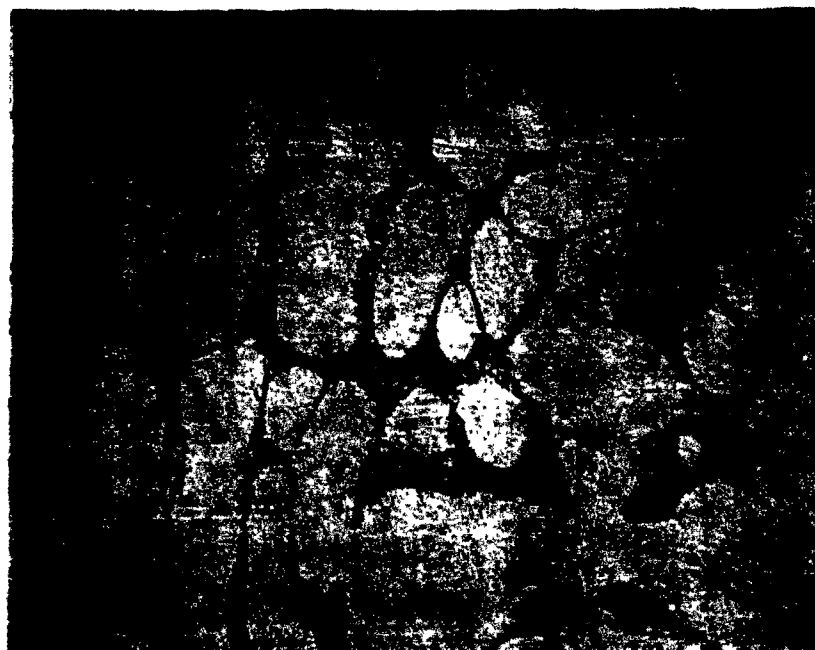
continued..

(figure 32b,c,d). The corresponding resistivity versus strontium content plot (figure 33) indicates that the resistivity decreases by only 0.21 n Ω .m from 43.75 n Ω .m to 43.54 n Ω .m with an increase in strontium concentration from 0.000 wt.% Sr to 0.044 wt.% Sr. All microstructures of A357 alloy contain Chinese script Mg₂Si incorporated in the eutectic silicon.

The correlation between D.C. resistivity and strontium content for A356 alloy with a high iron content (0.48 wt.%) was evaluated (figure 34). The resistivity decreases by 2.41 n Ω .m from 46.11 n Ω .m to 43.70 n Ω .m with an increase in strontium concentration from 0.000 wt.% Sr to 0.027 wt.% Sr. The resistivity again appears to increase at strontium contents greater than 0.027 wt.% Sr, however this assumption is based on only two data points. The corresponding microstructures (figure 35) show the alloy with 0.000 wt.% Sr (figure 35a) to have an unmodified structure; the alloy with 0.006 wt.% Sr to be undermodified (figure 35b), and alloys with strontium contents of 0.027 wt.% Sr and higher, to be modified and overmodified respectively, (figures 35c and 35d). All microstructures of the A356 alloy containing 0.48 wt.% Fe have needle-like Fe-Si-Al intermetallics dispersed throughout the primary aluminum and eutectic phases.

3.1.2 A.C. Resistivity

The differential A.C. resistivity technique, explained in detail in section 2.4.2 measures the difference in voltage,



(mag x 200)

32c: Modified 0.038 wt.% Sr



(mag x 200)

32d: Overmodified 0.068 wt.% Sr

Figure 32: Microstructures of A357 alloy at various strontium contents

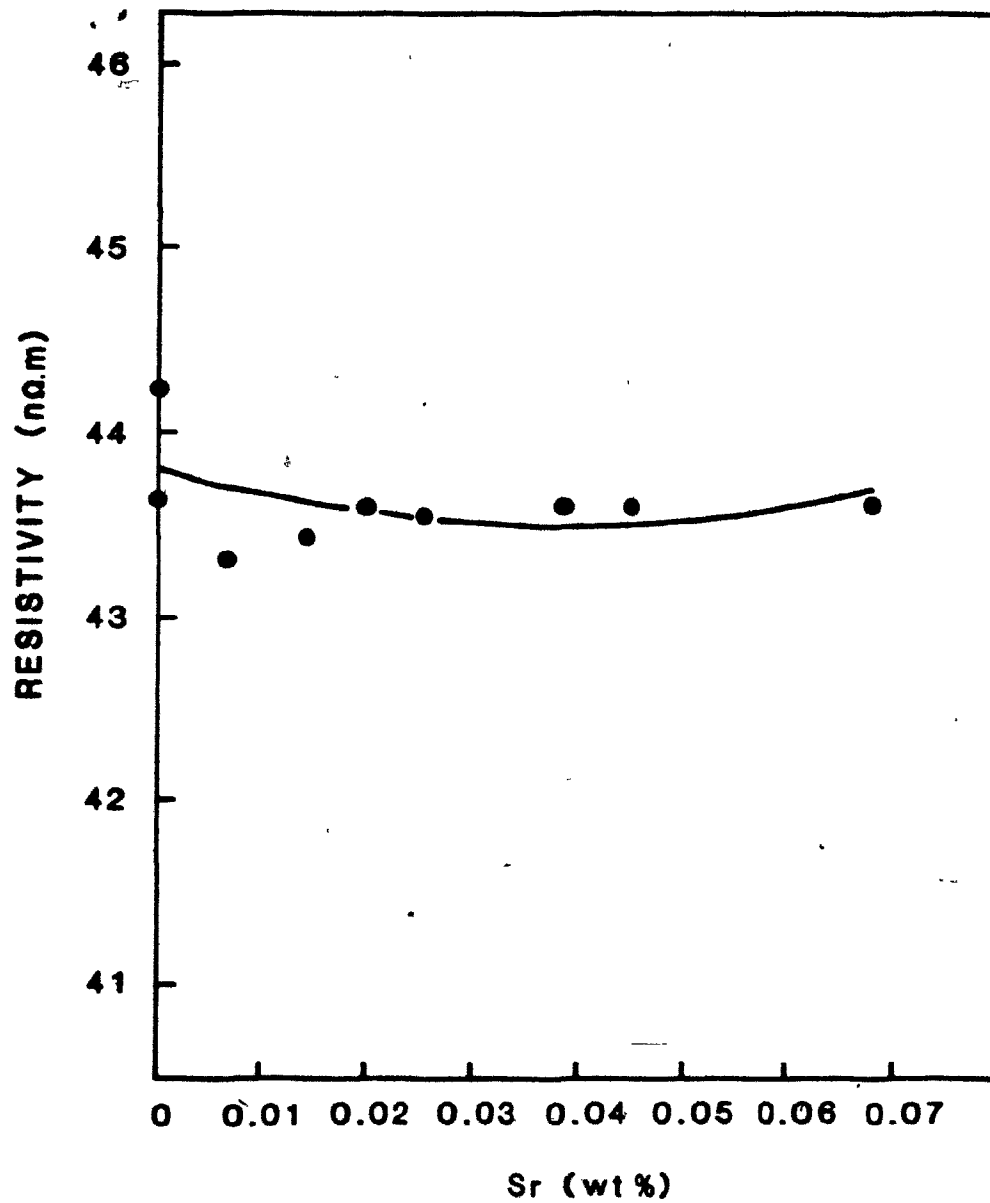


Figure 33: Variation of D.C. resistivity with strontium content for A357 alloy

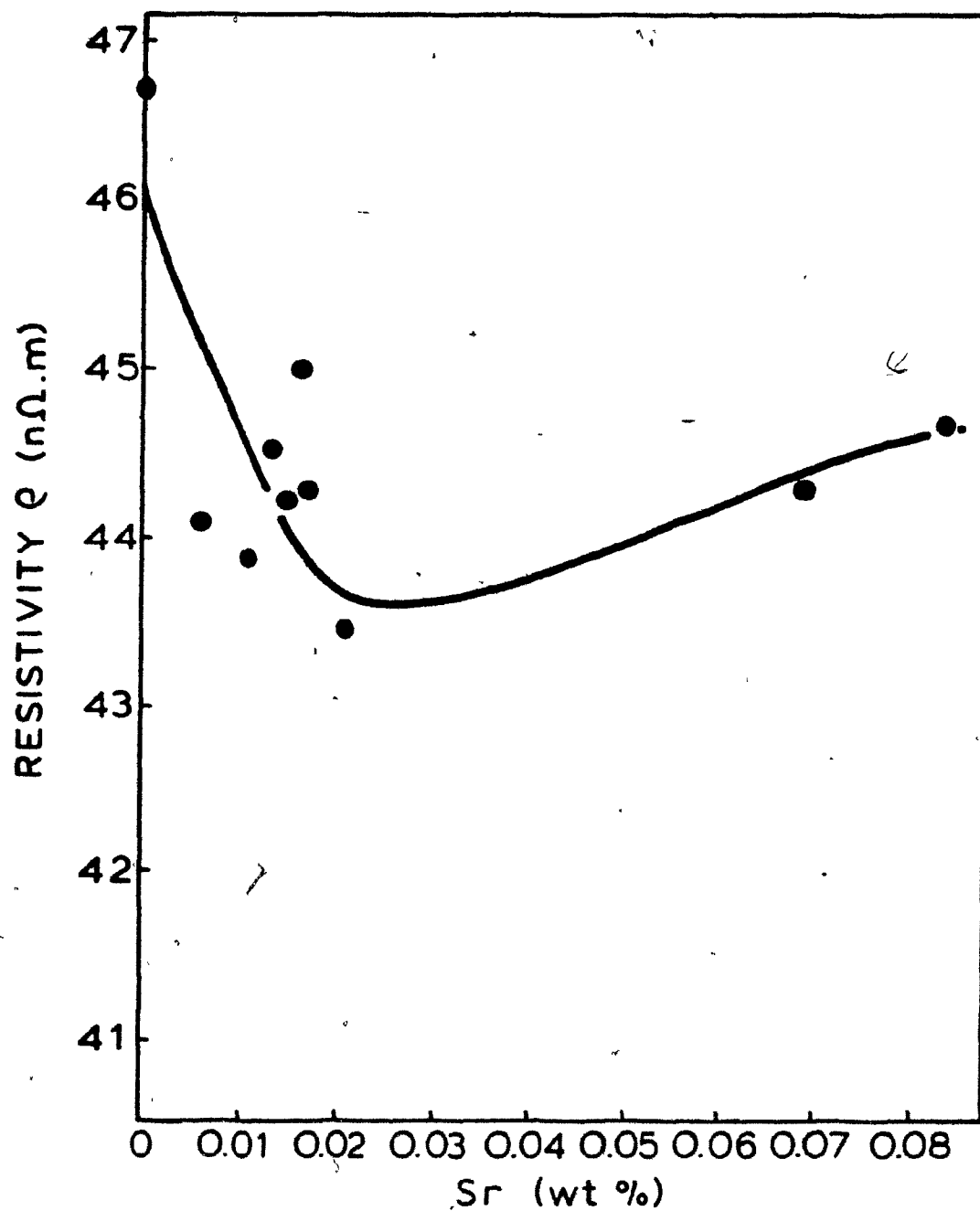


Figure 34: Variation of D.C. resistivity with strontium content for alloy A356 (0.48 wt.% Fe)



82

(mag x 200)

35a: Unmodified 0.000 wt.% Sr



(mag x 200)

35b: Undermodified 0.006 wt.% Sr

Figure 35: Microstructures of A356 alloy containing 0.48 wt.% Fe at various strontium contents. Long coarse needles are Fe-Si-Al intermetallics.

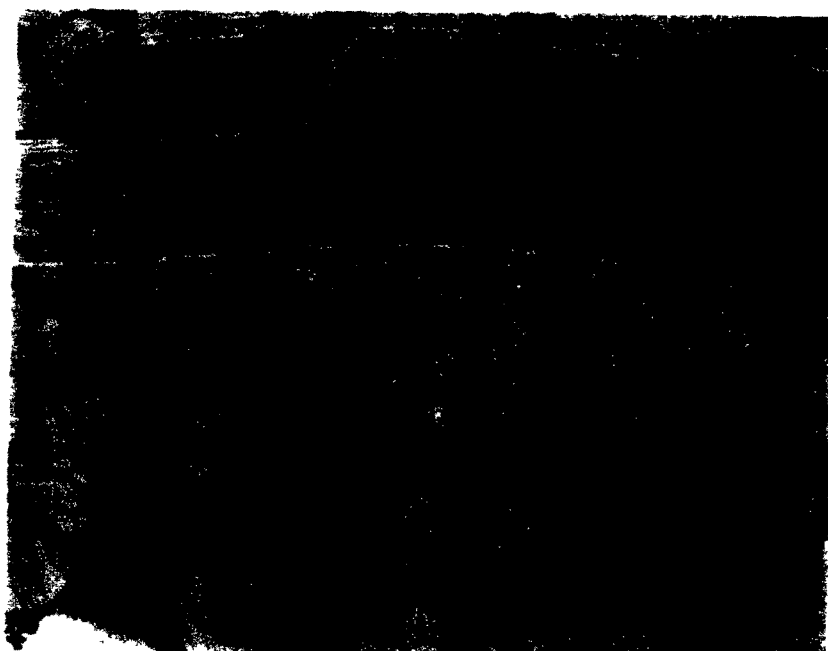
continued..



83

(mag x 200)

35c: Modified 0.027 wt.% Sr



(mag x 200)

35d: Overmodified 0.061 wt.% Sr

ΔV (mV), between a standard unmodified bar and a sample bar (experimental data, Appendix 6). Due to machining tolerances there were relatively large variations in diameter between the bars. Diameter ranges A,B and C were assigned to the bars and statistical analyses were performed on the ΔV versus strontium content data for each diameter range. F values, (see section 2.2 Statistical Analysis) were found in order to determine which diameter range yielded the graph with the least scatter between the points, that is, which yielded the most accurate graphical representation of the data. All three sets of data for the three diameter ranges had experimental F values (Table XI) greater than table F values (Table VII). Diameter range B however, had the highest experimental F value and therefore yielded the most accurate graphical representation of the data. For this reason, all the subsequent A.C. resistivity work was performed only on bars within diameter range B (15.22 mm to 15.31 mm).

The variation of ΔV (mV) versus strontium content (wt.%) for alloy A356 was correlated graphically (figure 36). ΔV increases by 1.00 mV from -0.13 mV to 0.87 mV with increase in strontium concentration from 0.000 wt.% Sr to 0.042 wt.% Sr. At strontium concentrations above 0.042 wt.% Sr ΔV appears to decrease, however as previously mentioned in the corresponding D.C. resistivity results, there are only a few data points at high strontium concentrations. The micrographs (figure 31) show the degree of modification for the various strontium contents.

	F Values		
	Diameter Range		
	A	B	C
	15.17 mm to 15.35 mm	15.22 mm to 15.31 mm	15.25 mm to 15.29 mm
Experimental F value	21.00	36.00	31.70
F value from tables	3.42	3.42	3.42

Table XI: Results of statistical analyses on the ΔV versus Sr wt.% data for the three bar diameter ranges using A356 alloy

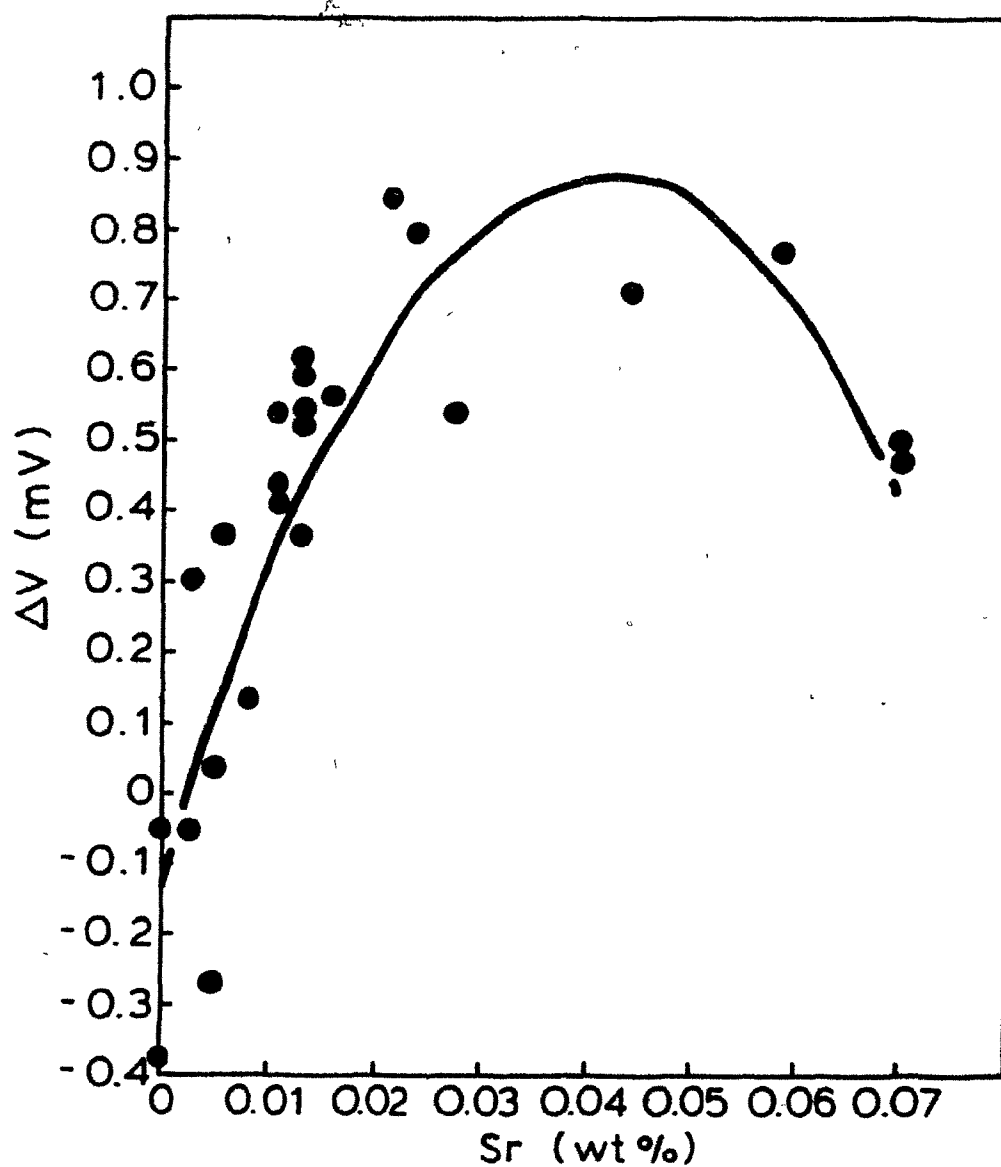


Figure 36: Variation of ΔV with strontium content for A356 alloy. (Bar diameter range B 15.22 to 15.31 mm)

The A357 alloy with the higher magnesium level again exhibits very different resistivity characteristics from the A356 alloy (figure 37). ΔV increases by only 0.18 mV from 0.16 mV to 0.34 mV with an increase in strontium concentration from 0.000 wt.% Sr to 0.040 wt.% Sr. There is a slight decrease in ΔV with increasing strontium contents above 0.040 wt.% Sr. The micrographs in figure 32 show the microstructures of the A357 bars which were used to obtain the data for figure 37.

The high iron content alloy, A356 containing 0.48 wt.% Fe, figure 38, again shows similar resistivity characteristics to the A356 alloy. ΔV increases by 0.34 mV from 0.17 mV to 0.51 mV with increasing strontium contents from 0.000 wt.% Sr to 0.027 wt.% Sr, and there appears to be a slight decrease above 0.04 wt.% Sr. The micrographs in figure 35 show the microstructures of A356 alloy containing 0.48 wt.% Fe.

3.2 The Factors Affecting Resistivity

3.2.1 Temperature

D.C. and A.C. resistivity measurements were made on A356 bars at various temperatures (see section 2.5.1). The D.C. results of unmodified, undermodified, modified and overmodified bars (Table XII) show that D.C. resistivity increases linearly with temperature (figure 39), the temperature coefficient being $0.1 \text{ n}\Omega.\text{mK}^{-1}$. This relationship is evident in bars exhibiting all degrees of modification and the temperature resistivity coefficient is identical to that for pure aluminum⁽²⁷⁾.

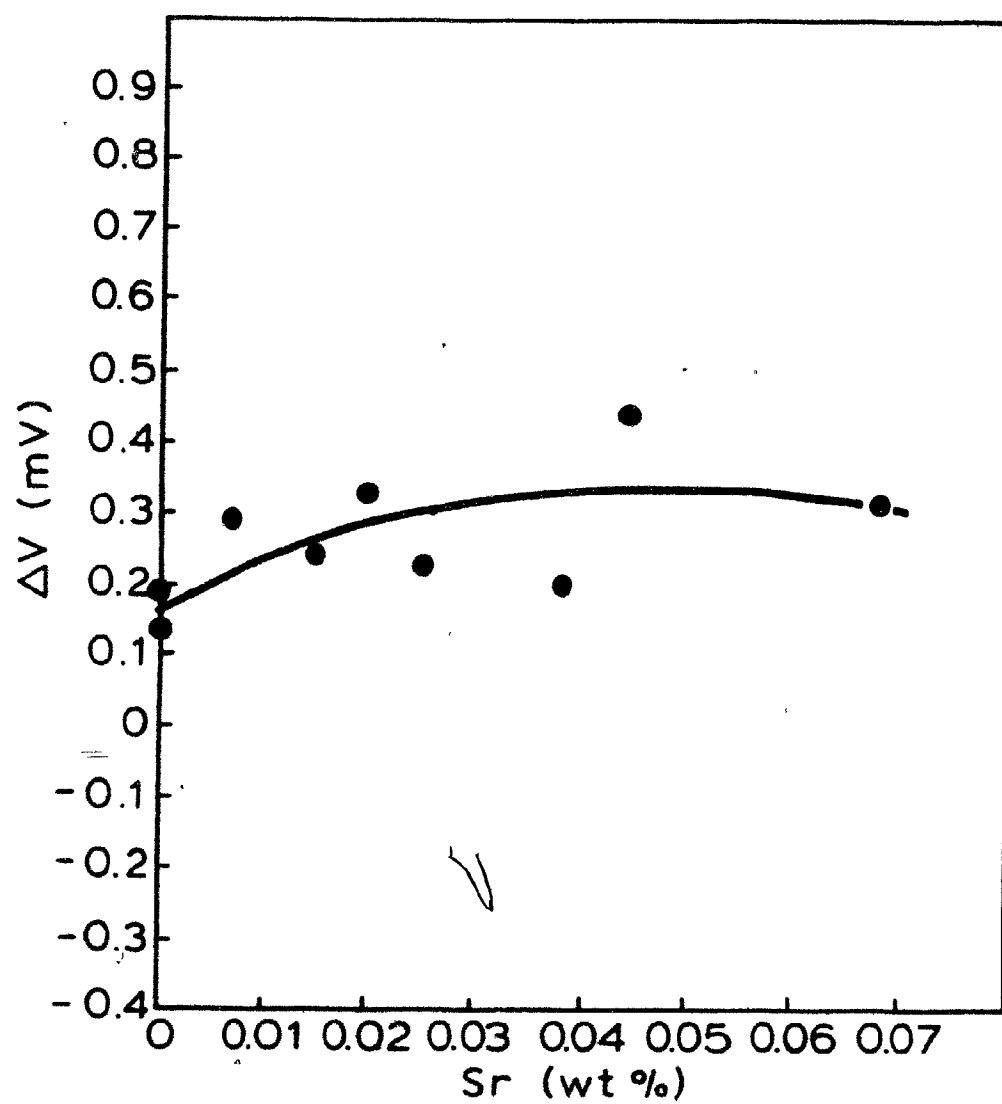


Figure 37: Variation of ΔV with strontium content for A357 alloy

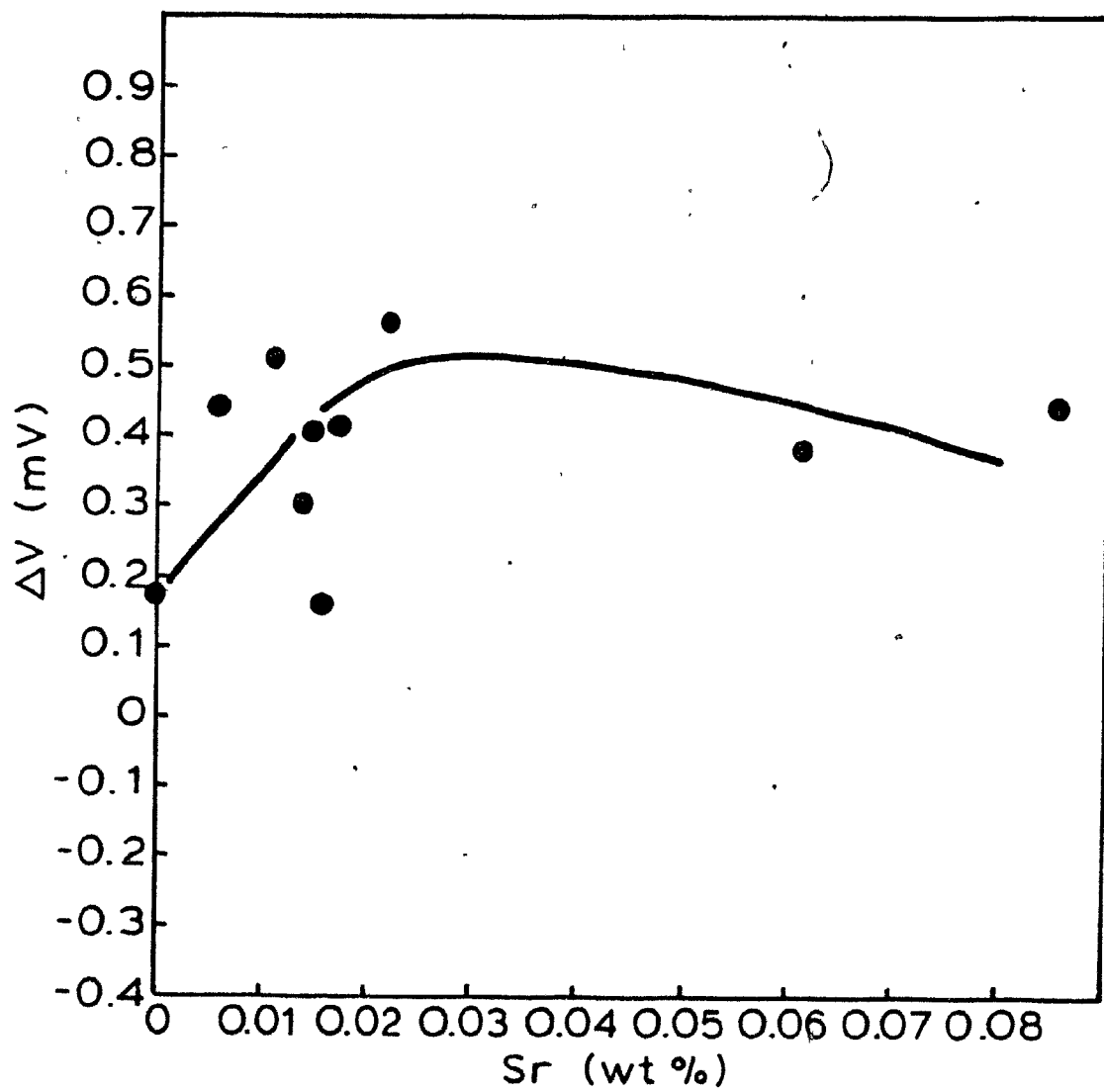


Figure 38: Variation of ΔV with strontium content for A356 alloy containing 0.48 wt.% Fe

Temperature C	D.C. Resistivity Values (n Ω .m)			
	State of Modification			
	unmodified	undermodified	modified	overmodified
24	46.47	43.02	41.72	42.51
0	44.04	40.60	39.34	40.09
-10	43.00	39.64	38.35	39.08

Table XII* D.C. resistivity values of A356 bars at various temperatures

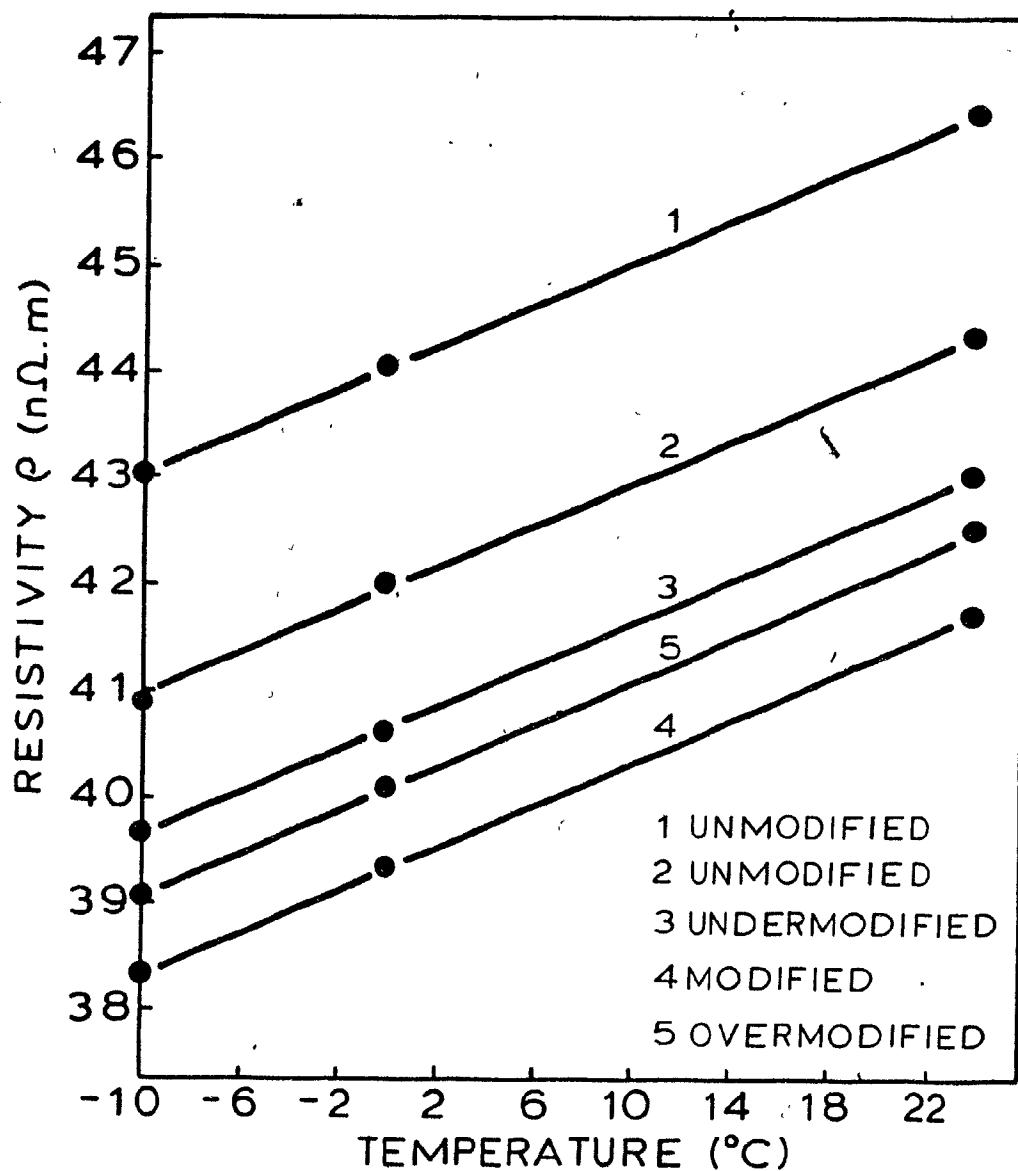


Figure 39: Variation of D.C. resistivity with temperature for A356 alloy.
(Gradients of graphs are 0.1 n Ω .mK $^{-1}$)

The A.C. resistivity results (Table XIII) show that the difference in voltage between the standard and sample remain constant (within the experimental error) with change in temperature.

3.2.2 Porosity

Porosity, evident in many of the castings, was quantified (Appendix 7) using the density technique explained in section 2.5.2. The majority of the A356 alloy castings had a porosity level between 0.00 vol.% and 0.20 vol.%, however porosities up to 0.99 vol.% were measured in a few of the bars. Average porosity and average resistivity values of the four bars from the same casting were used to increase the accuracy of the results. Comparisons that were made were therefore between castings and not between single bars. Castings with similar strontium contents were compared (Table XIV) and in every case but one, the casting with the highest resistivity exhibited the highest porosity.

Porosity was also examined by radiography. Although the individual pores were too small to be identified on the X-ray image (figure 40), the bars appeared homogeneous implying that the porosity was uniformly distributed in the casting. The porosity on the surface of the metallographic samples (figure 41) was also uniformly distributed.

3.2.2 Eutectic Segregation

During the course of experiments bar diameter was changed by machining and was found to affect D.C. resistivity markedly

Temperature C	A.C. Resistivity Values, ΔV (mV)			
	State of Modification			
	unmodified	undermodified	modified	overmodified
24	-0.062	0.454	0.540	0.432
0	-0.057	0.499	0.550	0.432
10	-0.061	0.454	0.547	0.430

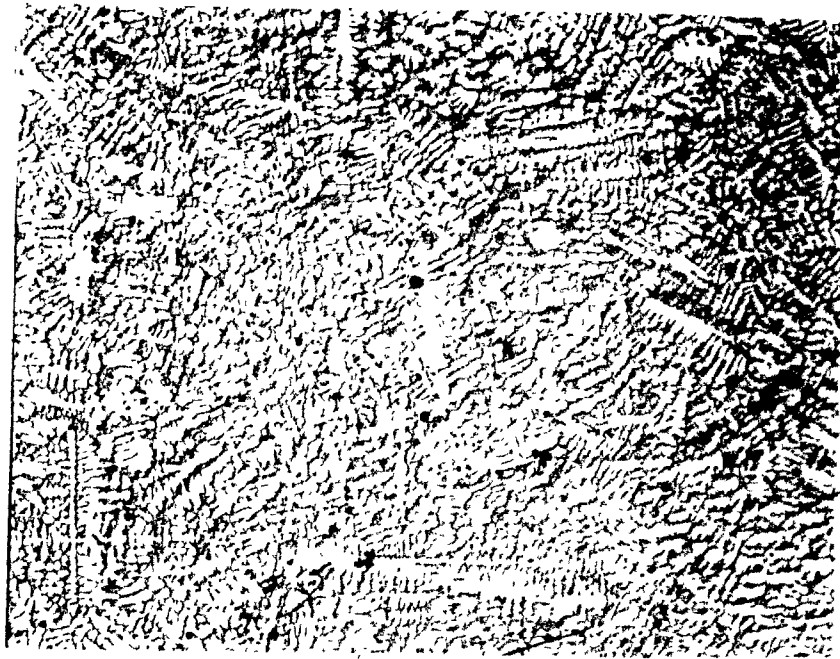
Table XIII: ΔV values from A.C. resistivity measurements at various temperatures, for alloy A356

Strontium content of castings (wt.%)	D.C. Resistivity, average of 4 bars in a casting (nΩ.m)	Porosity, average of 4 bars in a casting (vol.%)
0.000	44.82	0.30
0.000	44.79	0.09
0.004	44.39	0.000
0.005	44.77	0.100
0.007	42.20	0.009
0.006	44.55	0.990
0.011	42.32	0.025
0.010	42.50	0.101
0.013	42.08	0.000
0.013	42.12	0.019
0.014	41.67	0.009
0.015	41.96	0.097
0.017	41.91	0.000
0.015	41.96	0.097
0.021	41.55	0.020
0.024	42.80	0.333
0.025	40.94	0.010
0.024	42.80	0.333
0.028	42.08	0.121
0.029	42.12	0.265
0.069	41.81	0.033
0.069	42.15	0.445

Table XIV: The influence of porosity on electrical resistivity



Figure 40: X-ray images of the bars.
The bars were found to be
homogeneous.



(mag x 20)

Figure 41: Porosity on the surface of a metallographic sample

(Table XV). A decrease in bar diameter of approximately 3.0 mm increases the resistivity by approximately 28%. Studies were therefore made into the change in the amount of eutectic across the diameter of a bar (section 2.5.3). A 10% increase in the amount of eutectic towards the centre of the bar was found irrespective of whether the alloy was unmodified, under-modified, or modified, (Table XVI and figure 42).

3.2.4 Solute Concentrations

Microprobe analyses were performed in the centre of samples with various strontium contents in order to study the variation of solute concentration with change in strontium level. The results, (Table XVII) graphically represented (figure 43), show that the silicon content in the primary aluminum matrix does not vary with strontium content or degree of modification.

3.3 Heat Treatment

3.3.1 Heat Treatment of A356 Alloy

Three different heat treatments A, B and C with solution treatments of 8, 24 and 48 hours respectively were performed on bars as explained in section 2.6. D.C. and A.C. resistivity measurements were taken on the bars after solution treatment and after complete heat treatment (solution treatment followed by aging), (Appendix 8).

The average changes in D.C. resistivity upon solution treatment and aging for each type of heat treatment are given in table XVIII where each value is the average resistivity of

Sample	Diameter 1) mm	Resistivity ($n\Omega \cdot m$)	Diameter 2) mm	Resistivity ($n\Omega \cdot m$)	Resistivity Difference %
A6-2A	14.80	42.36	12.50	66.88	28.3
A6-2B	16.60	41.23	12.50	66.27	27.3
A6-2C	16.85	42.09	12.50	66.57	28.0
A6-2D	15.15	42.36	12.50	66.57	28.2

Table XV: Variation of D.C. resistivity with machined sample diameter

Sample	Volume Percent Eutectic			
	Radial distance from centre of bar (mm)			
	0mm (centre)	3.75 mm	7.5 mm	9.45 (Edge)
Un-modified	43	39	34	34
Under-modified	42	40	39	36
Modified	39	36	32	32

Table XVI: Variation of percent eutectic present with radial distance from the centre of a bar

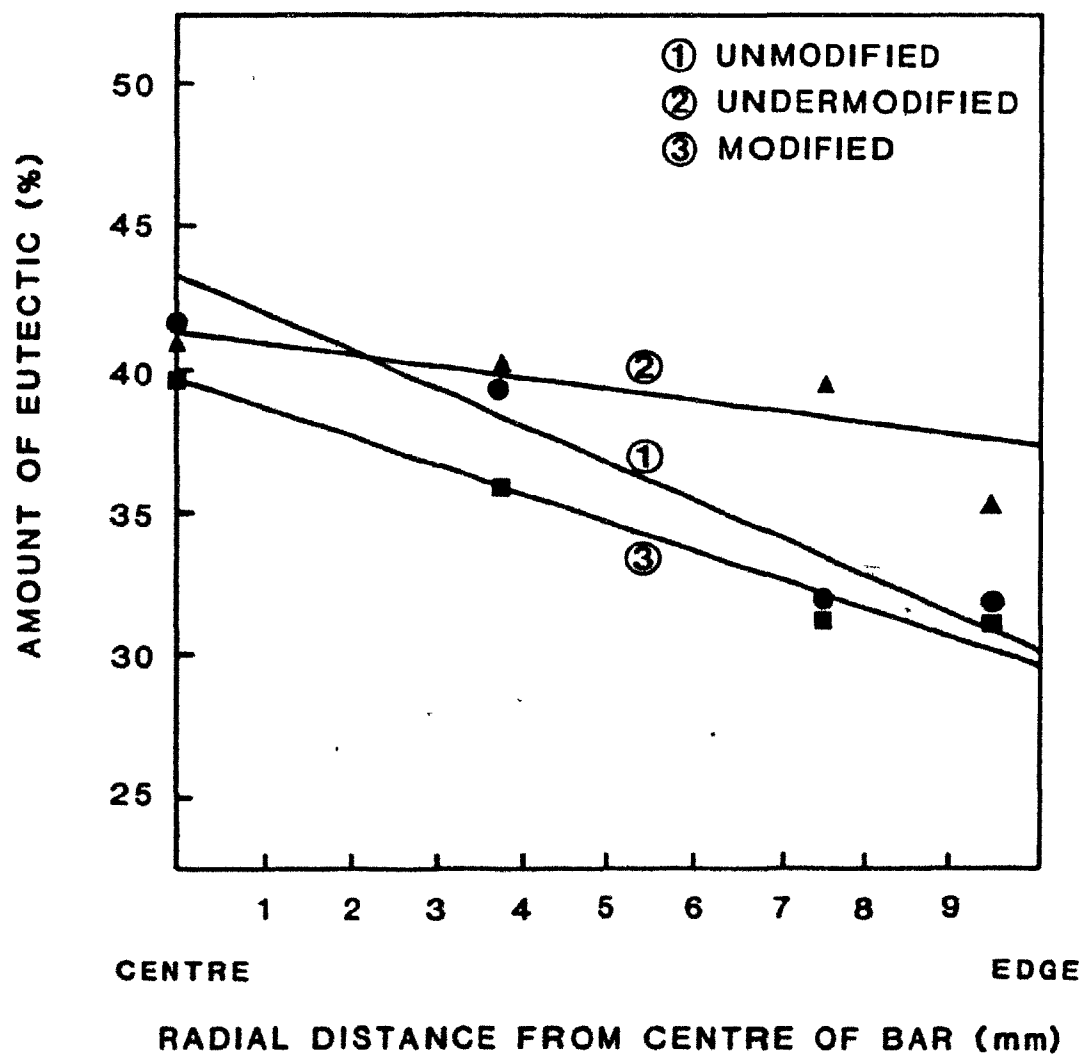


Figure 42: Variation of the amount of eutectic with radial distance from the centre of bars

Percent Strontium (by spectrometer analysis)	Percent Silicon (by microprobe analysis)
0.000	1.55
0.000	1.72
0.101	1.42
0.013	1.55
0.021	1.46
0.028	1.40
0.029	1.62
0.044	1.41
0.069	1.43
0.069	1.52

Table XVII: Correlation between percentage silicon in the aluminum matrix with strontium content

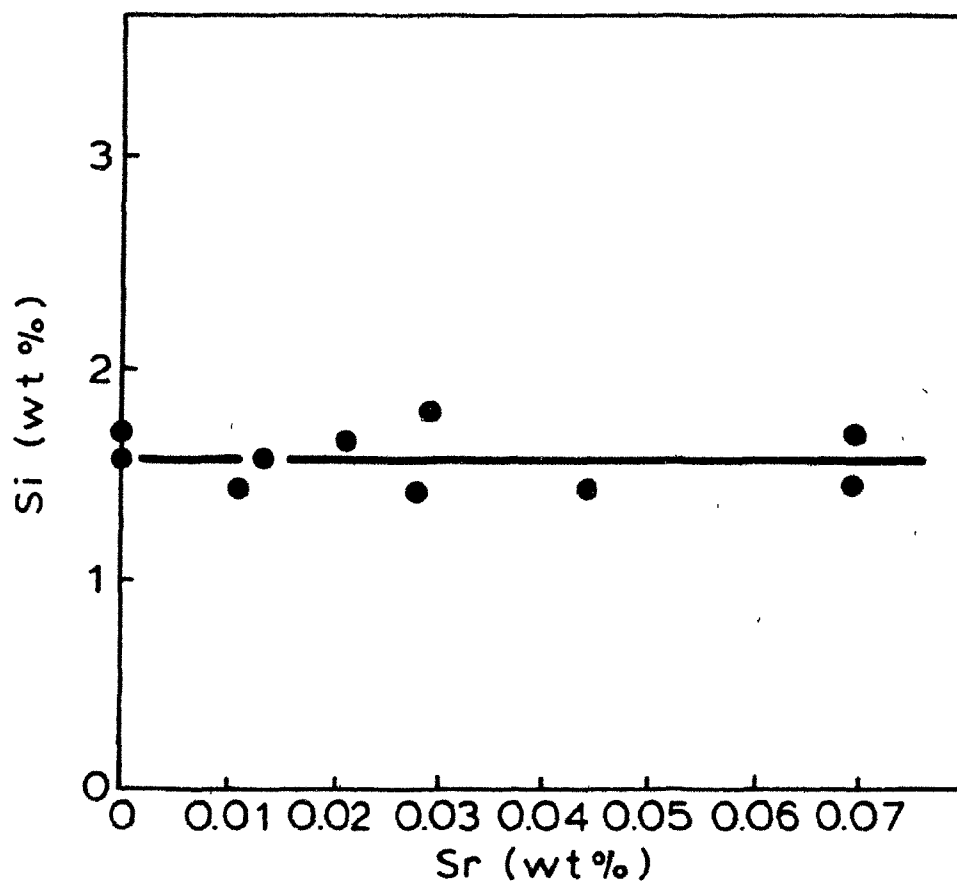


Figure 43: Variation of silicon content in the primary aluminum matrix with strontium content

Heat Treatment	Average change in D.C. Resistivity ($n\Omega.m$)	
	As a result of solution treatment	As a result of the aging process only
A (8 hours) solution treat)	3.15	-3.59
B (24 hours) solution treat)	2.60	-2.69
C (48 hours solution treat)	2.58	-1.57

Table XVIII: The average change in D.C. resistivity as a result of solution treatment and as a result of aging for A356 alloy heat treatments A, B and C.

26 A356 alloy bars containing varying amounts of strontium. The average increase in resistivity as a result of solution treatment (2.78 n Ω .m) in all cases is approximately the same as the average decrease in resistivity (2.62 n Ω .m) as a result of subsequent aging.

Although no clear trend is observed between the increase in resistivity upon solution treatment and the type of heat treatment, the resistivity change upon aging is interesting. For heat treatment A the decrease in resistivity on aging is larger than the increase observed on solution treatment. The resistivity of the completely heat treated (A) bar is therefore 0.44 n Ω .m lower than the original non-heat treated bar. By increasing the solution treatment time (heat treatment B) the decrease in resistivity is approximately the same as the increase on solution treatment. With heat treatment C, the decrease in resistivity on aging is less than the increase observed in solution treatment resulting in the completely heat treated (C) bar having a 1.01 n Ω .m higher resistivity than the original non-heat treated bar.

Another approach is to consider the change in resistivity upon heat treatment as a function of strontium content. There is one obvious trend (Table XIX): for all heat treatments, A, B and C, the modified bar shows a greater increase in resistivity than the unmodified bar, upon solution treatment. Additionally, for unmodified bars, the decrease in resistivity upon aging is always greater than the preceding increase upon

A356 ALLOY	CHANGE IN RESISTIVITY AS A RESULT OF HEAT TREATMENT ($n\Omega.m$)					
	Heat Treat- ment A		Heat Treat- ment B		Heat Treat- ment C	
	Solu- tion Treat- ment (8 hrs)	Aging	Solu- tion Treat- ment (24 hrs)	Aging	Solu- tion Treat- ment (48 hrs)	Aging
UNMODIFIED	+0.80	-2.69	+2.07	-3.26	+1.02	-2.51
MODIFIED	+3.65	-3.47	+3.63	-2.04	+2.29	-2.13

Table XIX: A comparison of the changes in resistivity brought about by various solution treatments and aging treatments, between unmodified and modified A356 alloys

solution treatment, and so heat treated modified bars exhibit higher resistivities than as-cast modified bars. To illustrate the resistivity changes graphically, the resistivity data from heat treatment A was plotted against strontium content. The resistivity data obtained after solution treatment (figure 44) for unmodified alloys (0.000 wt.% Sr) shows a small increase in resistivity (0.8 n Ω .m) upon solution treatment, and with increasing amounts of strontium, the change in resistivity gradually increases by 2.85 n Ω .m reaching a maximum change of 3.65 n Ω .m at 0.042 wt.% Sr. The corresponding A.C. resistivity plot (figure 45) again shows that unmodified alloys exhibit the smallest change in ΔV (-0.26 mV) upon solution treatment, and that modified alloys of 0.042 wt.% Sr exhibit the largest change in ΔV (-0.81 mV) on solution treatment.

The decrease in resistivity as a result of aging exhibits no correlation with the various heat treatments; however, as mentioned previously, completely heat treated modified bars exhibit a higher resistivity than as-cast modified bars, and heat treated unmodified bars exhibit a lower resistivity than the as-cast unmodified alloy. This is illustrated in figure 46; modified bars exhibit a 0.18 n Ω .m increase in resistivity as a result of complete heat treatment, and unmodified bars exhibit a decrease of 0.19 n Ω .m as a result of complete heat treatment.

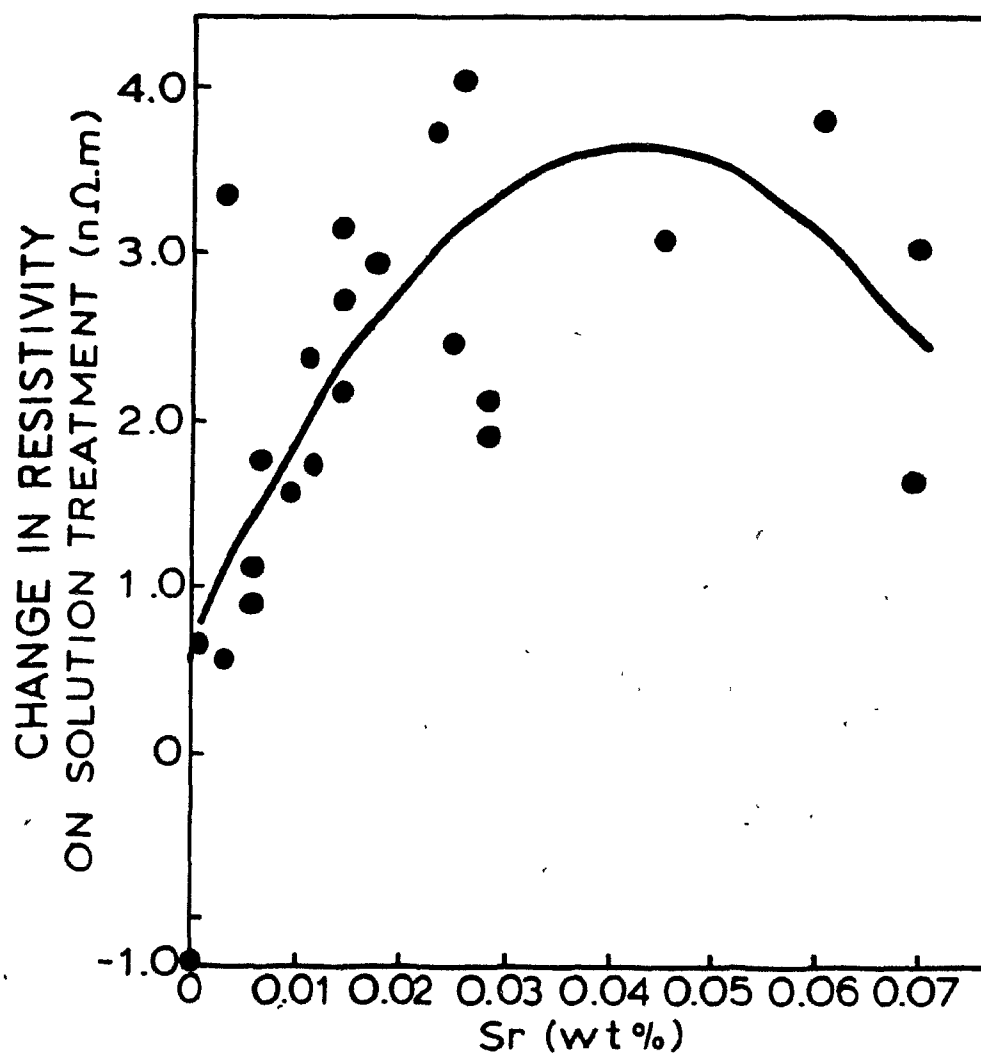


Figure 44: The difference in D.C. resistivity between as-cast and solution treated A356 bars of various strontium contents

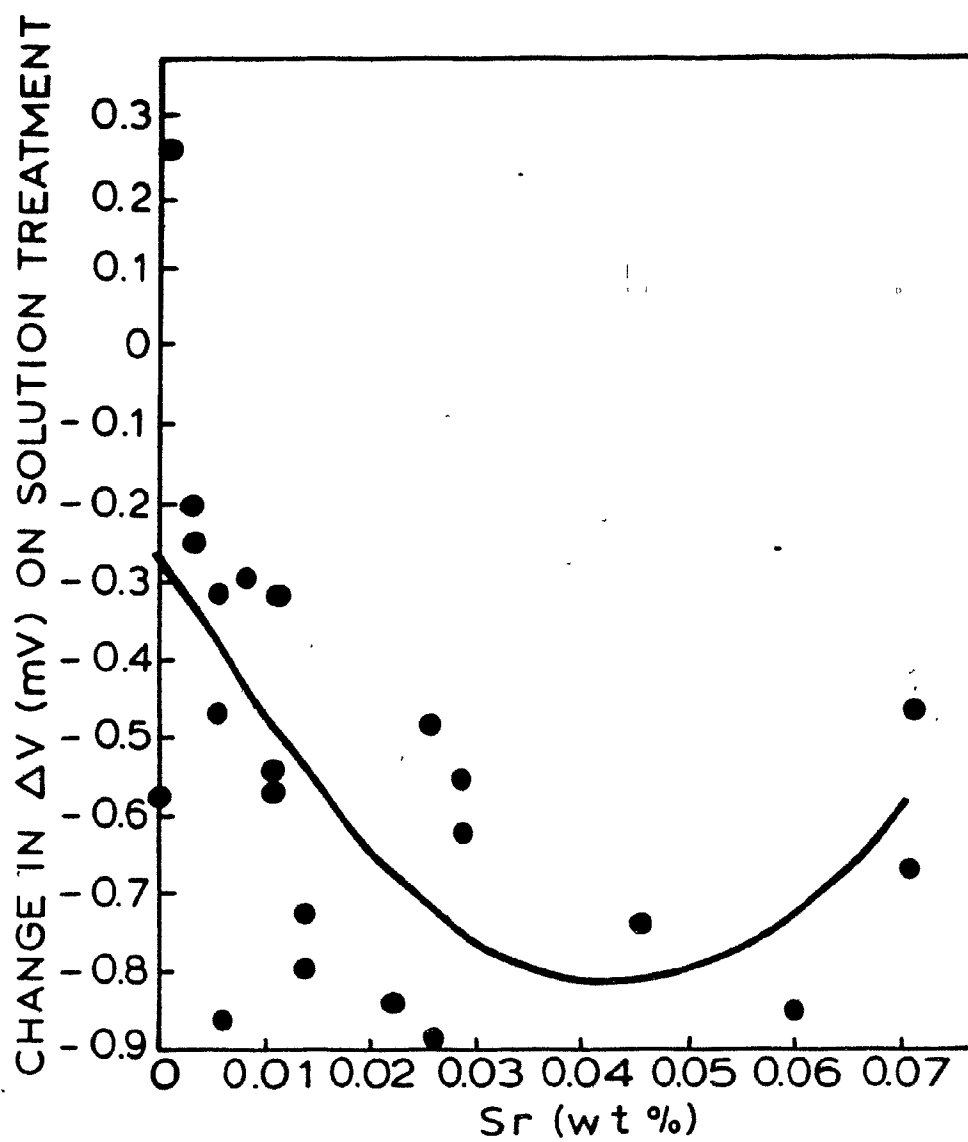


Figure 45: The difference in ΔV between as-cast and solution treated A356 bars of various strontium contents

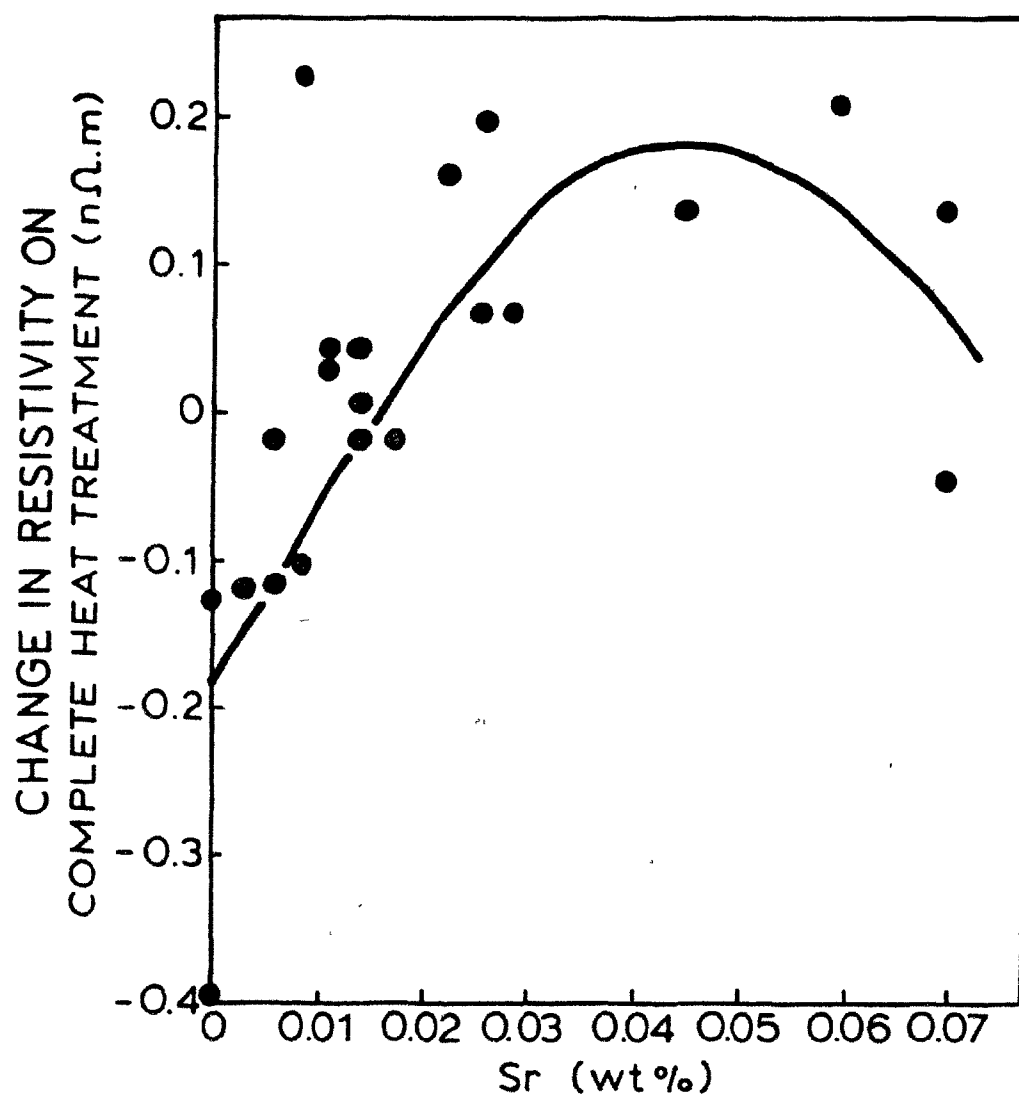


Figure 46: The difference in D.C. resistivity between as-cast and completely heat treated A356 bars of various strontium contents

The A.C. data shows the same results as the D.C. data (figure 47). Unmodified bars exhibit an increase in ΔV of 0.38 mV as a result of complete heat treatment and modified bars exhibit a decrease in ΔV of 0.37 mV.

The microstructures of both modified and unmodified samples after complete heat treatment are shown in figure 48. The microstructures are more or less identical for all three heat treatments and all show the heat treated modified eutectic to be more spheroidal than the unmodified heat treated eutectic.

3.3.2 Heat Treatment of A357 and A356 (0.48 wt.% Fe) Alloys

All three heat treatments, A, B, and C were performed on A357 alloys and A356 (0.48 wt.% Fe) alloys. D.C. and A.C. measurements were taken after solution treatment and aging (Appendix 8) and the results analysed in two ways as with the A356 alloy: irrespective of strontium content and as a function of strontium content.

The average changes in D.C. resistivity upon solution treatment and aging in the A357 alloy are given in table XX where each value is the average resistivity of 9 bars containing varying amounts of strontium. The one and only significant trend evident is the increase in resistivity on solution treatment and the decrease in resistivity on subsequent aging. Similar results are found for the A356 (0.48 wt.% Fe) alloy (Table XXI) where there is an increase in resistivity on solution treatment, and in two of the three cases there is a decrease in resistivity upon aging.

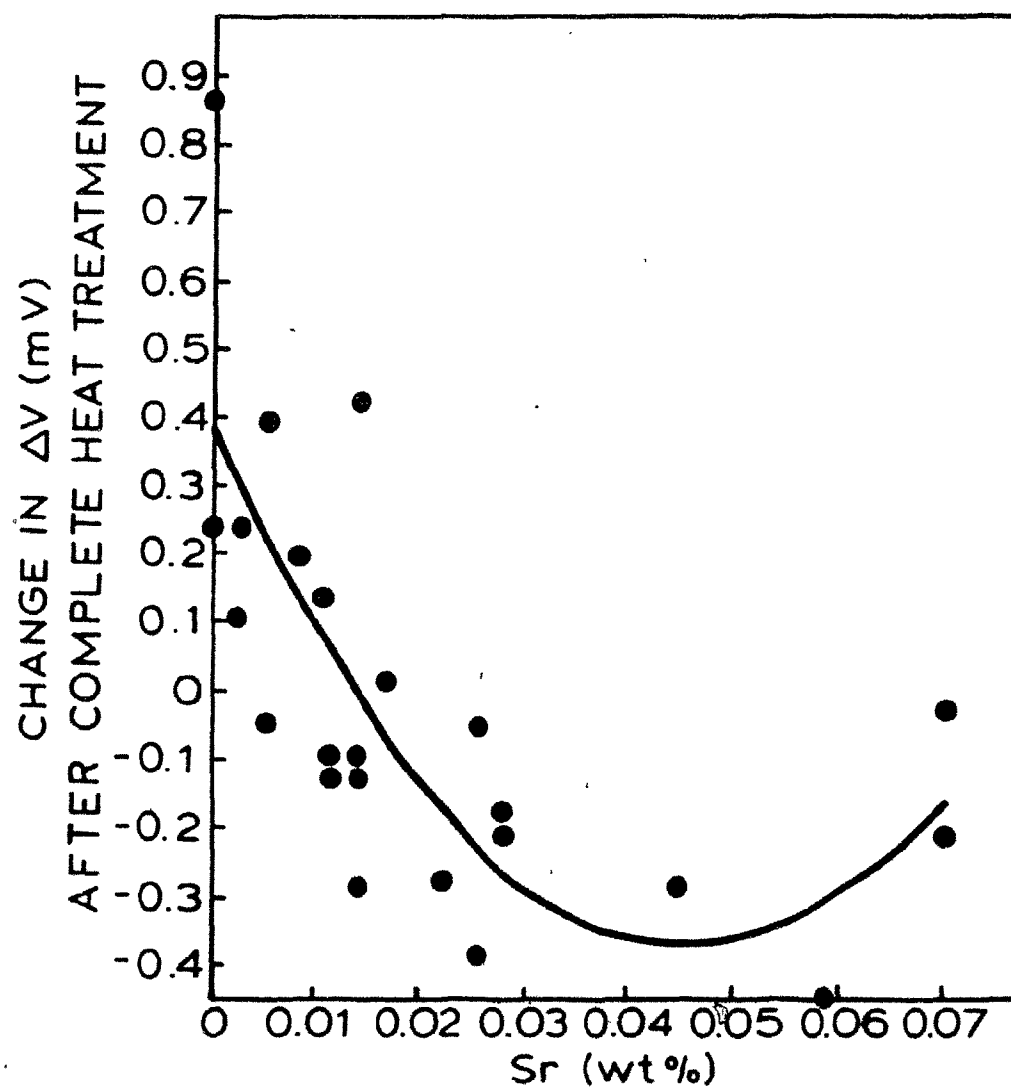
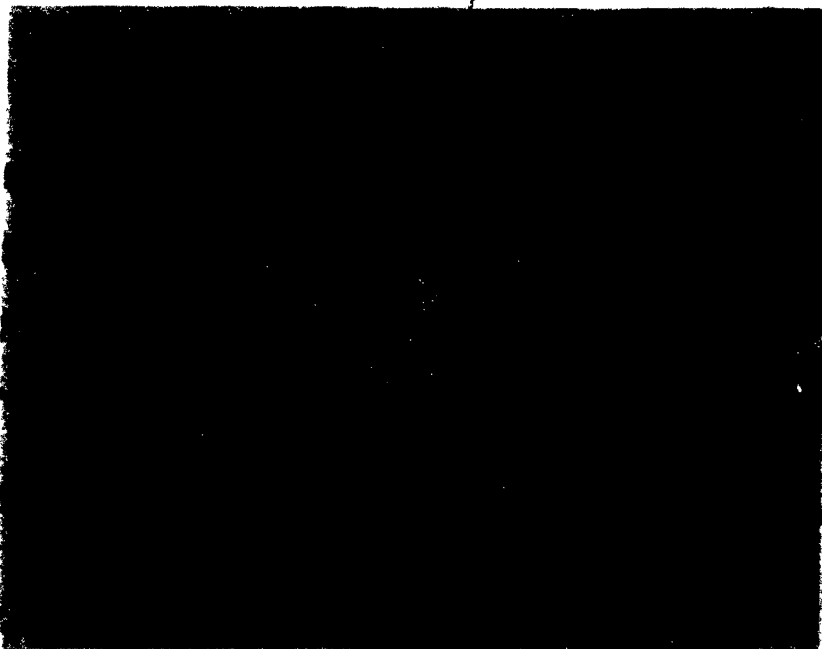


Figure 47: The difference in ΔV between as-cast and completely heat treated bars of various strontium contents



(mag x 200)

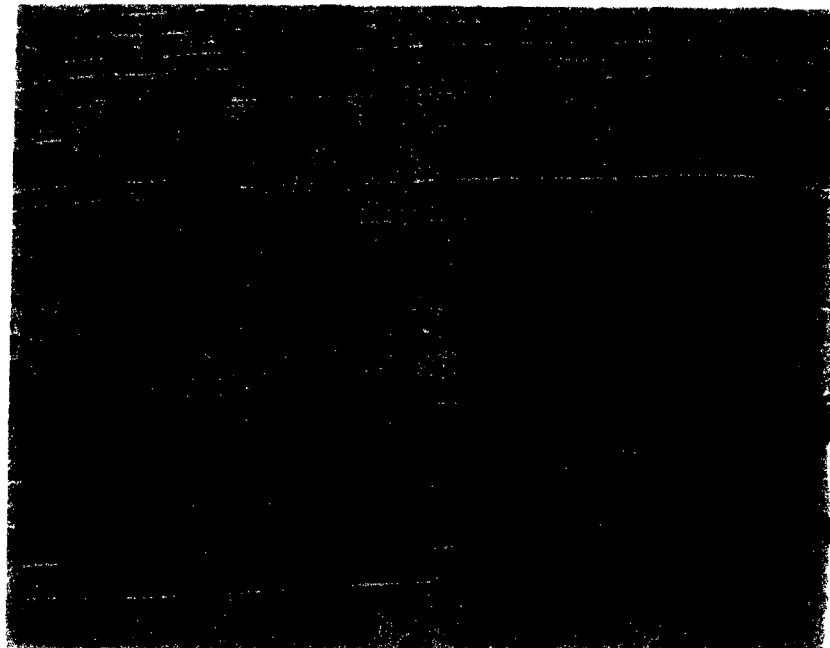
Unmodified



(mag x 200)

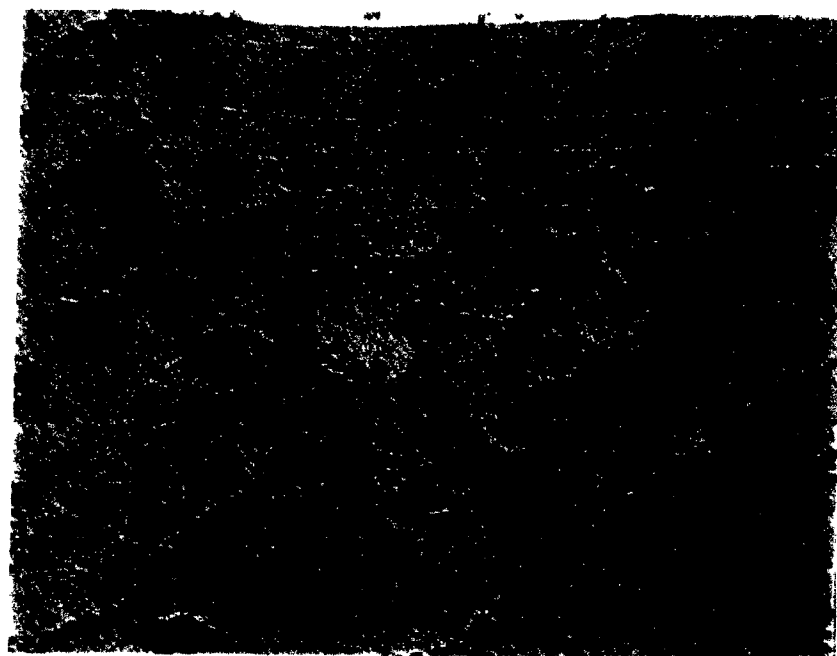
Modified

Figure 48a: Metallographic samples of unmodified and modified bars subject to complete heat treatment A



(mag x 200)

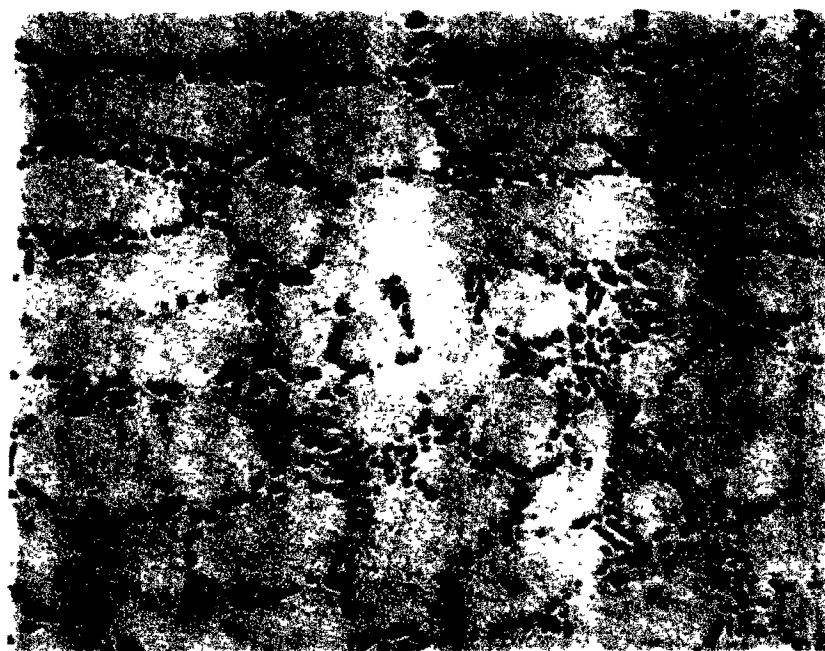
Unmodified



(mag x 200)

Modified

Figure 48b: Metallographic samples of unmodified and modified bars subject to heat treatment B



(mag x 200)

Unmodified



(mag x 200)

Modified

Figure 48c: Metallographic samples of unmodified and modified bars subject to heat treatment C

Heat Treatment	Average Change in D.C. Resistivity (nΩ.m)	
	As a result of solution treatment	As a result of aging only
A	+ 4.49	- 4.26
B	+ 3.06	- 2.97
C	+ 4.23	- 0.65

Table XX: The average change in D.C. resistivity as a result of solution treatment and as a result of aging for A357 alloy.

Heat Treatment	Average Change in D.C. Resistivity ($n\Omega.m$)	
	As a result of solution treatment	As a result of aging only
A	+ 2.72	- 3.20
B	+ 1.90	- 2.43
C	+ 1.82	+ 0.21

Table XXI: The average change in D.C. resistivity as a result of solution treatment and as a result of aging for A356 alloy containing 0.48 wt.% Fe.

Unlike the A356 alloy, heat treatment data of the A357 and A356 (0.48 wt.% Fe) alloys could not be analysed as a function of strontium content. Statistical analysis of the heat treatment vs. strontium content data (Appendix 9) suggested that data could not be graphically represented in a satisfactory way, possibly because too few data points were employed. There were 9 for the A357 alloy and 10 for the A356 (0.48 wt.% Fe) alloy while 26 data points were used in the analysis of the A356 alloy results.

4. DISCUSSION

4.1 Experimental Inaccuracies

A large part of experimental result analysis involves the calculation of experimental inaccuracies. Inaccuracies can be in an absolute form, for example $\pm x \text{ n}\Omega\cdot\text{m}$ or $\pm x \text{ mV}$, or they can be in the form of a percentage. The percentage values indicate the relative importance of inaccuracies upon the resistivity versus strontium content relationship, and can be used in D.C. and A.C. technique comparisons. The percentage inaccuracies were calculated on the basis that the total drop in resistivity ($4.07 \text{ n}\Omega\cdot\text{m}$) and the total increase in ΔV (1.00 mV) upon modification could be represented as 100%. Thus, for example, a $\pm 0.2 \text{ n}\Omega\cdot\text{m}$ inaccuracy is equivalent to an inaccuracy of $\pm 5.0\%$, and similarly a $\pm 0.05 \text{ mV}$ inaccuracy is also equivalent to an inaccuracy of $\pm 5.0\%$.

4.1.1 Instrumental Inaccuracies

The resistivity result from D.C. measurement includes the instrumental inaccuracies of the voltmeter, ammeter, micrometer screw gauge and vernier gauge giving a total instrumental inaccuracy of $\pm 0.20 \text{ n}\Omega\cdot\text{m}$ or $\pm 4.91\%$ (Appendix 10). Although the ΔV value of the A.C. technique apparently includes only the accuracy of the voltmeter, other factors such as the accuracy of the constant current setting, and of the constant voltage setting across the standard bar, and the accuracy of the lock-in amplifier must be taken into account. The total

instrumental inaccuracy of the AC apparatus is $\pm 2.0 \times 10^{-5}$ mV or $\pm 0.002\%$ (Appendix 10).

4.1.2 Inaccuracies Due to Inherent Differences between Similar Bars

In order to obtain a representative resistivity or ΔV value for a typical bar at a particular strontium level, the resistivity or ΔV values of the four bars from one casting were averaged. Standard deviations of the four bars in each casting were obtained and used to compute a standard error of ± 0.80 n Ω .m ($\pm 19.65\%$) and ± 0.189 mV (18.90%), (Appendix 11). This large variation or inaccuracy in resistivity between similar bars is probably due to the differences in porosity between the bars (section 4.3.2).

4.1.3 Dimensional Inaccuracies

The above inaccuracies are based upon the fact that four bars are used to obtain the average resistivity and ΔV values, and that the environmental conditions of all measurements are the same. An additional parameter however must be taken into account when considering ΔV inaccuracies. The A.C. technique is a comparison technique and requires the standard bar and sample bar to be identical in all respects except with respect to the morphology of the eutectic silicon. The measured voltage difference between the two bars is theoretically, due only to the difference in form of eutectic silicon. Practically, however, the bars were not dimensionally identical. The machining tolerances produced bars ranging in diameter from

15.17 mm to 15.35 mm, that is, a maximum diameter difference (δD) of 0.18 mm. In the extreme case where, for example the standard bar is 15.17 mm in diameter, and the sample bar is 15.35 mm in diameter, the maximum error on ΔV (δV) induced by δD alone is $\pm 0.21.2$ mV or 21.2% (Appendix 2). It should be noted that this extreme case would rarely occur, and the majority of measurements were taken using bars with δD less than 0.18 mm giving a δV less than 21.2%. In order to reduce the large inaccuracy due to varying bar diameter, the bars were grouped into three diameter ranges, A, B, and C, with δD values of 0.18 mm, 0.09 mm and 0.04 mm respectively. The corresponding inaccuracies are then 21.2%, 10.6% and 4.7% respectively.

Each set of data, that is, bars of range A, B and C were analysed separately as a function of strontium content and statistical tests showed range B to give the least amount of scatter in the results (section 3.1.2). Although the diameter range with the smallest δD would be expected to give the greatest accuracy, the ΔV values of this range are only the average values of a small number of bars. All A.C. tests were therefore performed using bars within the diameter range B, 15.31 mm to 15.22 mm.

4.1.4 Total Inaccuracies of D.C. and A.C. Techniques

The inaccuracy of the D.C. technique consists of;
instrumental inaccuracies: ± 0.20 n Ω .m or $\pm 4.9\%$

and

inherent differences between $\pm 0.80 \text{ n}\Omega\cdot\text{m}$ or $\pm 19.65\%$
similar bars:

giving a total inaccuracy of $\pm 1.00 \text{ n}\Omega\cdot\text{m}$ or $\pm 24.56\%$

The inaccuracy of the A.C. technique comprises of;

instrumental inaccuracies: $\pm 2.00 \times 10^{-5} \text{ mV}$ or $\pm 0.002\%$

inherent differences be- $\pm 0.189 \text{ mV}$ or $\pm 18.90\%$
tween bars:

and

dimensional inaccuracies: $\pm 0.106 \text{ mV}$ or $\pm 10.60\%$

giving a total inaccuracy of: $\pm 0.296 \text{ mV}$ or $\pm 29.60\%$

4.2 D.C. and A.C. Resistivity

4.2.1 A356 Alloy

The variation in D.C. resistivity with strontium content (figure 30) shows the expected trend that the acicular eutectic silicon imparts a greater resistivity to the A356 alloy than to the modified alloy which contains a fine fibrous eutectic. The drop in resistivity of $4.07 \text{ n}\Omega\cdot\text{m}$ between 0.000 wt. % Sr and 0.44 wt. % Sr is greater than the standard D.C. resistivity error of $\pm 1.00 \text{ n}\Omega\cdot\text{m}$, and can therefore be considered significant. Although the microstructures show modification to be complete at 0.015 wt. % Sr, the resistivity continues to decrease with increasing strontium content up to 0.044 wt. % Sr. This could either be due to a subtle continuation of the modifying process, or the shape of the graph at strontium levels

above 0.015 wt. % Sr could be considered questionable since it is only based on a few scattered data points. More experimental work is needed to determine the variation in resistivity with strontium content at high strontium levels, however it can be concluded from present data that D.C. resistivity can be used to distinguish modified A356 alloys from unmodified A356 alloys, provided that the two alloys are identical in every other respect, and that the environmental conditions in which the two are measured are the same.

The corresponding A.C. results (figure 36) show an expected increase in ΔV with increasing strontium content, since the difference in voltage between a standard unmodified bar and a modified sample is larger than the difference between a standard unmodified bar and a similar unmodified sample. The increase in ΔV of 1.0 mV is greater than the standard A.C. error ± 0.296 mV and can therefore be considered significant. The D.C. and A.C. graphs (figures 30 and 36) can be directly related. One is obviously the inverse of the other with the D.C. graph reaching a minimum resistivity at 0.044 wt. % Sr, and the A.C. graph reaching a maximum ΔV at 0.044 wt. % Sr. The form of the A.C. graph at high strontium contents is again questionable; however, it can be concluded that the A.C. technique is a satisfactory method with which to distinguish a modified alloy from an unmodified alloy.

4.2.2 A357 Alloy

The variation of D.C. resistivity with strontium content for the A357 alloy containing a high magnesium content (figure 33) is very different from the variation for the A356 alloy (figure 30). Magnesium has a modifying effect on A356 alloys and hence the 0.000 wt. % Sr alloy exhibits a partially modified structure (figure 32a). There is therefore no great change in eutectic morphology with increasing strontium content, and accordingly there is no great variation in resistivity. The slight decrease of 0.25 n Ω .m at the low strontium contents could well be due to the change in eutectic morphology from partially modified to completely modified; however, with consideration of experimental inaccuracies of ± 1.00 n Ω .m, the small drop in resistivity appears to be insignificant. In conclusion, D.C. resistivity cannot be used to measure modification in A357 alloys. From the micrographs (figure 32b) modification is complete at a lower strontium content (0.007 wt.% Sr) than for the A356 alloy (0.015 wt. % Sr). This is due to the modifying effect of magnesium. The A357 alloy also differs from the A356 alloy with respect to the resistivity value of the modified alloy. The resistivity of the modified A357 alloy is higher (43.50 n Ω .m) than that of the A356 alloy (40.75 n Ω .m) due to the presence of Mg₂Si Chinese script within the eutectic silicon phase.

The A.C. results for the A357 alloy (figure 37) are again an inverse form of the D.C. results (figure 30). There is a slight increase in ΔV (0.20 mV) at low strontium concentrations which lies within the inaccuracy range of ± 0.296 mV., and the A357 modified alloys exhibit a lower ΔV value (0.35 mV) than the modified A356 alloy (0.9 mV). Similar conclusions can be drawn that the A.C. technique, like the D.C. technique, cannot be used to control modification of A357 alloys.

4.2.3 A356 Alloy Containing 0.48 wt. % Fe

Iron does not have the modifying effect of magnesium. The variation of D.C. resistivity with strontium content for the A356 alloy with a high iron content (0.48 wt. % Fe, figure 34), is similar to that of the A356 alloy (0.20 wt. % Fe, figure 30). There is a significant decrease of 2.41 n Ω .m between the unmodified and modified alloy, implying that D.C. resistivity can be used to monitor modification of A356 alloys containing high iron concentrations.

The corresponding A.C. results (figure 38) show a significant increase in resistivity of 0.35 mV between unmodified and modified alloys, and therefore the A.C. technique can also be used to monitor modification in A356 alloys with high iron contents.

4.3 Factors Affecting Resistivity

Resistivity is dependent upon many variables and in order to control these during resistivity measurement, it was

necessary to investigate each factor separately. Temperature was varied and its effects upon resistivity found. The effects of porosity and eutectic segregation were also analysed.

4.3.1 Temperature

The variation of D.C. resistivity with temperature is linear over the temperature range -10°C to 24°C (figure 39). The temperature coefficient of resistivity, $0.1 \text{ n}\Omega\cdot\text{m K}^{-1}$, is the same as that for pure aluminum because the Al-Si-Mg alloy is primarily composed of an aluminum matrix. The presence of eutectic silicon causes no change in resistivity coefficient, but it does increase the absolute resistivity. This absolute resistivity varies with the morphology of eutectic silicon (figure 39). Unmodified alloys have the highest resistivities, undermodified alloys have lower resistivities and the modified and overmodified alloys exhibit the lowest resistivities.

Temperature fluctuations are especially important in D.C. resistivity measurement. For example, an increase in temperature of only 5°C will cause the resistivity to increase by $0.5 \text{ n}\Omega\cdot\text{m}$. When dealing with a $4.07 \text{ n}\Omega\cdot\text{m}$ resistivity range (the difference in resistivity between an unmodified and modified bar) any small temperature fluctuations will result in significant changes in resistivity. All samples to be compared using the D.C. resistivity technique must be measured at the same temperature. Temperature is a very difficult parameter to control in foundry conditions, therefore the temperature independent differential technique was studied. The difference

in voltage between an unmodified bar and a sample bar was measured over the temperature range -10°C to 24°C . The absolute resistivity of each bar changed with temperature, however, due to their identical thermal coefficients, the difference in resistivity between the two bars remained constant, (table XIII). The resistivity of sample bars containing various levels of strontium was measured. The unmodified sample exhibited the smallest constant ΔV values as expected, and the modified bar exhibited the largest constant ΔV value.

In summary, resistivity is considerably temperature dependent therefore the temperature independent A.C. technique would be favoured over the D.C. technique in foundry practice.

4.3.2 Porosity

Hydrogen porosity is a well known defect in aluminum castings. Although all melts were degassed for the same time period, the castings showed various porosity contents ranging from 0.00 vol % to 0.99 vol %. Average porosity and average resistivity values of four bars from the same casting were used to increase the accuracy of the results. Comparisons that were made were therefore between castings and not between individual bars. No two castings of identical strontium contents were obtained due to the unpredictable dissolution behaviour of strontium, and so castings with similar strontium contents were compared, (table XIV). In all comparisons but one, the casting with the highest resistivity exhibited the highest porosity content. The two unmodified castings were the

exception, with the highest resistivity occurring in the casting with lowest porosity. Strontium is known to increase hydrogen pick up in melts, and therefore has some effect upon porosity.

In summary, an increase in porosity will cause an increase in resistivity. In order to quantitatively analyse porosity, the standard deviations of porosity for the four bars in each casting were obtained and used to compute a standard error of ± 0.110 vol % porosity for each porosity result (Appendix 11). In other words, four bars, identical in every respect, can vary in porosity content by ± 0.110 vol % porosity. The errors computed in section 4.1 show that the inaccuracies due to inherent differences between identical bars are 19.55% for the D.C. technique and 18.9% for the A.C. technique. Since porosity was the only parameter found to vary between identical bars, it can be assumed that the inherent differences between identical bars are due to porosity differences. The variation of ± 0.110 vol % porosity therefore produces $\pm 19.55\%$ and $\pm 18.90\%$ inaccuracies in the D.C. and A.C. results respectively. Inaccuracies due to porosity are very large when compared with total inaccuracies of $\pm 24.63\%$ and $\pm 29.6\%$ of the D.C. and A.C. techniques. The scatter of results in the D.C. and A.C. versus strontium content curves can therefore be attributed largely to porosity variations.

4.3.3 Eutectic Segregation

During the course of the work, sample bar diameter was changed by machining and was found to affect D.C. resistivity. Microscopic examination revealed the presence of more eutectic in the centre of bars and hence experiments were conducted to measure the amount of eutectic across the sample bar diameter. A 10% increase in the amount of eutectic towards the centre of the bar was found and could certainly account for the increase in resistivity with decreasing bar diameter.

This variation is caused by normal segregation where the first solid phase to freeze during solidification (primary aluminum) is depleted in silicon. The liquid ahead of the solid-liquid interface which proceeds toward the centre of the bar is consequently enriched in silicon content. Thus the centre which is the last part of the bar to solidify, has a higher silicon content than the rest of the bar and therefore contains a greater proportion of eutectic. The variation is the same for unmodified, undermodified and modified bars because the change in silicon content across the bar only affects the amount of eutectic and not the eutectic morphology.

4.4 Heat Treatment

4.4.1 Introduction

The total inaccuracies of the D.C. and A.C. techniques were $\pm 1.00 \text{ n}\Omega\cdot\text{m}$ and $\pm 0.296 \text{ mV}$ respectively and were calculated taking into account instrumental inaccuracy, variation in resistivity between bars of the same strontium content, and in

the case of the A.C. technique, also taking into account the effects of machining tolerances. These inaccuracies were based on the premise that the resistivity values for the D.C. technique were an average of the resistivity of four bars, and the ΔV values were an average of ΔV values for two, three or four bars. (This variation in number of values for the average stems from the use of bars within range B diameter limits, section 2.4.2).

The heat treatment results, however, were those of single bars. No average values could be used because each of the bars obtained from one casting was heat treated differently. It is therefore valid to assume that the inaccuracies in the heat treatment results are at least $\pm 1.00 \text{ n}\Omega\cdot\text{m}$ and $\pm 0.296 \text{ mV}$ and could well be greater than these values.

4.4.2 Heat Treatment and Resistivity

Three heat treatments, A, B and C were performed on bars as explained in section 2.6. The resistivity values of all 26 A356 bars after solution treatment and after complete heat treatment were averaged (table XVIII), and it was found that the bars exhibited an average increase in resistivity on solution treatment of $2.78 \text{ n}\Omega\cdot\text{m}$ and an average decrease in resistivity on subsequent aging of $2.62 \text{ n}\Omega\cdot\text{m}$. These are significant changes since the standard D.C. error is $\pm 1.00 \text{ n}\Omega\cdot\text{m}$.

The increase in resistivity on solution treatment is mainly due to the effect of ripening and dissolution. The ripening process increases the resistivity of the alloy because it is a

eutectic coarsening process. Dissolution produces a solid solution which after quenching contains relatively high contents of silicon and magnesium. The atomic lattices of the solid solution are distorted to accomodate the excess silicon and magnesium atoms, and therefore impart a high resistivity on the alloy.

Spheroidization does in fact decrease resistivity because it changes plates and needles to spheroidal particles. An acicular eutectic is well known to give an alloy a higher resistivity than a spheroidal eutectic.

Homogenization would also be expected to decrease resistivity to a small extent because the aluminum matrix becomes more uniform, as the solute concentrations become uniform.

In conclusion, it can be postulated that the increase in resistivity due to solution treatment occurs because the resistivity effects of ripening and dissolution are greater than those of spheroidization and homogenization.

The decrease in resistivity on aging can possibly be attributed to the depletion of the silicon and magnesium concentrations in the matrix, however more extensive experimental work is necessary to substantiate this. It is thought that the depletion of solute content in the lattice allows the distorted lattice to become more uniform, and that a uniform lattice will impart a low resistivity to the alloy.

Ripening and spheroidization have different effects upon modified and unmodified structures and therefore studies were

performed to examine heat treatment as a function of strontium content.

For all types of heat treatment the modified alloy showed a greater increase in resistivity than the unmodified alloy upon solution treatment (table XIX). In every case, these differences were greater than the standard D.C. resistivity error of $\pm 1.00 \text{ n}\Omega\cdot\text{m}$. Ripening, an effect which increases resistivity, occurs more readily in modified alloys than in unmodified alloys due to the small interparticle distances in modified alloys. Spheroidization, however, an effect which decreases resistivity occurs to a lesser extent in modified alloys. In conclusion, the resistivity of modified alloys increases greatly on solution treatment due to extensive ripening and little spheroidization, while the resistivity of unmodified alloys increases slightly due to some ripening and much spheroidization.

Upon aging, all samples exhibit a decrease in resistivity and there is every indication that the decrease was approximately the same for all bars, irrespective of previous solution treatment time or state of modification. All bars were subject to the same aging treatment and all exhibited the same decrease on aging (table XIX) within the D.C. standard range of error (which is at least $\pm 1.00 \text{ n}\Omega\cdot\text{m}$).

Throughout the work no significant trend could be found between type of heat treatment and resistivity values and the micrographs of all modified and all unmodified alloys after

complete heat treatment were very much the same. Recent work⁽²⁸⁾ suggests that dissolution, ripening and spheroidizing processes occur within the first few hours of solution treatment and therefore no significant resistivity differences would be expected when comparing bars subjected to 8, 24 and 48 hours of solution treatment.

4.5 Comparison between D.C. and A.C. Resistivity Techniques

The D.C. resistivity of a cast Al-Si-Mg alloy is the sum of the resistivities due to eutectic morphology, dissolved impurity atoms, dislocations, vacancies, grain boundaries and porosity and yields no information about the effect of a single factor upon the total resistivity. The differential A.C. technique however, is a comparison technique and can measure changes in individual resistivity effects. The method uses a standard reference specimen and compares this with the sample under examination. In this way, the effects of resistivity due to factors that are present in both the standard and the sample are eliminated.

Although porosity was present in both standard and sample bars, it was not present in equal amounts. The effect of resistivity due to porosity was therefore partially eliminated using the A.C. technique where only the difference in porosity between the standard and sample affected the results.

Although porosity produces some inaccuracy in the results, the difference in resistivity due to porosity variations as measured in the A.C. technique is certainly less than the

absolute resistivity due to porosity measured in the D.C. technique. The inaccuracies due to porosity were calculated as 19.55% for the D.C. technique and 18.90% for the A.C. technique, (Appendix 11).

Instrument errors of the A.C. technique were less than those of the D.C. technique. This is to be expected since the direct ΔV values of the A.C. technique are not calculated from other parameters which themselves exhibit inaccuracies.

Considering solely the inaccuracies due to porosity and instrumental errors, it can be seen that the A.C. technique is more favourable, exhibiting 19% inaccuracy as compared with the 24.6% inaccuracy of the D.C. technique.

An additional factor however that had to be considered in the experimental work was the machining tolerances of the bars. These had no effect on D.C. resistivity but a 10.6% effect on A.C. results. The experimental results therefore showed a 24.6% inaccuracy in D.C. data and a 29.6% inaccuracy in A.C. data. Although the D.C. experimental data had the smaller inaccuracies the A.C. technique would certainly be favoured in foundry practice over the D.C. technique if bar machining tolerances could be eliminated.

5. SUMMARY

Both D.C. and A.C. resistivity techniques are satisfactory non-destructive techniques that can distinguish an unmodified A356 alloy from a modified A356 alloy and the results of both techniques can be directly related, where one is the inverse of the other. The work conducted on A357 alloys and A356 alloys containing 0.48 wt. % Fe, was limited, and further data points should be obtained to reach more satisfactory conclusions. The trends that were observed, however, do correspond to the microstructures and do suggest that modification can also be monitored in A356 alloys with 0.48% Fe contents. Magnesium, on the other hand, was found to have a modifying effect upon Al-Si-Mg alloys, and modification of A357 alloys cannot be studied using resistivity techniques.

Both D.C. and A.C. techniques apparently produced the same amount of scatter in the results implying that the scatter was due to some inherent variations in the castings and not resistivity measurement technique. There is sufficient evidence to assume that the inherent variations in the castings were due to porosity, and produced inaccuracies of approximately 19% in the results. If the resistivity techniques are to be improved it is imperative that the porosity of all castings must either be eliminated or kept constant.

Another factor to be considered if improvements are to be made is sample bar diameter. Firstly the presence of eutectic

segregation suggests that all bars must be cast to the same diameter, and secondly the sensitivity of the A.C. technique to variations in machined bar diameter suggests that bars must not be machined. Ideally, a mold should be developed which produces bars of constant diameter and good surface finish. The A.C. technique would then certainly be favoured in foundry practice; it has a low instrumental error and is insensitive to local temperature fluctuations.

Resistivity techniques can also be used in the heat treatment study of Al-Si-Mg alloys. The resistivity of bars increases on solution treatment and decreases on subsequent ageing. Modified alloys show a greater increase in resistivity upon solution treatment than unmodified alloys. The actual reasons for this are unclear at present but no doubt involve the processes of dissolution, spheroidization ripening and homogenisation.

6. CONCLUSIONS AND SUGGESTIONS FOR FURTHER WORK

In undertaking this work, the general objective was to study the resistivity technique in order to discover if it could be used in the foundry to monitor modification of Al-Si-Mg alloys. More specifically, the following questions were to be answered:

1. Is the change in resistivity between modified and unmodified Al-Si-Mg alloys due to the change in the form of the eutectic silicon or due to some other change such as composition of the aluminum matrix?
2. To what degree does resistivity due to porosity affect the resistivity measurements?
3. Are the inaccuracies observed in the results by Closset and Gruzleski⁽¹⁵⁾ (figure 16) due to poor apparatus or sample variation, and does differential electrical resistivity yield more accurate results?
4. Can electrical resistivity techniques be used to study compositional influences at various levels of modification?
5. Can the electrical resistivity technique be used to study heat treatment of Al-Si-Mg alloys at various levels of modification?

From the experimental results and discussions presented in the preceding chapters it is possible to use electrical resistivity to monitor modification of Al-Si-Mg alloys. In general, the following conclusions can be made:

1. There is every indication that the change in resistivity upon modification is due to changes in eutectic morphology; results show that there is no change in silicon content in the aluminum matrix upon modification.

2. Porosity increases the resistivity of Al-Si-Mg alloys and if the resistivities of bars are to be accurately compared then the porosity content of the bars must be the same.

3. The scatter in D.C. resistivity results is not due to poor instrumentation but due to sample variations. These sample variations are largely due to porosity and are therefore also observed in the differential A.C. technique.

4. Differential resistivity techniques will yield more accurate results than D.C. techniques provided that bars are produced with identical diameters.

5. The differential resistivity technique would be favoured in foundry practice primarily because it is temperature independent.

6. Both D.C. and A.C. resistivity techniques can be used to study compositional influences at various levels of modification. The results from these studies indicate that resistivity can successfully monitor modification in A356 alloys and A356 (0.48 wt. % Fe), however, it cannot successfully monitor modification in A357 alloys with higher magnesium contents.

7. Both D.C. and A.C. resistivity techniques can be used to study the heat treatment of Al-Si-Mg alloys at various levels

of modification. Results have shown an increase in resistivity on solution treatment and a decrease on subsequent aging. Additionally, modified alloys exhibit a greater increase in resistivity upon solution treatment than unmodified alloys.

The author suggests further work based on the results of this thesis:

1. The improvement of the resistivity techniques for use in the foundry;
 - a) A method must be developed by which the porosity of cast samples can be monitored, in order to produce bars of constant porosity level.
 - b) A mold should be developed that can produce bars with identical diameters and smooth surface finishes.
 - c) Studies of resistivity and modification should be performed on all Al-Si-Mg foundry alloys in order to identify the alloys that are sensitive to resistivity techniques.
2. The use of resistivity to monitor heat treatment in situ;
 - a) Studies of the variation in resistivity during heat treatment could be performed to gain an insight into the microstructural changes that occur upon heat treatment.
 - b) In situ resistivity data could be used to predict optimum heat treatment conditions.

- (
- c) Molds of different diameters could be developed in order to study the effects of cooling rate on heat treatment.

REFERENCES

1. L.F. Mondolfo. "Aluminum Alloys, Structure and Properties." Butterworth 1976, England. 1st ed., p. 368.
2. Metals Handbook, 9th ed., ASM, Metals Park, Ohio. Vol. 2, p. 164-167.
3. B. Closset and J.E. Gruzleski. "Structure and Properties of Hypoeutectic Al-Si-Mg Alloys Modified with Pure Strontium." Met. Trans., Vol. 13A, June 1982, p. 945, AIME.
4. G. Nagel, and R. Portalier. "Structural Modification of Aluminum-Silicon Alloys by Antimony Treatment." AFS International Cast Metals Journal, Dec. 1980.
5. A. Hellawell. "The Growth and Structure of Eutectics with Silicon and Germanium," Progress in Materials Science, Vol. 15, no. 1, 1970.
6. B.M. Thall and B.J. Chalmers. "Modification in Aluminum-Silicon Alloys." Inst. Metals, Vol. 77, 1950, p. 79.
7. V. de L. Davies and J.M. West. "Factors Affecting the Modification of Al-Si Eutectic," J. Inst. Metals, Vol. 92, 1963-1964, p. 175.
8. P.B. Crosley and L.F. Mondolfo, Modern Castings, Vol. 49, 1966, p. 63.
9. R.C. Harris, S. Lipson, and H. Rosenthal. "Tensile Properties of Al-Si-Mg Alloys and the Effects of Sodium Modification." Trans. AFS, Vol. 64, 1956, p. 470.
10. K.R. Todd and L.G. Yenta. "The Effect of Iron and Magnesium on Strontium Modified Al-Si Alloys." Dept. of Mining and Metallurgical Engineering, McGill University, Montreal, Quebec, Canada.
11. R.C. Lemon and H.Y. Hunsicker. "New Aluminum Permanent Mold Casting Alloys C355 and A356," Trans. AFS, Vol. 64, 1956, p. 255.
12. W.R. Opie and N.J. Grant: Foundry Vol. 78, 1950, p. 104. Also R. Jay and A. Cibula: Foundry Trade J., Vol. 101, 1956, p. 131 and 407.
13. B. Closset and J.E. Gruzleski. "A Study on the Use of Pure Metallic Strontium in the Modification of Al-Si Alloys," AFS Trans. Vol. 42, 1981, p. 801.

14. B. Closset, J.E. Gruzleski, S.A. Argyropoulos and H. Oger. "The Quantitative Control of Modification in Al-Si Foundry Alloys Using a Thermal Analysis Technique." Trans. AFS 1983, in press.
15. B. Closset, H. Oger and J.E. Gruzleski. "Methods for Non-Destructive and Quantitative Evaluation of Microstructures in Al-Si-Mg Alloys." Trans. AFS 1983, in press.
16. Handbook of Chemistry and Physics. 62nd ed. 1981-1982 CRC Press, p. F-112.
17. R.A.L. Drew, W.E. Muir and W.M. Williams. "Differential Resistivity Measurement for Monitoring Annealing." Met. Trans., Vol. 14A, Feb. 1983, p. 175.
18. K. Schröder. "Yield Phenomena in Copper-Arsenic Alloys." Procedures of the Philosophical Society, Vol. LXXII, 1958, I.
19. L.J. Cuddy. "An Electrical Resistivity Study of Deformation and Recovery of Iron at Low Temperatures." United States Steel Corporation, Research Centre, Monroeville, Pennsylvania, 1965.
20. V.M. Vinokur and V.Ya. Kravchenko. "Temperature Dependence of the Resistivity of a Metal with Dislocations." Sov. Physics. JETP Vol. 47(2), Feb. 1978, p. 369.
21. T. Alp, I. Brough, S.J. Sanderson, and K.M. Entwistle. "A Study of the Stability of Intermediate Precipitates in an Al-4.07 wt. % Cu Alloy Using Electrical Resistivity Measurements." Metals Science Vol. 9, 1975, p. 353.
22. K. Tanaka and T. Watanabe. "An Electrical Resistivity Study of Lattice Defects in Deformed Iron." J. of Applied Physics, Vol. 11, no. 10, 1972, p. 1429.
23. W.G. Pfann. "Zone Melting." Wiley and Sons Inc. 2nd ed. p. 170.
24. H. Oger, B. Closset and J.E. Gruzleski. "Characterization of the Eutectic Microstructure in Al-Si Foundry Alloys by Electrical Resistivity." Trans. AFS 1983, in press.
25. C. Chatfield. "Statistics for Technology." 2nd ed. 1979, Chapman and Hall, London, Halstead Press.
26. Handbook of Chemistry and Physics. 55th ed. 1974-1975. CRC Press p. B-4.

27. Metals Handbook, 9th ed., ASM, Metals Park, Ohio, Vol. 2, p. 64.
28. Work by B. Closset and R.A.L. Drew, McGill University, Dept. of Mining and Metallurgical Engineering, Montreal, Canada. To be Published.
27. Lange's Handbook of Chemistry, McGraw-Hill Book Co., New York, 1973.
30. D.E. Kundle and L.A. Willey: J. Materials, Vol. 1, 1966, p. 226.

APPENDICES

Appendix	Page
1. Spectrochemical Analyses of the Castings	146
2. Calculation of Errors in ΔV due to Machining Tolerances	150
3. Illustration of the Density Technique for Quantitative Determination of Porosity	151
4. Sample Calculation of Theoretical Density	152
5. D.C. Resistivity Data	153
6. A.C. Resistivity Data	161
7. Experimental Porosity Data	173
8. Heat Treatment Data	181
9. Results of Statistical Analysis of Heat Treatment Data	194
10. Calculation of Instrumental Inaccuracies for the D.C. and A.C. Techniques	198
11. Calculation of the Standard Resistivity Error between Bars of the Same Strontium Content	200

APPENDICES

Introduction

The experimental data for each sample bar are given where each sample is identified by using its sample number as follows:

VX-YZ

- (i) V denotes the type of Al-Si-Mg alloy used; A (A356 alloy); B (A357 alloy); C (A356 alloy containing 0.48 wt. % Fe).
- (ii) X denotes the number of the experiment in which two castings were poured.
- (iii) Y denotes the casting number within the particular experiment; 1 (first casting to be poured); 2 (second casting to be poured, usually having a higher strontium content than the first).
- (iv) Z denotes the bar location within the casting (figure 49).

When reference is made to a particular casting rather than a particular bar, the casting is identified as VX-Y.

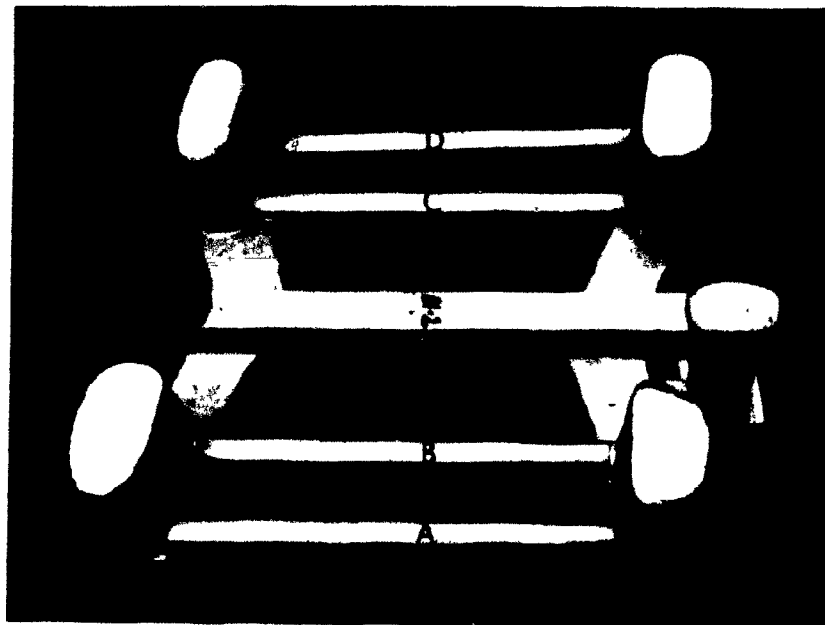


Figure 49: An Al-Si-Mg alloy casting showing the location of bars A, B, C and D.

APPENDIX 1Spectrochemical Analyses of the Castings

Casting Number	Element (wt. %)				
	Si	Fe	Cu	Mn	Mg
A1-1	7.076	0.061	0.008	0.000	0.366
A1-2	7.088	0.055	0.008	0.000	0.345
A2-1	7.038	0.058	0.008	0.000	0.361
A2-2	7.105	0.066	0.015	0.000	0.370
A3-1	7.485	0.069	0.007	0.008	0.372
A3-2	7.144	0.074	0.007	0.006	0.382
A4-1	7.333	0.069	0.006	0.004	0.369
A4-2	7.202	0.072	0.007	0.009	0.381
A5-1	7.209	0.056	0.006	0.009	0.355
A5-2	7.454	0.063	0.006	0.009	0.350
A6-1	7.385	0.059	0.007	0.011	0.364
A7-1	7.538	0.069	0.007	0.011	0.357
A8-1	7.332	0.066	0.007	0.012	0.375
A8-2	7.423	0.071	0.007	0.011	0.350
A9-1	6.913	0.061	0.008	0.021	0.356
A9-2	6.908	0.062	0.008	0.021	0.335
A10-1	7.037	0.058	0.007	0.021	0.340
A10-2	6.937	0.073	0.008	0.021	0.360
A11-1	6.993	0.064	0.008	0.022	0.359
A11-2	6.987	0.075	0.008	0.022	0.331
A12-1	7.035	0.062	0.007	0.022	0.373
A12-2	6.972	0.065	0.007	0.021	0.370
A13-1	7.266	0.050	0.007	0.021	0.360
A13-2	6.197	0.065	0.007	0.021	0.362
A14-1	6.990	0.074	0.000	0.003	0.323
A14-2	6.575	0.081	0.000	0.000	0.306

continued.

Spectrochemical Analysis of Castings (cont'd)

Casting Number	Element (wt. %)				
	Cr	Ni	Zn	Ti	Sr
A1-1	0.000	0.024	0.000	0.060	0.000
A1-2	0.000	0.026	0.000	0.059	0.015
A2-1	0.000	0.025	0.000	0.060	0.002
A2-2	0.000	0.022	0.037	0.061	0.006
A3-1	0.000	0.020	0.015	0.064	0.000
A3-2	0.000	0.022	0.095	0.059	0.005
A4-1	0.000	0.023	0.000	0.063	0.003
A4-2	0.000	0.022	0.000	0.063	0.008
A5-1	0.000	0.021	0.000	0.061	0.007
A5-2	0.000	0.021	0.000	0.059	0.013
A6-1	0.000	0.019	0.000	0.059	0.004
A7-1	0.000	0.019	0.000	0.061	0.014
A8-1	0.000	0.019	0.000	0.060	0.017
A8-2	0.000	0.019	0.000	0.061	0.013
A9-1	0.006	0.012	0.028	0.063	0.011
A9-2	0.006	0.012	0.028	0.063	0.069
A10-1	0.006	0.012	0.028	0.065	0.012
A10-2	0.006	0.012	0.028	0.064	0.069
A11-1	0.007	0.012	0.049	0.063	0.010
A11-2	0.007	0.012	0.056	0.062	0.028
A12-1	0.007	0.012	0.029	0.064	0.024
A12-2	0.006	0.012	0.029	0.063	0.029
A13-1	0.005	0.008	0.028	0.068	0.021
A13-2	0.005	0.008	0.028	0.069	0.025
A14-1	0.002	0.001	0.011	0.065	0.044
A14-2	0.001	0.001	0.010	0.061	0.058

N.B. The compositional balance is aluminum. continued.

Spectrochemical Analysis of Castings (cont'd)

Casting Number	Element (wt. %)				
	Si	Fe	Cu	Mn	Mg
B1-1	7.097	0.056	0.007	0.023	0.759
B1-2	7.172	0.062	0.007	0.023	0.783
B2-1	7.077	0.057	0.007	0.023	0.766
B3-1	7.338	0.056	0.007	0.023	0.783
B3-2	7.158	0.055	0.007	0.023	0.756
B4-1	6.482	0.070	0.000	0.000	0.653
B4-2	6.678	0.074	0.000	0.001	0.665
B5-1	8.143	0.089	0.000	0.007	0.682
B5-2	8.654	0.091	0.000	0.009	0.724
C1-1	7.681	0.456	0.000	0.007	0.348
C1-2	7.826	0.477	0.000	0.006	0.347
C2-1	7.762	0.514	0.000	0.007	0.348
C2-2	7.850	0.526	0.000	0.007	0.349
C3-1	7.319	0.434	0.009	0.011	0.335
C3-2	7.101	0.456	0.009	0.010	0.320
C4-1	6.789	0.464	0.000	0.009	0.309
C4-2	7.002	0.480	0.000	0.010	0.319
C5-1	7.305	0.478	0.000	0.011	0.337
C5-2	7.447	0.493	0.000	0.013	0.334

continued.

Spectrochemical Analysis of Castings (cont'd)

Casting Number	Element (wt. %)				
	Cr	Ni	Zn	Ti	Sr
B1-1	0.007	0.012	0.027	0.068	0.000
B1-2	0.007	0.012	0.027	0.068	0.014
B2-1	0.007	0.012	0.027	0.068	0.007
B3-1	0.007	0.012	0.027	0.068	0.023
B3-2	0.007	0.012	0.027	0.068	0.037
B4-1	0.002	0.001	0.011	0.062	0.000
B4-2	0.002	0.002	0.012	0.062	0.020
B5-1	0.006	0.003	0.000	0.063	0.044
B5-2	0.006	0.003	0.000	0.064	0.068
C1-1	0.005	0.002	0.000	0.063	0.000
C1-2	0.010	0.002	0.000	0.062	0.015
C2-1	0.000	0.002	0.000	0.063	0.014
C2-2	0.004	0.002	0.000	0.062	0.022
C3-1	0.001	0.002	0.011	0.064	0.006
C3-2	0.001	0.002	0.011	0.063	0.011
C4-1	0.055	0.002	0.000	0.063	0.016
C4-2	0.052	0.002	0.000	0.064	0.017
C5-1	0.034	0.002	0.000	0.065	0.061
C5-2	0.046	0.002	0.000	0.067	0.086

N.B. The compositional balance is aluminum.

APPENDIX 2

Calculation of Errors in ΔV due to Machining Tolerances

Unavoidable machining tolerances gave bar diameters ranging from 15.17 mm to 15.35 mm, that is, a maximum diameter difference between bars of 0.18 mm. The error incurred on ΔV can then be calculated as follows:

$$\frac{\delta V}{V} = \frac{2\delta D}{D}$$

where δV = error induced on ΔV

V = voltage across standard bar = 9.0 mV

δD = maximum diameter difference between bars

D = average bar diameter = 15.26 mm

For bars included in diameter range A, the maximum difference in diameter between bars is 0.18 mm giving an error on ΔV of ± 0.212 mV.

For bars included in diameter range B, the maximum difference in bar diameter between bars is 0.09 mm giving an error on ΔV of ± 0.106 mV.

For bars included in diameter range C, the maximum difference in bar diameter between bars is 0.04 mm giving an error on ΔV of ± 0.047 mV.

APPENDIX 3Illustration of the Density Technique for Quantitative
Determination of Porosity

Step 1: Calculate the experimental density - use weight of sample in air and in water.

$$\begin{aligned} \text{Experimental Density} &= \frac{\text{Mass in Air}}{\text{Mass in Air} - \text{Mass in Water}} \\ &\times \text{Density of Water} \end{aligned}$$

The density of water was taken from published values⁽²⁹⁾.

Step 2: Calculate theoretical density (Appendix 4)

Step 3: Calculate amount of porosity.

$$\begin{aligned} \text{Porosity, vol. \%} &= \frac{\text{Theoretical Density} - \text{Experimental Density}}{\text{Theoretical Density}} \\ &\times 100\% \end{aligned}$$

APPENDIX 4Sample Calculation of Theoretical Density⁽³⁰⁾

Alloy Composition: 7.076% Si, 0.061% Fe, 0.008% Cu, 0.366% Mg,
0.024% Ni, 0.060% Ti, balance Al.

Assume a 100 gm sample and calculate the mass and volume of
each species in the alloy.

Element	1/Density, cm ³ /gm	Amount Present, gm	Volume, cm ³
Si	0.429	7.076	3.035
Fe	0.127	0.061	0.008
Cu	0.112	0.008	0.001
Mg	0.575	0.366	0.210
Ni	0.112	0.024	0.003
Ti	0.220	0.060	0.013
Al	0.371	92.405	34.282
Total		100.000	37.552

$$\begin{aligned}
 \text{Theoretical Density} &= \frac{\text{Total Amount Present, gm}}{\text{Total Volume, cm}^3} \\
 &= \frac{100}{37.552} = 2.663 \text{ gm/cm}^3
 \end{aligned}$$

APPENDIX 5D.C. Resistivity Data

Sample	D.C. Resistivity (nΩ.m)	Average D.C. Resistivity (nΩ.m)
A1-1A	44.39	
A1-1B	45.38	
A1-1C	44.68	44.82
A1-1D	41.90	
A1-2A	42.40	
A1-2B	41.71	
A1-2C	41.72	41.96
A1-2D	41.99	
A2-1A	43.39	
A2-1B	42.80	
A2-1C	42.34	42.90
A2-1D	43.08	
A2-2A	45.01	
A2-2B	44.43	
A2-2C	44.08	44.59
A2-2D	44.84	

D.C. Resistivity Data (cont.)

Sample	D.C. Resistivity (nΩ.m)	Average D.C. Resistivity (nΩ.m)
A3-1A	46.47	
A3-1B	46.10	
A3-1C	45.73	44.79
A3-1D	44.85	
A3-2A	44.56	
A3-2B	44.44	
A3-2C	43.94	44.21
A3-2D	43.88	
A4-1A	45.14	
A4-1B	44.27	
A4-1C	44.31	44.66
A4-1D	44.90	
A4-2A	44.28	
A4-2B	43.28	
A4-2C	43.53	43.73
A4-2D	43.84	
A5-1A	43.42	
A5-1B	42.79	
A5-1C	42.62	42.74
A5-1D	42.31	
A5-2A	42.34	
A5-2B	41.88	
A5-2C	41.93	42.12
A5-2D	42.34	

D.C. Resistivity Data (cont.)

Sample	D.C. Resistivity (n Ω .m)	Average D.C. Resistivity (n Ω .m)
A6-1A	44.16	
A6-1B	44.51	
A6-1C	44.84	44.50
A6-1D	47.93	
A7-1A	41.72	
A7-1B	41.48	
A7-1C	41.59	41.67
A7-1D	41.89	
A8-1A	42.40	
A8-1B	41.48	
A8-1C	41.99	41.91
A8-1D	41.77	
A8-2A	42.34	
A8-2B	41.80	
A8-2C	41.70	42.08
A8-2D	42.48	
A9-1A	42.82	
A9-1B	42.05	
A9-1C	41.97	42.32
A9-1D	42.46	
A9-2A	41.84	
A9-2B	42.16	
A9-2C	42.13	42.22
A9-2D	42.75	

D.C. Resistivity Data (cont.)

Sample	D.C. Resistivity (n Ω .m)	Average D.C. Resistivity (n Ω .m)
A10-1A	42.45	42.09
A10-1B	41.71	
A10-1C	41.70	
A10-1D	42.51	
A10-2A	42.51	42.10
A10-2B	41.14	
A10-2C	41.77	
A10-2D	42.96	
A11-1A	43.02	42.50
A11-1B	42.33	
A11-1C	41.75	
A11-1D	42.91	
A11-2A	42.51	42.08
A11-2B	41.54	
A11-2C	41.91	
A11-2D	42.34	
A12-1A	43.14	42.60
A12-1B	41.35	
A12-1C	42.22	
A12-1D	43.71	
A12-2A	42.74	42.12
A12-2B	41.77	
A12-2C	42.27	
A12-2D	41.71	

D.C. Resistivity Data (cont.)

Sample	D.C. Resistivity (n Ω .m)	Average D.C. Resistivity (n Ω .m)
A13-1A	41.26	40.91
A13-1B	40.46	
A13-1C	40.38	
A13-1D	41.54	
A13-2A	41.66	40.94
A13-2B	40.38	
A13-2C	40.24	
A13-2D	41.47	
A14-1A	41.83	41.41
A14-1B	40.85	
A14-1C	40.84	
A14-1D	42.11	
A14-2A	42.16	41.31
A14-2B	40.59	
A14-2C	40.57	
A14-2D	42.94	
B1-1A	44.68	44.18
B1-1B	43.53	
B1-1C	44.05	
B1-1D	44.45	
B1-2A	43.99	43.40
B1-2B	42.84	
B1-2C	42.84	
B1-2D	43.94	

D.C. Resistivity Data (cont.)

Sample	D.C. Resistivity (n Ω .m)	Average D.C. Resistivity (n Ω .m)
B2-1A	43.70	43.31
B2-1B	43.02	
B2-1C	42.79	
B2-1D	43.76	
B3-1A	43.99	43.59
B3-1B	43.42	
B3-1C	43.02	
B3-1D	43.94	
B3-2A	44.16	43.67
B3-2B	43.35	
B3-2C	43.36	
B3-2D	43.93	
B4-1A	43.99	43.68
B4-1B	43.30	
B4-1C	43.53	
B4-1D	43.93	
B4-2A	44.51	43.66
B4-2B	43.12	
B4-2C	43.53	
B4-2D	43.47	
B5-1A	43.71	43.63
B5-1B	43.13	
B5-1C	43.30	
B5-1D	44.39	

D.C. Resistivity Data (cont.)

Sample	D.C. Resistivity (nΩ.m)	Average D.C. Resistivity (nΩ.m)
B5-2A	43.93	43.64
B5-2B	43.35	
B5-2C	43.12	
B5-2D	44.16	
C1-1A	47.19	46.74
C1-1B	46.41	
C1-1C	46.21	
C1-1D	47.17	
C1-2A	45.03	44.26
C1-2B	43.76	
C1-2C	43.87	
C1-2D	44.39	
C2-1A	45.66	44.47
C2-1B	43.85	
C2-1C	43.82	
C2-1D	44.58	
C2-2A	44.22	43.41
C2-2B	43.52	
C2-2C	42.95	
C2-2D	42.94	
C3-1A	44.62	44.10
C3-1B	44.08	
C3-1C	43.36	
C3-1D	44.34	

D.C. Resistivity Data (cont.)

Sample	D.C. Resistivity (nΩ.m)	Average D.C. Resistivity (nΩ.m)
C3-2A	44.37	43.82
C3-2B	43.94	
C3-2C	43.42	
C3-2D	43.82	
C4-1A	45.32	44.98
C4-1B	44.71	
C4-1C	44.59	
C4-1D	45.32	
C4-2A	44.32	44.28
C4-2B	43.91	
C4-2C	44.46	
C4-2D	44.42	
C5-1A	45.01	44.36
C5-1B	43.79	
C5-1C	43.71	
C5-1D	44.92	
C5-2A	45.27	44.64
C5-2B	44.92	
C5-2C	44.22	
C5-2D	44.16	

APPENDIX 6A.C. Resistivity Data

A. Bars Within Diameter Range A (15.17 mm to 15.35 mm)
(includes all 130 bars)

Sample	ΔV (mV)	ΔV average (mV)
A1-1B	-0.395	
A1-1C	0.036	-0.321
A1-1D	-0.603	
A1-2A	0.485	
A1-2B	0.650	
A1-2C	0.500	-0.387
A1-2D	-0.086	
A2-1A	0.305	
A2-1B	0.393	
A2-1C	0.324	0.328
A2-1D	0.290	
A2-2A	-0.059	
A2-2B	0.183	
A2-2C	0.244	0.075
A2-2D	-0.068	
A3-1A	-0.792	
A3-1B	-0.062	
A3-1C	-0.164	0.502
A3-1D	-0.988	

continued ..

A.C. Resistivity Data (diameter range A cont.)

Sample	ΔV (mV)	ΔV average (mV)
A3-2A	0.056	
A3-2B	0.089	
A3-2C	0.212	0.091
A3-2D	0.008	
A4-1A	-0.100	
A4-1B	-0.017	
A4-1C	0.042	-0.013
A4-1D	0.023	
A4-2A	0.074	
A4-2B	0.235	
A4-2C	0.147	0.125
A4-2D	0.042	
A5-1A	0.352	
A5-1B	0.478	
A5-1C	0.438	0.416
A5-1D	0.397	
A5-2A	0.499	
A5-2B	0.651	
A5-2C	0.589	0.567
A5-2D	0.527	
A6-1A	-0.086	
A6-1B	0.062	
A6-1C	-0.122	-0.238
A6-1D	-0.805	

continued ..

A.C. Resistivity Data (diameter range A cont.)

Sample	ΔV (mV)	ΔV average (mV)
A7-1A	0.548	
A7-1B	0.713	0.597
A7-1C	0.667	
A7-1D	0.461	
A8-1A	0.497	
A8-1B	0.629	0.591
A8-1C	0.674	
A8-1D	0.564	
A8-2A	0.499	
A8-2B	0.677	0.572
A8-2C	0.657	
A8-2D	0.456	
A9-1A	0.458	
A9-1B	0.593	0.532
A9-1C	0.458	
A9-1D	0.617	
A9-2A	0.206	
A9-2B	0.560	0.298
A9-2C	0.418	
A9-2D	0.008	
A10-1A	0.433	
A10-1B	0.543	0.463
A10-1C	0.580	
A10-1D	0.296	

continued..

A.C. Resistivity Data (diameter range A cont.)

Sample	ΔV (mV)	ΔV average (mV)
A10-2A	0.324	
A10-2B	0.680	0.512
A10-2C	0.605	
A10-2D	0.439	
A11-1A	0.454	
A11-1B	0.604	0.490
A11-1C	0.467	
A11-1D	0.435	
A11-2A	0.432	
A11-2B	0.732	0.621
A11-2C	0.820	
A11-2D	0.501	
A12-1A	0.304	
A12-1B	0.670	0.480
A12-1C	0.593	
A12-1D	0.352	
A12-2A	0.416	
A12-2B	0.666	0.582
A12-2C	0.571	
A12-2D	0.673	
A13-1A	0.746	
A13-1B	0.983	0.881
A13-1C	1.025	
A13-1D	0.770	

continued..

A.C. Resistivity Data (diameter range A cont.)

Sample	ΔV (mV)	ΔV average (mV)
A13-2A	0.702	
A13-2B	0.910	
A13-2C	0.881	0.973
A13-2D	0.698	
A14-1A	0.605	
A14-1B	0.828	
A14-1C	0.895	0.740
A14-1D	0.630	
A14-2A	0.691	
✓ A14-2B	0.968	
A14-2C	0.908	0.858
A14-2D	0.736	

A.C. Resistivity Data**B. Bars Within Diameter Range B (15.22 mm to 15.31 mm)
(includes 80 bars)**

Sample	ΔV (mV)	ΔV average (mV)
A1-2A	0.485	0.387
A1-2B	0.650	
A1-2C	0.500	
A1-2D	-0.086	
A2-1A	0.305	0.329
A2-1B	0.393	
A2-1D	0.290	
A2-2A	-0.059	-0.059
A3-1A	-0.792	-0.339
A3-1B	-0.062	
A3-1C	-0.164	
A3-2A	0.056	0.057
A3-2B	0.089	
A3-2D	0.008	
A4-1A	-0.100	-0.013
A4-1B	-0.017	
A4-1C	0.042	
A4-1D	0.023	
A4-2A	0.074	0.155
A4-2B	0.235	

continued..

A.C. Resistivity Data (diameter range B cont.)

Sample	ΔV (mV)	ΔV average (mV)
A5-1A	0.352	
A5-1C	0.438	0.396
A5-1D	0.397	
A5-2A	0.499	
A5-2B	0.651	0.567
A5-2C	0.589	
A5-2D	0.527	
A6-1A	-0.086	
A6-1B	0.062	-0.238
A6-1C	-0.122	
A6-1D	-0.805	
A7-1A	0.548	
A7-1B	0.713	0.643
A7-1C	0.667	
A8-1A	0.497	
A8-1B	0.629	0.591
A8-1C	0.674	
A8-1D	0.564	
A8-2A	0.499	
a8-2C	0.657	0.537
A8-2D	0.456	
A9-1A	0.458	
A9-1B	0.593	0.556
A9-1D	0.617	

continued..

A.C. Resistivity Data (diameter range B cont.)

Sample	ΔV (mV)	ΔV average (mV)
A9-2B	0.560	0.489
A9-2C	0.418	
A10-1A	0.433	0.463
A10-1B	0.543	
A10-1C	0.580	
A10-1D	0.296	
A10-2A	0.324	0.512
A10-2B	0.680	
A10-2C	0.605	
A10-2D	0.439	
A11-1A	0.454	0.445
A11-1D	0.435	
A11-2A	0.432	0.555
A11-2B	0.732	
A11-2C	0.501	
A12-1A	0.304	0.416
A12-1C	0.593	
A12-1D	0.352	
A12-2A	0.416	0.585
A12-2B	0.666	
A12-2D	0.673	
A13-1A	0.746	0.847
A13-1C	1.025	
A13-1D	0.770	

continued..

A.C. Resistivity Data (diameter range B cont.)

Sample	ΔV (mV)	ΔV average (mV)
A13-2A	0.702	
A13-2B	0.910	
A13-2C	0.881	0.798
A13-2D	0.698	
A14-1A	0.605	
A14-1B	0.828	
A14-1C	0.895	0.740
A14-1D	0.630	
A14-2A	0.691	
A14-2C	0.908	
A14-2D	0.736	0.778

A.C. Resistivity Data (Cont.)

C. Bars Within Diameter Range C (15.25 mm to 15.29 mm)
(includes 52 bars).

Sample	ΔV (mV)	ΔV average (mV)
A1-2A	0.485	
A1-2B	0.650	0.350
A1-2D	-0.086	
A2-1A	0.305	0.305
A3-1A	-0.792	
A3-1B	-0.062	-0.427
A4-1A	-0.100	
A4-1C	0.042	-0.012
A4-1D	0.023	
A4-2A	0.074	
A4-2B	0.235	0.155
A5-1A	0.352	
A5-1C	0.438	0.395
A5-2A	0.499	
A5-2B	0.651	0.567
A5-2C	0.589	
A5-2D	0.527	
A6-1A	-0.086	
A6-1B	-0.062	
A6-1C	-0.122	-0.238
A6-1D	-0.805	

continued..

A.C. Resistivity Data (diameter range C cont.)

Sample	ΔV (mV)	ΔV average (mV)
A7-1A	0.548	0.643
A7-1B	0.713	
A7-1C	0.667	
A8-1A	0.497	0.563
A8-1B	0.629	
A8-1D	0.564	
A8-2A	0.499	0.478
A8-2D	0.456	
A9-1A	0.458	0.526
A9-1B	0.593	
A9-2C	0.418	0.418
A10-1A	0.433	0.424
A10-1B	0.543	
A10-1D	0.296	
A10-2A	0.324	0.512
A10-2B	0.680	
A10-2C	0.605	
A10-2D	0.439	
A11-1A	0.454	0.445
A11-1D	0.435	
A11-2B	0.732	0.617
A11-2D	0.501	

continued..

A.C. Resistivity Data (diameter range C cont.)

Sample	ΔV (mV)	ΔV average (mV)
A12-1C	0.593	0.473
A12-1D	0.352	
A12-2B	0.666	0.670
A12-2D	0.673	
A13-1A	0.746	0.758
A13-1D	0.770	
A13-2A	0.702	0.702
A14-1B	0.828	0.729
A14-1D	0.630	
A14-2C	0.908	0.822
A14-2D	0.736	

APPENDIX 7Experimental Porosity Data

Sample	% Porosity	Average % Porosity
A1-1A	0.19	0.30
A1-1B	0.38	
A1-1C	0.38	
A1-1D	0.26	
A1-2A	0.18	0.00
A1-2B	0.00	
A1-2C	0.21	
A1-2D	0.00	
A2-1A	0.15	0.14
A2-1B	0.11	
A2-1C	0.11	
A2-1D	0.18	
A2-2A	0.97	0.99
A2-2B	0.86	
A2-2C	1.01	
A2-2D	1.12	
A3-1A	0.11	0.09
A3-1B	0.18	
A3-1C	0.03	
A3-1D	0.03	

continued..

Porosity Data (cont.)

Sample	% Porosity	Average % Porosity
A3-2A	0.00	
A3-2B	0.11	
A3-2C	0.11	0.10
A3-2D	0.18	
A4-1A	0.27	
A4-1B	0.37	
A4-1C	0.49	0.37
A4-1D	0.34	
A4-2A	0.15	
A4-2B	0.45	
A4-2C	0.45	0.26
A4-2D	0.00	
A5-1A	0.00	
A5-1B	0.04	
A5-1C	0.00	0.01
A5-1D	0.00	
A5-2A	0.00	
A5-2B	0.00	
A5-2C	0.08	0.02
A5-2D	0.00	
A6-1A	0.00	
A6-1B	0.00	
A6-1C	0.00	0.00
A6-1D	0.00	

continued..

Porosity Data (cont.)

Sample	% Porosity	Average % Porosity
A7-1A	0.00	
A7-1B	0.00	
A7-1C	0.04	0.01
A7-1D	0.00	
A8-1	0.00	
A8-1	0.00	
A8-1	0.00	0.00
A8-1	0.00	
A8-2	0.00	
A8-2	0.00	
A8-2	0.00	0.00
A8-2	0.00	
A9-1	0.10	
A9-1	0.00	
A9-1	0.00	0.03
A9-1	0.00	
A9-2	0.13	
A9-2	0.00	
A9-2	0.00	0.03
A9-2	0.00	
A10-1	0.09	
A10-1	0.00	
A10-1	0.00	0.03
A10-1	0.05	

continued..

Porosity Data (cont.)

Sample	% Porosity	Average % Porosity
A10-2	0.67	
A10-2	0.22	0.45
A10-2	0.22	
A10-2	0.67	
A11-1A	0.08	
A11-1B	0.11	0.10
A11-1C	0.11	
A11-1D	0.11	
A11-2A	0.22	
A11-2B	0.08	0.12
A11-2C	0.00	
A11-2D	0.19	
A12-1A	0.44	
A12-1B	0.26	
A12-1C	0.22	0.33
A12-1D	0.41	
A12-2A	0.35	
A12-2B	0.15	
A12-2C	0.45	0.27
A12-2D	0.11	
A13-1A	0.00	
A13-1B	0.00	
A13-1C	0.00	0.02
A13-1D	0.08	

continued..

Porosity Data (cont.)

Sample	% Porosity	Average % Porosity
A13-2A	0.04	
A13-2B	0.00	0.01
A13-2C	0.00	
A13-2D	0.00	
A14-1A	1.01	
A14-1B	0.71	0.86
A14-1C	0.78	
A14-1D	0.93	
A14-2A	0.67	
A14-2B	0.30	0.39
A14-2C	0.15	
A14-2D	0.45	
B1-1A	0.18	
B1-1B	0.18	0.16
B1-1C	0.15	
B1-1D	0.10	
B1-2A	0.19	
B1-2B	0.30	0.29
B1-2C	0.19	
B1-2D	0.45	
B2-1A	0.21	
B2-1B	0.10	0.12
B2-1C	0.04	
B2-1D	0.00	

continued..

Porosity Data (cont.)

Sample	% Porosity	Average % Porosity
B3-1A	0.24	
B3-1B	0.11	0.24
B3-1C	0.04	
B3-1D	0.56	
B3-2A	0.10	
B3-2B	0.15	0.11
B3-2C	0.07	
B3-2D	0.00	
B4-1A	0.47	
B4-1B	0.00	0.33
B4-1C	0.23	
B4-1D	0.53	
B4-2A	0.38	
B4-2B	0.11	0.329
B4-2C	0.26	
B4-2D	0.56	
B5-1A	0.43	
B5-1B	0.26	0.44
B5-1C	0.44	
B5-1D	0.64	
B5-2A	0.42	
B5-2B	0.08	0.315
B5-2C	0.00	
B5-2D	0.45	

continued..

Porosity Data (cont.)

Sample	% Porosity	Average % Porosity
C1-1A	0.76	
C1-1B	0.50	
C1-1C	0.64	0.60
C1-1D	0.50	
C1-2A	0.53	
C1-2B	0.34	
C1-2C	0.26	0.40
C1-2D	0.48	
C2-1A	0.00	
C2-1B	0.41	
C2-1C	0.27	0.35
C2-1D	0.37	
C2-2A	0.36	
C2-2B	0.06	
C2-2C	0.06	0.20
C2-2D	0.32	
C3-1A	0.33	
C3-1B	0.19	
C3-1C	0.30	0.28
C3-1D	0.30	
C3-2A	0.13	
C3-2B	0.58	
C3-2C	0.47	0.49
C3-2D	0.77	

continued..

Porosity Data (cont.)

Sample	% Porosity	Average % Porosity
C4-1A	1.33	1.25
C4-1B	1.22	
C4-1C	1.22	
C4-1D	1.25	
C4-2A	1.30	0.19
C4-2B	1.15	
C4-2C	1.08	
C4-2D	1.22	
C5-1A	0.86	0.71
C5-1B	0.45	
C5-1C	0.38	
C5-2D	1.16	
C5-2A	0.86	0.69
C5-2B	0.60	
C5-2C	0.52	
C5-2D	0.78	

APPENDIX 8Heat Treatment Data

Three alloys were heat treated, A356 alloy, A357 alloy and A356 alloy containing 0.48 wt. % Fe. D.C. and A.C. resistivity measurements were taken after solution treatment and after aging when the bars had attained room temperature.

Heat Treatment Data -A356 AlloyHeat Treatment A (8 hours solution treatment)

Sample	Resistivity after Solution Treatment (nΩ.m)	Resistivity after aging (nΩ.m)
A1-1B	44.13	41.46
A1-2B	44.90	42.40
A2-1B	43.48	41.44
A2-2B	46.28	43.50
A3-1B	46.79	43.36
A3-2B	45.35	43.08
A4-1B	47.68	43.14
A4-2B	44.87	42.37
A5-1B	44.63	42.79
A5-2B	44.16	41.88
A6-1B	45.65	43.36
A7-1B	44.73	42.18
A8-1B	44.45	41.48
A8-2B	44.57	42.26
A9-1B	44.56	42.50
A9-2B	43.99	41.93
A10-1B	43.54	41.71
A10-2B	44.34	42.74
A11-1B	44.63	43.02
A11-2B	43.59	42.45
A12-1B	43.88	42.27
A12-2B	44.05	42.68
A13-1B	44.37	42.30
A13-2B	44.51	42.67
A14-1B	44.01	42.45
A14-2B	44.51	42.90

Heat Treatment Data - A356 AlloyHeat Treatment A (8 hours solution treatment)

Sample	ΔV after solution treatment (mV)	ΔV after aging (mV)
A1-1B	-0.124	0.463
A1-2B	-0.124	0.383
A2-1B	0.122	0.497
A2-2B	-0.203	0.368
A3-1B	-0.487	0.287
A3-2B	-0.203	0.169
A4-1B	-0.235	0.202
A4-2B	-0.034	0.406
A5-1B	0.017	0.427
A5-2B	0.101	0.521
A6-1B	-0.229	0.278
A7-1B	0.000	0.420
A8-1B	0.019	0.639
A8-2B	0.144	0.569
A9-1B	0.070	0.453
A9-2B	0.112	0.531
A10-1B	0.241	0.655
A10-2B	0.031	0.467
A11-1B	0.044	0.489
A11-2B	0.207	0.528
A12-1B	0.200	0.604
A12-2B	0.077	0.451
A13-1B	0.147	0.689
A13-2B	0.021	0.504
A14-1B	0.124	0.520
A14-2B	0.128	0.492

Heat Treatment Data - A356 AlloyHeat Treatment B (24 hours solution treatment)

Sample	Resistivity after Solution Treatment (n Ω .m)	Resistivity after Aging (n Ω .m)
A1-1C	46.07	43.76
A1-2C	46.71	41.72
A2-1C	45.95	42.12
A2-2C	47.08	42.93
A3-1C	47.20	43.99
A3-2C	47.85	42.56
A4-1C	47.05	43.16
A4-2C	46.01	42.18
A5-1C	44.90	41.94
A5-2C	45.16	41.97
A6-1C	45.53	43.48
A7-2C	43.42	41.82
A8-1C	46.12	42.90
A8-2C	45.14	42.62
A9-1C	45.58	43.04
A9-2C	44.85	42.79
A10-1C	44.45	42.16
A10-2C	46.19	43.14
A11-1C	44.69	41.98
A11-2C	44.45	41.91
A12-1C	44.51	42.68
A12-2C	45.49	42.73
A13-1C	44.74	42.44
A13-2C	45.01	42.28
A14-1C	43.36	41.53
A14-2C	44.45	42.40

Heat Treatment Data - A356 AlloyHeat Treatment B (24 hours solution treatment)

Sample	ΔV after solution treatment (mV)	ΔV after aging (mV)
A1-1C		0.208
A1-2C		0.317
A2-1C	NO RESULTS	0.321
A2-2C		0.345
A3-1C		0.108
A3-2C		0.487
A4-1C		0.212
A4-2C		0.355
A5-1C		0.490
A5-2C		0.503
A6-1C		0.080
A7-1C		0.543
A8-1C		0.415
A8-2C		0.392
A9-1C		0.459
A9-2C		0.362
A10-1C		0.528
A10-2C		0.287
A11-1C		0.317
A11-2C		0.543
A12-1C		0.414
A12-2C		0.337
A13-1C		0.486
A13-2C		0.374
A14-1C		0.595
A14-2C		0.388

Heat Treatment Data - A356 AlloyHeat Treatment C (48 hours solution treatment)

Sample	Resistivity after Solution Treatment (nΩ.m)	Resistivity after aging (nΩ.m)
A1-1D	45.36	42.50
A1-2D	45.87	43.59
A2-1D	45.60	43.31
A2-2D	45.29	42.57
A3-1D	44.76	41.85
A3-2D	43.19	41.60
A4-1D	44.67	42.40
A4-2D	45.20	42.71
A5-1D	44.36	41.86
A5-2D	45.07	41.88
A6-1D	49.30	46.10
A7-1D	43.70	40.99
A8-1D	41.99	40.40
A8-2D	44.53	42.25
A9-1D	43.82	41.32
A9-2D	44.06	43.18
A10-1D	44.79	42.97
A10-2D	44.34	41.82
A11-1D	44.51	42.45
A11-2D	43.25	41.92
A12-1D	43.48	41.88
A12-2D	45.13	41.94
A13-1D	44.96	41.54
A13-2D	45.14	42.62
A14-1D	45.07	42.79
A14-2D	43.99	41.71

Heat Treatment Data -A356 AlloyHeat Treatment C (48 hours solution treatment)

Sample	Resistivity after Solution Treatment (nΩ.m)	Resistivity after aging (nΩ.m)
A1-1D	-1.237	-0.549
A1-2D	-0.230	0.392
A2-1D	-0.104	0.437
A2-2D	-0.154	0.39
A3-1D	-0.996	-0.333
A3-2D	-0.343	0.679
A4-1D	0.151	0.544
A4-2D	-0.204	0.306
A5-1D	0.061	0.592
A5-2D	-0.059	0.595
A6-1D	-0.938	-0.193
A7-1D	0.215	0.663
A8-1D	0.575	0.933
A8-2D	0.128	0.543
A9-1D	0.191	0.681
A9-2D	-0.353	0.024
A10-1D	-0.014	0.460
A10-2D	0.213	0.626
A11-1D	0.050	0.518
A11-2D	0.322	0.658
A12-1D	0.324	0.722
A12-2D	0.012	0.590
A13-2D	-0.014	0.787
A13-1D	-0.009	0.505
A14-2D	-0.041	0.476
A14-1D	0.223	0.587

Heat Treatment Data of A357 Alloy and
A356 (0.48 wt.% Fe) Alloy

Heat Treatment A (8 hours solution treatment)

Sample	Resistivity after Solution Treatment (nΩ.m)	Resistivity after aging (nΩ.m)
B1-1B	47.20	43.08
B1-2B	47.85	44.40
B2-1B	47.47	42.22
B3-1B	48.53	43.81
B3-2B	47.47	43.82
B4-1B	48.09	43.96
B4-2B	48.33	43.73
B5-1B	46.13	42.71
B5-2B	48.41	43.36
C1-1B	48.93	45.72
C1-2B	46.07	43.30
C2-1B	45.61	42.84
C2-2B	47.71	43.52
C3-1B	46.62	43.62
C3-2B	46.01	43.48
C4-1B	47.94	44.71
C4-2B	47.00	43.82
C5-1B	46.53	43.34
C5-2B	47.71	43.75

Heat Treatment Data of A357 Alloy
and A356 (0.48 wt.% Fe) Alloy

Heat Treatment A (8 hours solution treatment)

Sample	ΔV after solution treatment (mV)	ΔV after aging (mV)
B1-1B	-0.330	0.247
B1-2B	-0.408	0.187
B2-1B	-0.361	0.440
B3-1B	-0.751	0.067
B3-2B	-0.423	0.261
B4-1B	-0.483	0.184
B4-2B	-0.555	0.191
B5-1B	-0.145	0.362
B5-2B	-0.456	0.239
C1-1B	-0.547	-0.171
C1-2B	-0.057	0.351
C2-1B	-0.045	0.423
C2-2B	-0.281	0.295
C3-1B	-0.230	0.284
C3-2B	-0.106	0.328
C4-1B	-0.547	-0.003
C4-2B	-0.399	0.084
C5-1B	-0.335	0.331
C5-2B	-0.193	0.351

Heat Treatment Data of A357 Alloy
and A356 (0.48 wt.% Fe) Alloy

Heat Treatment B (24 hours solution treatment)

Sample	Resistivity after Solution treatment (nΩ.m)	Resistivity after aging (nΩ.m)
B1-1C	47.26	44.10
B1-2C	47.72	44.05
B2-1C	43.99	42.40
B3-1C	47.67	42.88
B3-2C	47.34	44.82
B4-1C	45.83	43.31
B4-2C	47.18	43.99
B5-1C	47.78	44.57
B5-2C	44.68	42.62
C1-1C	47.58	44.39
C1-2C	46.65	43.88
C2-1C	45.65	43.82
C2-2C	46.19	43.18
C3-1C	45.41	42.68
C3-2C	45.26	43.41
C4-1C	46.13	43.87
C4-2C	46.67	44.60
C5-1C	44.84	42.57
C5-2C	45.14	42.85

Heat Treatment Data of A357 Alloy
and A356 (0.48 wt. % Fe) Alloy

Heat Treatment B (24 hours solution treatment)

Sample	ΔV after solution treatment (mV)	ΔV after aging (mV)
B1-1C	-0.609	0.075
B1-2C	-0.598	0.195
B2-1C	0.115	0.546
B3-1C	-0.657	0.340
B3-2C	-0.543	0.054
B4-1C	-0.150	0.338
B4-2C	-0.394	0.154
B5-1C	-0.619	0.067
B5-2C	0.024	0.460
C1-1C	-0.616	0.022
C1-2C	-0.304	0.281
C2-1C	-0.187	0.258
C2-2C	-0.165	0.372
C3-1C	-0.136	0.344
C3-2C	-0.045	0.417
C4-1C	-0.383	0.126
C4-2C	-0.359	0.104
C5-1C	0.032	0.417
C5-2C	-0.113	0.405

Heat Treatment Data of A357 Alloy
and A356 (0.48 wt.% Fe) Alloy

Heat Treatment C (48 hours solution treatment)

Sample	ΔV after solution treatment (mV)	ΔV after aging (mV)
B1-1D	48.61	46.56
B1-2D	48.26	46.89
B2-1D	48.44	47.52
B3-1D	48.35	46.30
B3-2D	48.09	46.27
B4-1D	48.54	47.40
B4-2D	46.50	45.81
B5-1D	48.00	45.95
B5-2D	49.26	47.66
C1-1D	48.22	46.53
C1-2D	45.31	44.39
C2-1D	46.86	45.95
C2-2D	45.90	45.22
C3-1D	45.26	45.26
C3-2D	46.33	45.19
C4-1D	47.17	46.25
C4-2D	46.70	46.01
C5-1D	46.51	45.38
C5-2D	45.98	45.75

Heat Treatment Data of A357 Alloy
and A356 (0.48 wt.% Fe) Alloy

Heat Treatment C (48 hours solution treatment)

Sample	ΔV after solution treatment (mV)	ΔV after aging (mV)
B1-1D	-1.135	-1.20
B1-2D	-0.816	-0.883
B2-1D	-1.021	-0.950
B3-1D	-0.899	-0.707
B3-2D	-0.826	-0.718
B4-1D	-0.102	-0.992
B4-2D	-0.629	-0.682
B5-1D	-1.222	-0.659
B5-2D	-1.173	-1.390
C1-1D	-1.711	-1.403
C1-2D	-0.286	-0.115
C2-1D	-0.608	-0.365
C2-2D	-0.462	-0.214
C3-1D	-0.308	-0.174
C3-2D	-0.580	-0.273
C4-1D	-0.559	-0.376
C4-2D	-0.615	-0.367
C5-1D	-0.676	-0.350
C5-2D	-0.457	-0.415

APPENDIX 9Results of Statistical Analysis of Heat Treatment Data

Heat treatment measurements were taken after solution treatment and after aging. One part of the result analysis involved the study of the changes in resistivity that occur upon heat treatment as a function of strontium content. For each alloy and for each heat treatment two relationships were examined:

- i) The difference in resistivity between an as-cast and a solution treated bar versus strontium content
- ii) The difference in resistivity between an as-cast and an aged bar versus strontium content

The data was statistically analysed (section 2.2) and graphs plotted of the two relationships. Each relationship was characterized by a specific F value. If this F value was higher than the table F values (table VII) then the graphs were satisfactory representations of the data.

Results of Statistical Analysis of Heat Treatment Data
A356 Alloy

Heat Treatment	Statistical F values	
	Difference in D.C. resistivity between an as-cast bar and a heat treated bar (X) vs. strontium content	
	X = solution treated bar	X = completely heat treated bar
A	11.61 (3.42)	32.50 (3.42)
B	3.38 (3.42)	18.16 (3.42)
C	1.29 (3.42)	2.31 (3.42)

The corresponding table F values for 95% significance level are shown in brackets beside the experimental F values.

Results of Statistical Analysis of Heat Treatment Data
A357 Alloy

Heat Treatment	Statistical F values			
	Difference in D.C. resistivity between an as-cast bar and a heat treated bar (X) vs. strontium content.			
	X = solution treated bar		X = completely heat treated bar	
A	6.19	(6.39)	0.52	(6.39)
B	28.95	(9.01)	3.36	(5.41)
C	2.11	(5.14)	2.36	(5.41)

The corresponding table F values for 95% significance level are shown in brackets beside the experimental F values.

Results of Statistical Analysis of Heat Treatment Data
A356 Alloy containing 0.48 wt.% Fe

Heat Treatment	Statistical F values	
	Difference in D.C. resistivity between an as-cast bar and a heat treated bar (X) vs. strontium content.	
	X = solution treated bar	X = completely heat treated bar
A	2.59 (5.19)	4.19 (4.74)
B	3.89 (4.74)	12.34 (4.76)
C	1.34 (4.76)	2.72 (4.76)

The corresponding table F values for 95% significance level are shown in brackets beside the experimental F values.

APPENDIX 10Calculation of Instrument Inaccuracies for the D.C. and A.C. Techniques1. D.C. Technique

Accuracy of voltmeter = ± 0.03 % of reading

Accuracy of Ammeter = ± 0.4 % of reading

Accuracy of vernier gauge = $\pm 0.0005\%$ of reading

Accuracy of micrometer screw gauge = ± 0.03 % of reading

Total error in resistivity reading

= $(\pm 0.03\%) + (\pm 0.40\%) + (\pm 0.0005\%) + 2(\pm 0.03\%)$

= $\pm 0.491\%$ of reading.

Taking the resistivity reading as the lowest resistivity measurement - $40.91 \text{ n}\Omega\cdot\text{m}$

$\pm 0.491\%$ of $40.91 \text{ n}\Omega\cdot\text{m}$ = $\pm 0.20 \text{ n}\Omega\cdot\text{m}$

Instrumental Inaccuracy of D.C. technique = $\pm 0.20 \text{ n}\Omega\cdot\text{m}$

2. A.C. Technique

Accuracy of voltmeter = $\pm 0.03\%$ of reading in mV

Accuracy of current setting = $\pm 0.1\%$ of reading in mV

Accuracy of voltage setting = $\pm 0.01\%$ of reading in mV

Accuracy of lock-in amplifier = $\pm 0.01\%$ of reading in mV

Total error in ΔV reading

$$= (\pm 0.03\%) + (\pm 0.1\%) + (\pm 0.01\%) + (\pm 0.01\%)$$

$$= \pm 0.15\% \text{ of reading}$$

Taking the ΔV reading as the smallest ΔV measurement;

$$0.013 \text{ mV } \pm 0.15\% \text{ of } 0.013 \text{ mV} = \pm 2.0 \times 10^{-5} \text{ mV}$$

$$\underline{\text{Instrumental Inaccuracy of A.C. technique} = +2.0 \times 10^{-5} \text{ mV}}$$

APPENDIX 11

Calculation of the Standard Resistivity Error between Bars of the Same Strontium Content

The resistivity between similar bars from the same casting was found to vary. In order to quantify the variation in resistivity between similar bars the following procedure was performed;

1. The standard deviation of resistivity values of the four bars in each casting was calculated = S_D .
2. The sum of the squares of the standard deviations was found, and divided by the number of castings = $\sum S_D^2 / .26$
3. The square root of $\sum S_D^2 / .26$ was determined to give the standard error in resistivity between similar bars.

The same procedure was performed on porosity data to find the standard porosity variation between bars of the same strontium content.